**The Dissertation Committee for Matthew Solomon Khosh Certifies that this is the approved version of the following dissertation:**

# Seasonal dynamics of organic matter and inorganic nitrogen in surface waters of Alaskan Arctic streams and rivers

**Committee:**

James W. McClelland, Supervisor

Kenneth H. Dunton

Zhanfei Liu

Gerald C. Shank

Amy Townsend-Small

# Seasonal dynamics of organic matter and inorganic nitrogen in surface waters of Alaskan Arctic streams and rivers

**by**

**Matthew Solomon Khosh, B.S.**

**Dissertation**

Presented to the Faculty of the Graduate School of

The University of Texas at Austin

in Partial Fulfillment

of the Requirements

for the Degree of

**Doctor of Philosophy**

**The University of Texas at Austin**

**December 2015**

## Acknowledgements

There are numerous people to thank who helped me in one way or another throughout this journey, but I would like to call special attention to a few. I would like to especially thank my advisor Jim McClelland whose guidance was immeasurable during this process and from whom I have learned a tremendous amount. Thanks are also deserved to the other members of my research committee, Ken Dunton, Zhanfei Liu, Chris Shank, and Amy Townsend-Small, whose advice and assistance were integral to this research.

I would also like to thank past and present members of the McClelland lab; Patty Garlough, Claire Griffin, Karen Bishop, Stephanie Smith, Tara Connelly, Steven Cao, Rae Mooney, and Craig Connelly. Additionally, I would like to thank all the graduate students, postdocs, research technicians, faculty, and staff who overlapped with me during my time at UTMSI for helping make working and living in Port Aransas a positive experience.

Special thanks are deserved to my parents and sister for their endless love and support of all of my life decisions. Finally, many thanks are deserved to my best friend, partner, and fellow dog hoarder, Rachel Clarkson, who was a constant source of unwavering support and positive encouragement. Thank you for putting up with me.

# Seasonal dynamics of organic matter and inorganic nitrogen in surface waters of Alaskan Arctic rivers

Matthew Solomon Khosh, Ph.D.

The University of Texas at Austin, 2015

Supervisor: James W. McClelland

Climate-linked changes in hydrology and biogeochemical processes within Arctic watersheds are likely already affecting fluvial export of waterborne materials, including organic matter (OM) and dissolved inorganic nitrogen (DIN). Our understanding of Arctic watershed OM and DIN export response to climate change is hampered by a lack of contemporary baselines, as well as a dearth of seasonally comprehensive studies. This work focuses on characterizing OM and DIN concentrations and sources in six streams/rivers on the North Slope of Alaska during the entirety of the hydrologic year (May through October) in 2009 and 2010. The highest OM concentrations occurred during spring snowmelt, with results indicating that terrestrial vegetation leachates are the major source of dissolved OM, while particulate OM originates from a degraded soil source. Over the hydrologic year, soils became a progressively increasing source of dissolved OM, while autochthonous production made up a sizeable proportion of particulate OM during base flow conditions. DIN concentrations were low throughout the spring and summer and increased markedly during the late summer and fall. Our findings suggest that penetration of water into thawed mineral soils, and a reduction in nitrogen assimilation relative to remineralization, may increase DIN export from Arctic watersheds during the late summer and fall. Although recent studies of Arctic rivers have emphasized the importance of the

spring thaw period on OM export, our understanding of the mechanisms that control water chemistry observations during this time are still lacking. Experimental leaching results, from experiments conducted in 2014, suggest that aboveground plant biomass is a major source of dissolved OM in Arctic catchments during the spring, and that the timing of freezing and drying conditions during the fall may impact dissolved OM leaching dynamics on that same material the following snowmelt. Improved knowledge of OM and DIN temporal trends and the mechanisms that control seasonal concentrations is essential for understanding export dynamics of these water constituents in Arctic river systems. Perhaps more importantly, increased understanding of the seasonal controls on OM and DIN export in Arctic rivers is critical for predicting how these systems will respond under future climate change scenarios.

# Table of Contents

# List of Tables

# List of Figures

# Introduction

Rivers serve as an important connection between terrestrial and ocean ecosystems, transporting freshwater, nutrients, and organic matter (OM) from their contributing upstream land area to coastal aquatic environments. This linkage is especially pronounced in the Arctic land-ocean system, where Arctic rivers account for greater than 10% of annual global river discharge, yet the Arctic Ocean comprises only about 1% of the world's ocean volume [*Menard and Smith*, 1966; *Aagaard and Carmack*, 1989]. Similarly, Arctic rivers transport large quantities of OM, mainly in the dissolved form [*Dittmar and Kattner*, 2003; *Guo and Macdonald*., 2006; *McClelland et al*., 2014], with contemporary estimates reporting that Arctic rivers export 11-13% of the total global dissolved OM flux. This globally significant amount of fluvial OM is a result of high dissolved OM concentrations in Arctic rivers [e.g., *McClelland et al*., 2012], owing to large stores of soil OM in high latitude soils, peatlands, and permafrost [*Tarnocai et al*., 2009]. As recent studies estimate that approximately 50% of the global soil organic carbon pool is contained within Arctic and high latitude soils, there is concern that warming of the Arctic could mobilize carbon from previously frozen soils, reintroducing it to the contemporary global carbon cycle, potentially resulting in a global warming positive feedback loop [e.g., *Billings et al.*, 1983; *Schuur et al*., 2013]. There has been much focus on the potential release of carbon through soil-atmosphere interactions via enhanced greenhouse gas emissions through microbial remineralization [e.g., *Oechel et al*., 1993; *Koven et al*., 2011; *Schuur et al*., 2015]. However, the lateral transport of OM by rivers is a major component of Arctic carbon cycling, and merits attention as the annual flux of carbon is of similar magnitude to that of carbon sequestration by Arctic terrestrial vegetation [*McGuire et al*., 2009]. Additionally,

changes in river water chemistry may be useful indicators of climate change impacts on landscape processes at watershed scales as they integrate over the entire drainage area.

Over the past 100 years the largest increases in warming have occurred in the Arctic, with rates of warming nearly double the observed global average, and a consensus among contemporary climate models projects additional increases in air temperature of 4-7°C by the end of the 21st century for the region [*IPCC*, 2007; *ACIA*, 2005]. The impacts of warming include modifications to the Arctic hydrologic cycle, including changes in the quantity, seasonality, and flow paths of water in the Arctic freshwater system [*Peterson et al.*, 2002; *Peterson et al.*, 2006; *Holland et al.*, 2007; *White et al.*, 2007; *Rawlings et al.*, 2010; *Romanovsky et al.*, 2010]. These responses to warming have already been documented over recent decades and are expected to intensify with continued warming. Tight coupling between catchment hydrology and terrestrial biogeochemical processes [*Johnson et al*., 1996; *Steiglitz et al*., 2000; *Judd and Kling*, 2002], in addition to river water chemistry [*Striegl et al*., 2005; *Finlay et al*., 2006; *McNamara et al.*, 2008; *Townsend-Small et al.*, 2011], suggest that riverine OM export dynamics are likely already occurring and will continue to intensify with projected climate change scenarios. Likewise, impacts on the fluvial export of inorganic forms of nitrogen are of interests as they serve as important resources for downstream Arctic freshwater [e.g., *Levine and Whalen*, 2001; *MacIntyre et al.*, 2006; *Gettel et al.*, 2013] and coastal ecosystems [e.g., *Amon and Meon*, 2004; *Tank et al.*, 2011; *McClelland et al.*, 2014].

Currently, the biogeochemical response of Arctic river catchments, and associated OM and inorganic nitrogen export response, to climate change over the next century is not entirely clear. Increases in dissolved OM export with warming have been reported in northern temperate peatlands [*Freeman et al*., 2001; *Freeman et al*., 2004] and Siberian Arctic peatlands [*Frey & Smith*, 2005]. *Frey & Smith* [2005] report that increases in fluvial

dissolved OM fluxes correlate with increases in warming, and suggest that soil OM storage will be reduced and increases in riverine dissolved OM concentrations and export are expected. An alternative is that warmer temperatures will lead to an increase in the depth of the seasonally thawed top layer of permafrost soil (active layer), diverting flow paths of water below organic rich soils and into mineral soils with lower organic carbon content [*Striegl et al*., 2005]. Increased temperatures and longer water flow paths and residence times in mineral soils would increase both soil microbial remineralization of dissolved OM and adsorption of dissolved OM to mineral soil particle surfaces leading to a decreases in OM export [*Striegl et al*., 2005]. Although increased flow of water through deeper soils may reduce dissolved OM export, this may be accompanied by a concurrent increase in the export of inorganic nitrogen [*Jones et al*., 2005] due to increased dissolved OM remineralization [*Harms and Jones*, 2012]. Similarly, *Frey et al*. [2007] project increases in the export of nitrogen from western Siberian peatlands with further warming, and an analysis of nitrate export from a watershed in the Alaskan Arctic between the late 1970s and early 2000s found that export has increased in recent years [*McClelland et al*., 2007]. Though relationships linking warmer temperatures and hydrology with OM and inorganic nitrogen concentrations and export have been established, permafrost degradation [*Frey and McClelland*, 2009], and changes in terrestrial biogeochemical processes [e.g., *Neff and Hooper*, 2002] may complicate expected catchment OM and inorganic nitrogen export responses.

Owing to highly remote locations and logistical difficulties associated with working in the Arctic, there is a general dearth of quality-controlled long-term water chemistry data sets [*Holmes et al*., 2000; ; *Holmes et al.*, 2001], and those that are available are exceptionally rare and spatially sparse [e.g., *McClelland et al.*, 2007]. As such, evaluating the predicted responses of waterborne materials exported from Arctic watersheds is

hindered by a lack of contemporary baselines by which to compare future changes. An improved understanding of fluvial constituent seasonal dynamics in Arctic rivers may offer critical insights into anticipated responses to climate change as the seasonal transitions from winter-to-spring and summer-to-winter are important periods of biogeochemical processing and export of water, OM, and inorganic nitrogen from watersheds. For example, discharge during the spring freshet may account for up to three quarters of the yearly annual runoff in Arctic watersheds [*Kane et al.*, 1989; *Kane et al.*, 1997; *McNamara et al.*, 1997; *McNamara et al.*, 1998; *Bowling et al.*, 2003], and recent investigations indicate that the majority of the annual OM export from Arctic rivers occurs during this period [e.g., *Finlay et al.*, 2006; *Raymond et al.*, 2007; *Townsend-Small et al.*, 2011; *McClelland et al.*, 2014]. The importance of the spring freshet on annual fluxes of OM and inorganic nitrogen has received recognition during the past decade as studies have made a concentrated effort to sample during this historically under-studied time period. However, studies with a similar concentrated focus on late summer and fall dynamics have remained limited [e.g., *Cai et al.*, 2008; *Holmes et al.*, 2012]. Projections of a future Arctic include longer snow and ice-free free periods [*Ueyama et al.*, 2003; *Pearson et al.*, 2013], deeper active layers [*Jorgenson et al.*, 2006], and permafrost degradation [*Frey and McClelland*, 2009], all of which are likely to affect soil and stream biogeochemistry and would be expected to be most apparent in the late summer to early fall during maximum seasonal soil thaw extent. As such, a greater knowledge of the seasonal dynamics of both OM and inorganic nitrogen concentrations during the late summer and fall, in addition to the spring, is fundamental for predicting how fluvial export of these constituents from Arctic watersheds will respond to warming and associated climate change impacts to hydrology and biogeochemical processing.

The primary goals of this study were to expand upon current knowledge regarding the seasonal dynamics of fluvial OM and inorganic nitrogen in Arctic catchments, specifically focusing on streams and rivers on The North Slope of Alaska, and investigating possible mechanisms that control observed constituent concentrations. As it has been previously demonstrated that a significant portion of the annual flux of OM, inorganic nitrogen, and water occurs in early spring, primarily during the spring snowmelt, [e.g., *Finlay et al*., 2006; *Raymond et al.*, 2007; *Townsend-Small et al.*, 2011; *McClelland et al.*, 2014], the observational components of this dissertation also emphasized sampling during the spring, however the high resolution sampling conducted during the late summer and fall as part of this study offers a unique seasonally comprehensive data set that provides new insights into dissolved OM and inorganic nitrogen export dynamics from Arctic catchments during the understudied late season. In Chapter 1, dissolved and particulate OM dynamics from six river catchments in Arctic Alaska were examined during the entirety of the hydrologic year (May through October) in 2009 and 2010. Specifically, we focused on quantifying dissolved organic carbon (DOC) and particulate organic carbon concentrations, and using carbon to nitrogen ratios (C:N) and stable isotope ratios ($\delta^{13}C$) to characterize these OM pools and elucidate possible sources. Chapter 2 focuses on dissolved nitrogen seasonal dynamics from the same six streams and rivers over the same study period, measuring dissolved organic nitrogen (DON) and dissolved inorganic nitrogen (DIN) concentrations and using soil temperature data and nitrogen to chloride molar ratios ($N:Cl^-$) to determine possible mechanisms and watershed processes to explain seasonal DON and DIN concentration patterns. Finally, in Chapter 3, a leaching experiment using aboveground material from three species of common Alaskan Arctic vascular plants was conducted to determine the effects of drying and freezing on dissolved

OM leaching dynamics from vegetation material and its possible role in OM export from Arctic watersheds during the spring snowmelt.

# Chapter 1: Seasonally dynamics of dissolved and particulate organic matter in Alaskan Arctic tundra and mountain streams


## ABSTRACT

Climate-linked changes in hydrology and biogeochemical processes within Arctic watersheds are altering fluvial export of water-borne materials, including organic matter (OM) in both dissolved and particulate forms. These changes in export are likely to become most apparent during an earlier spring snowmelt and in the late summer and early fall when soil active layer depths are at maximum extent. As seasonally comprehensive studies of water-borne constituents in Arctic rivers remain relatively rare, an improved understanding of seasonal OM dynamics may help us to better understand how these systems are responding to climate change. Our study focuses on characterizing organic carbon concentrations and sources in six streams/rivers on the North Slope of Alaska during the entirety of the hydrologic year (May through October) in 2009 and 2010. Specifically, we examined seasonal variations in dissolved organic carbon (DOC) and particulate organic carbon (POC) concentrations, and we used carbon to nitrogen molar ratios (C:N) as indicators of OM sources. We also used stable isotope ratios ($\delta^{13}C$) of POC to elucidate sources. The highest concentrations of both dissolved and particulate OM occurred during spring snowmelt. However, high C:N ratios of dissolved OM measured during this period indicate vegetation leachates as a major source, while low C:N ratios of particulate OM suggest a primarily degraded soil source. Dissolved OM C:N ratios declined over the course of the hydrologic year, signaling a progressively increasing soil source, while particulate OM C:N ratios displayed only small variations during the year. However, seasonal decreases in $\delta^{13}C$ of POC values point to an increase in the proportion of autochthonous particulate OM production during summer and fall base flow conditions.

Our results indicate that hydrology, active layer depth, and water flow paths are important mechanisms controlling fluvial OM concentrations and composition in Arctic rivers.

## INTRODUCTION

Historically, prevailing cold climactic conditions and waterlogged anaerobic soils at high latitudes have resulted in the storage of large amounts of organic matter (OM) in Artic soils, peatlands, and permafrost, with recent estimates reporting that as much as 50% of the global soil organic carbon pool is contained within these systems [*Tarnocai et al*., 2009]. Knowledge of how OM cycling will respond to climate change is critical as warming of the Arctic may result in the mobilization of carbon from previously frozen soils, reintroducing it into contemporary biogeochemical cycling [e.g., *Billings et al.*, 1983; *Schuur et al*., 2013]. Previous studies investigating the response of northern latitude soils to climate change have primarily focused on soil-atmosphere interactions of enhanced greenhouse gas emissions via microbial remineralization [e.g., *Oechel et al*., 1993; *Koven et al*., 2011; *Schuur et al*., 2015]. Although the vertical fluxes of carbon are significantly larger, the lateral transport rate of organic carbon by rivers is of similar magnitude, although smaller, to the rate of net carbon sequestration by terrestrial vegetation and therefore represents a major component of high latitude carbon cycling [*McGuire et al*., 2009].

In addition to increases in air temperature, the effects of climate change include alterations to Arctic hydrologic cycles, such as longer snow and ice free seasons, increased river discharge, and altered quantity and seasonality of precipitation [*Peterson et al.*, 2002; *Peterson et al.*, 2006; *Holland et al.*, 2007; *White et al.*, 2007; *Rawlings et al.*, 2010]. As hydrology has been demonstrated to affect terrestrial OM processes [*Johnson et al*., 1996; *Steiglitz et al*., 2000; *Judd and Kling*, 2002], as well as river water chemistry [*Finlay et al*., 2006; *McNamara et al.*, 2008; *Townsend-Small et al.*, 2011], perturbations to riverine OM export dynamics from Arctic watersheds are most likely already occurring and will continue to intensify with projected climate change scenarios. While linkages between

hydrology and biogeochemistry within Arctic river catchments have been demonstrated at various locations throughout the Arctic [e.g., *Striegl et al*., 2005; *Holmes et al.*, 2012; *McClelland et al.*, 2014], OM export responses to climate warming induced changes to hydrology may be complicated by permafrost degradation [*Frey and McClelland*, 2009], and changes in terrestrial OM production [*Neff and Hooper*, 2002]. One hypothesis is that OM export from the region will increase with projected climate change. This is supported by studies in northern temperate peatlands [*Freeman et al*., 2001; *Freeman et al*., 2004] and Siberian Arctic peatlands [*Frey & Smith*, 2005] that correlated increases in fluvial OM fluxes to warming, suggesting reduced soil OM storage and increased riverine OM concentrations and export. Alternatively, warmer temperatures are expected to lead to an increase in the depth of the seasonally thawed soil layer (active layer), diverting flow paths of water below organic rich soils and into mineral soils with lower organic content [*MacLean et al.*, 1999*; Striegl et al*., 2005; *Petrone et al.*, 2006]. It is argued that the coupled effect of increased temperatures and longer water flow paths and residence times in mineral soils would increase both adsorption of OM to mineral soil surfaces and increase soil microbial remineralization leading to a decrease in OM export [*MacLean et al.*, 1999; Striegl et al., 2005; *Petrone et al.*, 2006].

Our understanding of Arctic watershed OM export response to climate change is hampered by a general lack of contemporary baselines by which to compare future changes in river water chemistry [*Holmes et al*., 2000; ; *Holmes et al.*, 2001], as quality-controlled long-term water chemistry data sets are exceptionally rare [*McClelland et al.*, 2007]. Furthermore, logistical difficulties associated with working in remote regions resulted in past studies often sampling primarily during summer months. Although a lack of long-term data records makes assessment of alterations in OM export from Arctic watersheds challenging, an improved understanding of seasonal fluvial constituent export dynamics

from these systems may offer critical insights into anticipated responses to climate change. For example, the seasonal transition from winter to spring is highly important in terms of annual fluxes of both water [e.g., *Kane et al.*, 1989; *Kane et al.*, 1997; *McNamara et al.*, 1997; *McNamara et al.*, 1998; *Bowling et al.*, 2003] and OM [e.g., *Finlay et al*., 2006; *Raymond et al.*, 2007; *Townsend-Small et al.*, 2011; *McClelland et al.*, 2014], with a majority of export occurring during this brief period. Although studies with a concentrated effort on sampling during the spring snowmelt have improved our estimates of OM fluxes from Arctic river systems , studies with a similar focus on late summer and fall dynamics have remained limited [e.g., *Cai et al.*, 2008; *Holmes et al.*, 2012]. As projections of a future Arctic include longer snow and ice-free free periods [*Ueyama et al.*, 2003; *Pearson et al.*, 2013] and deeper active layer thaw depths, mobilization of previously frozen soil organic material is likely to occur and would be most apparent in the late summer to early fall during maximum seasonal soil thaw extent. A greater understanding of seasonal variability of fluvial OM concentrations and composition, especially during the under-studied shoulder seasons of spring and fall, may help us better predict how these systems will respond to projected climate change.

This study focused on quantifying fluvial dissolved organic carbon (DOC) and particulate organic carbon (POC) concentrations and identifying seasonal trends throughout the hydrologic year (spring snowmelt in May through fall freeze-up in October) for six watersheds in the Alaskan Arctic. Additionally, OM carbon to nitrogen molar ratios (C:N) were used to identify potential sources contributing to both the dissolved and particulate fractions, while stable carbon isotope ratios ($\delta^{13}C$) were used to further characterize the particulate OM pool. We also employed stable oxygen isotope ratios ($\delta^{18}O$) of water as a tracer for river water sources in an effort to link hydrology with river chemistry data. While we placed a particular emphasis on sampling during the spring

snowmelt period, the seasonally comprehensive scope of our study provides an unprecedented opportunity to characterize OM concentrations and composition in Arctic river catchments during the historically under-studied late summer and fall.

## METHODS

### Study Area

The six river catchments of this study are located on the north side of the Brooks Range in Alaska, USA (Figure 1.1) and range in size from 1.7 to 608.3 $km^2$. The study sites are all within the vicinity of Toolik Field Station; approximately 250 km north of the Arctic Circle. The region north of the Brooks Range is underlain by continuous permafrost 200 to 300 m thick [*Osterkamp and Payne*, 1981; *Jorgenson et al.*, 2008]. Mean annual air temperature for the area is -8.6°C, with summer temperatures commonly between 10°C and 18°C, and winter temperatures between -30°C and -40°C typical [*Zhang et al.*, 1996]. Snowfall between September and May accounts for 30-50% of total annual precipitation in the area, which averages around 30 cm $year^{-1}$ [*Zhang et al.*, 1996, *McNamara et al.*, 1997].

According to the river catchment classification scheme of *Craig and McCart* [1975], the six study sites were divided into two groups of three; "tundra sites" and "mountain sites." The tundra sites (Kuparuk, Imnavait, and Oksrukuyik) are located in the northern foothills of the Brooks Range and have lower gradient watersheds relative to the mountain sites (Atigun, Roche, and Trevor), which are located within higher gradient mountainous terrain (Table 1.1 and Figure 1.1). It should be noted that the Roche and Trevor sites are separate sub-catchments within the larger Atigun watershed. Vegetation communities at all sites are comparable at lower elevations, although the tundra sites have

larger proportions of vegetated area compared to the mountain sites. Similarly, the tundra sites have greater proportional extents of organic-rich soil coverage compared to the mountain sites that have sizeable areas of exposed rocky uplands. Tussock-forming *Eriophorum vaginatum* dominates the vascular plant community at these sites, with non-vascular sphagnum mosses and lichens common among the inter-tussock space. Wet sedges (e.g., *Carex spp*.) and dry heath plant communities are also present, with dwarf birch (*Betula spp.*) and willow (*Salix spp.*) found extensively along stream banks and other low lying terrain [*Walker et al.*, 1989].

Although the two site types have large differences in geomorphology and landscape coverage, the general hydrology is similar across all sites. The river channels of these six basins are frozen for a large part of the year; typically from complete freeze-up in October until breakup in mid- to late May or early June. In larger Arctic rivers, the spring snowmelt period is the dominate annual hydrological event, accounting for up to three quarters of yearly runoff [*Kane et al.*, 1989; *Kane et al.*, 1997; *McNamara et al.*, 1997; *McNamara et al.*, 1998; *Bowling et al.*, 2003]. At the smaller catchments of this study, runoff from snowmelt is also a period of significant discharge accounting for a large percentage of total annual runoff. However, summer storms can produce high discharge events with peaks comparable in magnitude or even larger than those associated with spring snowmelt [*Kriet et al.*, 1992, *McNamara et al.*, 1998, *Kane et al.*, 2003]. After the large discharge pulse associated with snowmelt, base flows decrease through the summer and into the fall until freeze-up. The catchments of all sites are free from major inputs from deep springs or glaciers [*Kriet et al*., 1992; *Huryn et al.*, 2005], and subsurface flow is constrained by the presence of permafrost to the active layer, which increases in depth over the summer typically to a maximum extent of 25-40 cm [*Hinzman et al*., 1991].

**Sample Collection and Analyses**

Surface water samples were collected from all six study sites from mid-May through mid- to late October in 2009 and again in 2010. Each year, samples were collected during several two to six week long field campaigns that aimed at capturing the spring snowmelt, summer base flow, and late summer to fall freeze-up time periods. In 2009, a greater focus was placed on sampling during the winter to spring seasonal transition, while in 2010 a greater emphasis was placed on daily resolution sampling during the late summer and fall. The Kuparuk, Imnavait, Atigun, and Roche sites were sampled on a near-daily basis during scheduled sampling periods, which resulted in approximately 60 discrete daily sample collections from each site per year. The Oksrukuyik and Trevor sites were sampled at approximately weekly intervals during field sampling campaigns, yielding approximately 15 sample collections from each of these sites per year.

In the field, surface water samples were collected near each river channel's edge (i.e. within ~2 meters), but with specific sampling sites selected to draw from high flow locations. The river channels of all of the sites are relatively small, and the waters well mixed, so it was assumed that samples were representative of average river water chemistry. However, care was taken to avoid sampling of pools, backwaters, and other microenvironments that may not have been representative of bulk water chemistry. Additional precautions were taken to collect samples well upstream of each site's respective intersection with the Dalton Highway. This was done in an effort to minimize possible anthropogenic inputs and/or contamination from the road surface or from passing vehicles. It should be noted though that stretches of the Dalton Highway do intersect with portions of the Atigun and Oksrukuyik watersheds upstream of each site's respective sampling location. At the Kuparuk site, the Arctic LTER maintains an experimental

phosphorus addition stream reach, but samples were collected well upstream of that location.

Water samples were collected using a field portable peristaltic pump with MasterFlex Tygon tubing (Cole-Parmer, Vernon Hills, IL, USA), and filtered in the field using pre-cleaned 0.45 μm Versapore® membrane capsule filters (GeoTech Environmental Engineering Inc., Denver, CO, USA). Subsamples for analysis of dissolved constituents were collected in polycarbonate bottles, while subsamples for stable oxygen isotope ratios ($\delta^{18}O$) were collected in HDPE bottles. At each site, whole water samples were also collected for particulate analyses. Whole waters were collected from the subsurface using a 1 L polycarbonate bottle attached to an extendable pole sampler that was used to fill two 2 L polycarbonate bottles. After collection, dissolved constituent subsample bottles and whole water subsample bottles were transported on ice to Toolik Field Station for additional sample processing.

At Toolik Field Station, samples for DOC analyses were acidified for preservation using ultra-pure hydrochloric acid and stored at room temperature in the dark prior to analysis. Whole water samples were filtered through 25 mm pre-combusted Whatman® glass fiber filter discs (0.7 μm nominal pore size), and depending on total particulate loads, filtrate volumes ranged from 40 mL to 2000 mL. Two filters were collected; one filter for carbon analyses and one filter for nitrogen analyses. Filters were dried at 60°C for 24 hours and stored in a desiccator cabinet.

DOC concentrations were measured at the University of Texas Marine Science Institute using high temperature catalytic oxidation on a Shimadzu total organic carbon analyzer (Shimadzu Corporation, Kyoto, Japan). To ensure accuracy, a low carbon water standard and a seawater reference standard were routinely measured. When compared to consensus values, repeated measurements of standards over multiple analytical runs

resulted in a sample analysis accuracy of <5 μmol C $L^{-1}$, with instrument precision <2% based on replicate sample measurement. C:N ratios of dissolved OM were calculated using measured DOC concentrations and dissolved organic nitrogen concentration estimates presented in Chapter 2 of this dissertation.

POC concentrations and $\delta^{13}C$ values were measured at the University of Texas Marine Science Institute using a Carlo Erba 1500 elemental analyzer coupled to a Finnigan MAT Delta Plus continuous flow isotope ratio mass spectrometer (EA-IRMS). Prior to analysis, filters were acidified to remove inorganic carbon. Filters were triple acidified with sulfurous acid ($H_2SO_3$, ACS 6% $SO_2$ minimum), with a 20 minute drying period in a 60°C oven between the first two acid applications, and a 24 hour drying period after the third acid application [*Verado et al*., 1990]. PON concentrations for C:N estimates were measured on the same EA-IRMS system, but filters for nitrogen analysis were not acidified. Additionally, $\delta^{15}N$ values were measured in parallel with PON concentrations from the same filters. The PON concentration data and $\delta^{15}N$ data are provided as supplementary material in Appendix A.

Samples for analysis of stable oxygen isotope ratios of water ($\delta^{18}O$) were filtered through acid-washed 0.45 μm polypropylene filters, and then measured using Wavelength-Scanned Cavity Ringdown Spectroscopy on a Picarro L2120i (Sunnyvale, California) at the U.S. Army Cold Regions Research and Engineering Laboratory's Alaska Geochemistry Laboratory on Fort Wainwright, Alaska. Repeated analyses of five internal laboratory standards and analyses of SMOW, GISP, and SLAP standards (International Atomic Energy Agency) were used to calibrate the analytical results. Based on thousands of these standards analyses and of sample duplicate analyses precision is estimated at ± 0.2‰ for $\delta^{18}O$.

## RESULTS

Temporal variations in riverine surface water $\delta^{18}O$ values are shown in Figure 1.2. The $\delta^{18}O$ values generally increased during the snowmelt period from May through June at the tundra and mountain sites. The increase from relatively lower values observed during the spring to higher values post snowmelt was more pronounced at the tundra sites, while the increase was more gradual at the mountain sites. Through the summer and into the fall until freeze-up, $\delta^{18}O$ values were relatively constant at both site types in each study year.

Seasonal variations in fluvial DOC concentrations at the three tundra and three mountain sites are shown in Figure 1.3. Generally, the highest DOC concentrations during the hydrologic year were measured soon after the initiation of spring melt, in mid- to late May. Following snowmelt, DOC values at all sites declined from peak concentrations observed during the spring to lower values in the summer. The exception to this trend was the Imnavait site in 2010 where DOC concentrations increased from early June to early August. DOC concentrations typically declined during September and October at the Kuparuk, Oksrukuyik, and all three mountain sites. Again the exception was the Imnavait site in 2010 in which DOC concentrations increased in the late summer through the fall.

Although seasonal DOC patterns were qualitatively similar between the tundra and mountain sites, distinct quantitative differences between the site types were apparent (Figure 1.3). At all times during the sampling period, DOC concentrations were higher at the tundra sites compared to the mountain sites. During the spring freshet, peak DOC concentrations were over twice as high at the tundra sites compared to those observed at the mountain sites in 2009, and over four times as high in 2010. Differences in DOC concentrations between the two site types became even larger during the summer, with July and August DOC concentrations being over ten times as high at the tundra sites compared to the mountain sites at times. At the mountain sites, DOC concentrations were highly

comparable in 2009 and 2010, while at the tundra sites there were noticeable inter-site differences. Among the three tundra sites, Imnavait had higher peak concentrations during the spring, as well as higher average concentrations during the summer and fall. The Kuparuk and Oksrukuyik sites had similar peak DOC concentrations during snowmelt, but concentrations were typically higher at Oksrukuyik during all other periods.

In general, POC concentrations exhibited similar seasonal patterns to DOC concentrations at the Kuparuk, Oksrukuyik, and all three mountain sites (Figure 1.4). At these sites, POC concentrations were typically higher during spring snowmelt and declined thereafter. More specifically, POC concentrations decreased rapidly following the spring freshet and then continued to decline more slowly through the summer and into the fall during both years. In the summer of 2010, however, POC concentrations were more variable, with concentrations on some dates approaching or even exceeding the high values observed during snowmelt. Seasonal trends in POC concentrations at the Imnavait site were less apparent compared to the other study sites during both years. POC concentrations were typically high during snowmelt and declined after at the Imnavait site, but in 2009 POC concentrations were highly variable during the summer and fall, while concentrations displayed a distinct temporal increase from September to October in 2010.

Among the mountain sites, POC concentrations were highest at Atigun during all seasons (Figure 1.4). POC concentrations were also higher at Roche than at Trevor during the spring snowmelt period, but were similar during the remainder of the hydrologic year. Among the tundra sites, Kuparuk had higher POC concentrations during snowmelt compared to Oksrukuyik, but concentrations at Oksrukuyik were usually higher during the summer and fall. POC concentrations at Imnavait were similar to those at Oksrukuyik during the spring, but higher than both of the other tundra sites later in the summer.

Seasonal changes in DOC concentrations (Figure 1.3) were accompanied by changes in molar C:N ratios of dissolved OM at all sites in both years (Figure 1.5). C:N ratios of dissolved OM generally decreased over the spring-fall timeframe, but this seasonal shift was more clearly defined at the tundra sites than the mountain sites. Although dissolved OM C:N ratios were highly variable at the mountain sites, temporal patterns trended towards values lower than those observed at the tundra sites. At both site types, C:N ratios of dissolved OM were higher in 2009 compared to 2010 during all times from May through October. Among the tundra sites, Imnavait C:N ratios of dissolved OM were slightly higher than at either the Kuparuk or Oksrukuyik sites in the summer of 2009, although in 2010 C:N ratios were similar among all three sites. There were no consistent differences in C:N ratios of dissolved OM among the mountain sites in either study year. Dissolved OM C:N ratios were negatively correlated with surface water $\delta^{18}O$ values in 2009 and 2010 (Figure 1.6), however, as dissolved OM C:N ratios were highly variable at the mountain sites, the relationship between C:N ratios and $\delta^{18}O$ values was generally more consistent at the tundra sites.

C:N ratios of particulate OM also varied over the spring-fall timeframe, but less strongly than those of dissolved OM (Figure 1.7). In 2009, C:N ratios of particulate OM were slightly elevated (compared to summer values) at both site types. Whereas in 2010, C:N ratios increased from relatively low values during the spring to higher values in the summer and fall. Overall, C:N ratios of particulate OM were much lower than C:N ratios of dissolved OM, and were not markedly different between the tundra and mountain sites.

Temporal variations in $\delta^{13}C$ values of particulate OM were similar at the tundra and mountain sites (Figure 1.8). With the exception of a few outliers, POC $\delta^{13}C$ values tended to decrease from higher values in the spring to lower values in the summer and fall. At the tundra sites, POC $\delta^{13}C$ values decreased faster during the spring compared to the mountain

sites, but otherwise values were quantitatively similar between the different site types. Among the catchments of each site type, POC $\delta^{13}C$ values and temporal patterns were comparable, with the exception of the Atigun in 2010, which had relatively elevated $\delta^{13}C$ values during the summer compared to all other sites. POC $\delta^{13}C$ values were strongly correlated with POC concentrations at all sites during both years, with the exception of Imnavait (Figure 1.9).

## DISCUSSION

Temporal patterns in both concentration and composition of dissolved OM and particulate OM were observed at each of our study sites in both years. While generalized seasonal patterns were evident among all six sites, distinguishing quantitative and qualitative differences were apparent between the two site types. Shifts in OM quantity and quality between the spring and the summer highlight controls on the seasonality of Arctic river OM dynamics; specifically hydrology, active layer depth, and water flow paths through soils. High concentrations of both dissolved and particulate OM measured during the spring at our study sites are consistent with previous work emphasizing the importance of the snowmelt period for OM export from Arctic catchments [e.g., *Finlay et al*., 2006; *Townsend-Small et al.*, 2011; *Holmes et al*., 2012; *McClelland et al.*, 2014]. In addition to capturing the early season transition period between winter and spring, an emphasis of the current study was placed on sampling throughout the entire hydrologic year. While our early season sampling offers a point of comparison to previous work, this high resolution data set provides new insights into OM concentrations and composition during the understudied later summer and fall.

**Dissolved Organic Matter Seasonal Dynamics**

High DOC concentrations at all study sites during the spring (Figure 1.3) corresponded with low $\delta^{18}O$ values (Figure 1.2), characteristic of snowfall, reflecting the dominant influence of snowmelt on dissolved OM export at the beginning of the hydrologic year. Low $\delta^{18}O$ values, combined with the fact that soils are still largely frozen during the spring freshet, suggest that high DOC concentrations are derived from leaching of senescent vegetation and surface soils into meltwaters during this time. During the initial stages of snowmelt, frozen ground, and the snowpack itself, constrain runoff to the soil surface [*Woo*, 1986; *Kane et al*., 1989]. This temporary restriction of water to the surface and upper soil horizons, facilitates leaching of aboveground vegetation, leaf litter, and high OM content surface soils, contributing to the high DOC concentrations during snowmelt [*MacLean et al*., 1999; *Guo and Macdonald*, 2006; *Petrone et al*., 2006; *Spencer et al.*, 2008].

In addition to high dissolved DOC concentrations observed during the spring, the relatively high C:N ratios during this period (Figure 1.5) are consistent with the paradigm that dissolved OM originates from leaching of aboveground vegetation material, as well as high organic content surface litter layers and soils. Likewise, a study investigating the chemical composition of dissolved OM from the Yukon River, Alaska, reported that during the spring, the dissolved OM pool has a substantially higher proportion of vascular plant material chemical markers [*Spencer et al.*, 2008]. Additionally, incubation experiments indicate that microbial decomposition of riverine dissolved OM is highest during the spring, suggestive of a fresh labile source [*Holmes et al*., 2008]. The combination of high C:N ratios, high terrestrial plant chemical composition, high lability, and young radiocarbon age of dissolved OM exported during the spring [*Benner et al*., 2004; *Guo and Macdonald*, 2006; *Raymond et al*., 2007] indicates that the pool of dissolved OM exported

during the spring is dominated by relatively fresh, labile leachates derived from aboveground vegetation and high OM content litter and surface soils.

Observed decreases in DOC concentrations over the course of the spring and summer may be an indication of a seasonal shift in dissolved OM sources/sinks and/or export processes (Figure 1.3). The lower DOC concentrations observed post snowmelt at our study sites are accompanied by higher $\delta^{18}O$ values (Figure 1.2), reflecting an increased rainwater and/or soil-water signal from progressive seasonal thawing of the active layer. Thawing of the active layer during the spring and into the summer facilitates the flow of water through deeper soil horizons [*Woo*, 1986; *Kane et al*., 1989; *Keller et al.*, 2010; *Barker et al.*, 2014]. Compared to shallow (0-5 cm) and near surface (>5 cm) organic soil horizons in the area, which may have a carbon composition of 35 to 45%, deeper mineral soil horizons (20 cm or deeper) are a smaller source of easily leachable DOC as they typically have a carbon composition of <15% [*Mack et al*., 2004; *Guo et al*., 2007; *Shaver et al*., 2014]. As depth of the active layer extends through the summer, exposing deeper flow paths, the residence time of waters flowing through soils also increases [*McNamara et al.* 1997]. Longer soil water residence times, in conjunction with warmer soil temperatures, increases soil bacterial remineralization rates [*Nadelhoffer et al*., 1991; *Chapin et al*., 1995; *Bekku et al*., 2003], which has been shown to be a substantial OM transformation process in the area [*Kling et al.*, 2014]. Flow paths through deeper soil horizons (>20 cm) with elevated mineral content [*Mack et al*., 2004; *Shaver et al*., 2014] may also facilitate lower DOC concentrations through soil mineral particle adsorption of dissolved OM [*MacLean at al.*, 1999; *Kawahigashi et al.*, 2006; *Petrone et al.*, 2006].

Instream processing of OM is also an important consideration during the spring to summer transition. Recently, photochemical oxidation of aquatic dissolved OM has been identified as a major carbon loss pathway from Arctic inland waters; exceeding rates of

bacterial remineralization and accounting for 70-95% of total DOC processed in Arctic lakes and rivers during the summer [*Cory et al*., 2014]. In addition to complete photochemical oxidation of DOC to inorganic carbon, partial photochemical oxidation stimulates additional bacterial remineralization of dissolved OM [*Cory et al.*, 2013]. Bottle incubations suggest that bacterial remineralization of dissolved OM exported during spring snowmelt may be substantial, with losses of 20-40% measured, however, the lability of dissolved OM exported during the summer has been demonstrated to be minimal [*Holmes et al.*, 2008]. Photochemical mediated bacterial remineralization of less labile and/or recalcitrant dissolved OM may play an increasingly important role post snowmelt. Likewise, as discharge and flow rates decrease in the summer, water residence times in river channels increase resulting in longer instream microbial processing times and reductions in dissolved OM concentrations [*Peterson et al*., 1997; *Wollheim et al*., 2001].

In addition to declining DOC concentrations, decreases in C:N ratios post snowmelt also support seasonal shifts in dissolved OM sources and/or processing (Figure 1.5). High C:N ratios of dissolved OM observed in the spring at the tundra and mountain sites in 2009 and 2010 are consistent with measured C:N ratios of >40 for standing vegetation, litter, and shallow organic soil layers (<5 cm) [*Mack et al*., 2004]. Decreases in C:N ratios from spring to summer suggest that subsurface (>5 cm) organic soil horizons (C:N ratios <25) becoming an increasingly dominant dissolved OM source material [*Gersper et al*., 1980; *Mack et al*., 2004]. Additionally, autochthonous production of dissolved OM by benthic microalgae, with C:N ratios of 5-10 under optimal growing conditions [*Hillebrand and Sommer*, 1999], may make up a sizeable fraction of fluvial DOC during summer base flow conditions when transport of allochthonous dissolved OM to river channels is relatively low. Continued decreases in C:N ratios of dissolved OM through the summer and into the fall suggest that the proportion of dissolved OM exported to river channels derived from

deeper organic and mineral soil horizons (C:N ratios <20) increases, while dissolved OM from surface vegetation and organic rich soils decreases [*Gersper et al*., 1980; *Mack et al*., 2004].

The observed decreases in DOC concentrations and C:N ratios of dissolved OM at our study sites are consistent with observed reductions in discharge-normalized export of DOC from spring to summer in rivers of the North Slope and the Yukon River basin [*Striegel et al*., 2005; *Townsend-Small et al*., 2011]. Specifically, *Striegel et al.* [2005] attributes the decrease from spring to summer to increased flow path depth, water residence time, and microbial remineralization of OM within the active layer. Similarly, seasonal decreases in dissolved OM $^{14}C$ content over the course of the hydrologic year suggest an increase in older soil OM sources versus comparatively fresh vegetation and detritus [*Guo and Macdonald*, 2006; *Guo et al*., 2007; *Raymond et al*., 2007]. The relationship between $\delta^{18}O$ values and dissolved OM C:N ratios (Figure 1.6) suggests similar seasonal shifts in hydrology and OM processing control dissolved OM dynamics at our study sites. In the spring, low $\delta^{18}O$ values, indicative of a snowmelt dominated water source, correspond with high dissolved OM C:N ratios, corroborating the influence of meltwaters on leaching of vegetation and surface soils. An increase to relatively higher $\delta^{18}O$ values during the summer suggests that decreasing dissolved OM C:N ratios are associated with a shift to rain fall and soil melt water sources, supporting increased export of dissolved OM from deeper soils as seasonal thawing of the active layer increases the depth of water flow paths [*Woo*, 1986; *Kane et al*., 1989; *Keller et al.*, 2010; *Barker et al.*, 2014].

Comparable qualitative seasonal trends in DOC concentrations and C:N ratios of dissolved OM observed at the tundra and mountain sites indicate that similar dissolved OM export processes operate at both site types. However, quantitative differences in dissolved OM concentrations between the two sites types (Figure 1.3) reflect the high contrast in

organic soil stores and vegetation coverage between the tundra and mountain sites (Figure 1.1). The tundra sites have proportionally greater organic soil stores and aboveground vegetation coverage, both of which are strongly correlated with production and export of DOC in the area [*Judd and Kling*, 2002]. Similarly, lower OM soil stocks at the mountain sites are consistent with the rapid decreases in DOC concentrations observed during the spring. Assuming similar soil thaw dynamics between the two site types, the thinner organic soils at the mountain sites would result in earlier thawing of mineral soil horizons compared to the tundra sites. Earlier exposure of mineral soils at the mountain sites would result in reduced production and export of DOC due to the lower leaching potential of mineral soils with lower OM content [*Gersper et al*., 1980; *Mack et al*., 2004; *Guo et al*., 2007]. Likewise, we would expect a higher amount of adsorption of dissolved OM to mineral soil particles at the mountain sites compared to the tundra sites. Although C:N ratios of exported dissolved OM were highly variable at the mountain sites, the general trend towards values lower than the tundra sites is also consistent with lower stocks of organic-rich soil horizons and earlier thawing of mineral soils [*Gersper et al*., 1980; *Mack et al*., 2004].

Variations in DOC concentrations among the six study sites during the hydrologic year correlate well with differences in mean watershed slope values (Table 1.1); sites with lower slopes generally had higher fluvial DOC concentrations. DOC concentrations were comparable among all the mountain sites during the hydrologic year, attributable to each site having proportionally similar areas of exposed rocky uplands and lower elevation vegetated terrain. Among the tundra sites, the relationship between site geomorphological characteristics and dissolved OM concentrations also correlated well, with the lower slope Oksrukuyik site generally having higher concentrations of DOC compared to the Kuparuk site. The Imnavait site was the one exception to this relationship among the tundra sites.

Imnavait had much higher DOC concentrations than the other two tundra sites even though its mean watershed slope was intermediate relative to those sites. Observed differences in both concentrations (2009 and 2010) and seasonal patterns (2010) between the Imnavait and the other study sites may be related to the site's comparatively smaller watershed size and dissimilar stream channel geomorphology. Upstream of our Imnavait collection site, the river channel is classified as a pool-run morphology; small ponds connected by intermittingly flowing water tracks [*Arp et al.*, 2015], whereas the other five study sites are *Strahler* [1957] 3$^{rd}$ order streams or higher. Although C:N ratios of dissolved OM at Imnavait indicate similar seasonal dissolved OM source dynamics to the other study sites, quantitative and qualitative differences in seasonal DOC concentration dynamics suggest differences in dissolved OM production and/or processing rates. The smaller catchment size and unique channel morphology of the Imnavait may result in differential strengths of landscape versus stream channel dissolved OM source/sink processes compared to the Kuparuk and Oksrukuyik sites, as well as all of the mountain sites.

**Particulate Organic Matter Seasonal Dynamics**

Seasonal variations in DOC concentrations were accompanied by comparable temporal trends in POC concentrations (Figure 1.4), with high concentrations observed during the spring signaling parallel timing in transport mechanisms between dissolved and particulate OM fractions. During snowmelt, relatively high POC concentrations were accompanied by low $\delta^{18}O$ values (Figure 1.2), again pointing to meltwaters as an important conveyor of OM during this period. High energy flows and large magnitude discharge during the freshet results in a substantial amount of riverbank erosion [*Rember and Trefry*, 2004]. Additionally, whereas initial restriction of meltwaters during snowmelt results in

high dissolved OM concentrations from leaching of surface vegetation and soils, as snowmelt proceeds the subsequent movement of meltwaters across the landscape [*Woo*, 1986; *Kane et al*., 1989] supports increased particulate transport from the landscape to river channels. Decreases in POC concentrations from spring to summer at all sites were consistent with increasing $\delta^{18}O$ values (signaling a shift from snowmelt to rainwater and thawed soil waters) along with an overall decrease in river discharge post snowmelt. However, during the summer of 2010, storm activity in the area that produced discharge events similar to or greater than peak flows associated with snowmelt, resulted in elevated POC concentrations. In any case, generally low POC concentrations observed during the summer and fall until freeze-up correspond with decreases in river base flow, and are consistent with previously identified positive correlations between particulate OM concentrations and river discharge [*Guo and Macdonald*, 2006; *McClelland et al*., 2014].

POC $\delta^{13}C$ values that largely fall between -25 and -28‰ during May at all sites (Figure 1.8) suggest that particulate OM exported during this time is dominated by allochthonous terrestrial material derived from C3 vegetation [*Schell*, 1983; *O'Leary*, 1988; *Kendal et al*., 2001; *Guo and Macdonald*, 2006; *Guo et al*., 2007]. In comparison with the dissolved OM fraction, however, much lower C:N ratios of particulate OM during snowmelt (Figure 1.7) point to a highly reworked soil OM source [*Ping et al*., 1998]. This is consistent with research showing that bulk POC exported from large Arctic rivers is greater than 3000 years old during the spring, as determined by $^{14}C$ measurements [*Guo and Macdonald*, 2006; *Guo et al*., 2007].

The general decrease in POC $\delta^{13}C$ values from spring to summer suggests a seasonal shift in particulate OM sources (Figure 1.8). Lower POC $\delta^{13}C$ values observed during the summer and fall are consistent with an increase in autochthonous contributions, as $\delta^{13}C$ values less than -30‰ are indicative of *in situ* production [*Mook and Tan*, 1991;

*Finlay*, 2001]. The relationship between POC concentrations and POC $\delta^{13}C$ values (Figure 1.9) suggests that as allochthonous inputs of particulate OM subside with decreases in river flow during summer and fall, autochthonous contributions becomes increasingly dominant. C:N ratios of particulate OM are less useful for separating allochthonous and autochthonous contributions because reworked soil OM and new production within freshwater systems (i.e. phytoplankton and benthic microalgae) both have relatively low C:N ratios [*Hillebrand and Sommer*, 1999; *Mack et al*., 2004]. During periods of high particulate OM concentrations post snowmelt (e.g., summer of 2010), it is likely that the instream primary production $\delta^{13}C$ signal is masked by an increased terrestrial particulate OM load associated with storm flows. While older $^{14}C$ ages associated with soil inputs to Arctic rivers [*Schell*, 1983; *Guo and Macdonald*, 2006; *Guo et al.*, 2007] may similarly obscure a modern $^{14}C$ signal from autochthonous production, it is also possible for newly produced OM to have depleted $^{14}C$ values due to uptake of aged dissolved inorganic carbon, which can be several thousand years old in Arctic rivers [*Guo and Macdonald*, 2006]. In any case, continued decreases in $\delta^{13}C$ values from summer through fall support the conclusion that autochthonous particulate OM production becomes increasingly dominant during base flow conditions in latter periods of the hydrologic year.

In contrast to the dissolved OM pool, POC concentrations and seasonal trends were highly comparable between the tundra sites and mountain sites, in spite of large differences in organic soil coverage and watershed topography between the site types (Table 1.1 and Figure 1.4). In larger rivers of the North Slope, variations in particulate OM loads between sites were attributed to differences in catchment water yields [*McClelland et al*., 2014]. Thus, our results may imply that water yields are similar among the tundra and mountain catchments that are included in the present study. On the other hand, it is possible that total particle loads at the mountain sites are higher [*Millman and Syvitski*, 1992] and have lower

OM content (i.e., percent of total suspended solids) than the tundra sites [*Rember and Trefry*, 2004]. In this case, greater water yields at the mountain sites may compensate for lower OM content of exported particulate material.

Overall, our results show distinct seasonal variations in both the quantity and quality of fluvial OM at each of our study sites during the course of the hydrologic year. Runoff from snowmelt in the spring is accompanied by high concentrations of both dissolved and particulate OM. However, large differences in C:N ratios between the dissolved and particulate OM pools precludes a similar source material and suggests a decoupling in export mechanisms between these two fractions early in the hydrologic year. In the case of the dissolved OM pool, high C:N ratios during the spring point to relatively fresh terrestrial vegetation leachates, while low C:N ratios of particulate OM point to a bulk soil source. Declining C:N ratios of dissolved OM through the summer and into the fall are indicative of increasing contributions from deeper soils horizons and instream algal production. Although particulate OM C:N ratios displayed little seasonal variation, temporal trends in $\delta^{13}C$ values point to seasonal shifts in POC sources. Specifically, decreasing $\delta^{13}C$ values from spring through fall are consistent with increased proportional contributions of autochthonous particulate OM during base flow conditions.

## IMPLICATIONS

Warmer temperatures, altered precipitation regimes, and longer snow and ice free seasons associated with climate change have the potential to substantially alter OM cycling and export from Arctic watersheds. As a consequence, there has been a strong push by the scientific community to improve our understanding of OM dynamics in Arctic rivers during the past decade. Recent studies of OM in Arctic rivers have focused particular

attention on the spring freshet period [e.g., *McNamara et al*., 2008; *Townsend-Small et al*., 2011, *Holmes et al*., 2012; *McClelland et al*., 2014] since a large proportion of annual water discharge from river occurs during and shortly after snowmelt. However, understanding fluvial OM dynamics later in the year may also be important with respect to climate change. While export of OM from Arctic rivers during the summer and fall may be relatively small compared to during the spring, the effects of increases in seasonal active layer thaw depth, and extension of the snow and ice free seasons are more likely to be apparent during the late summer and fall when the active layer depth is at its maximum.

Previous studies characterizing sources of dissolved OM in Arctic rivers have concluded that DOC originates mainly from leachates of relatively recent terrestrial vegetation [e.g., *Benner et al*., 2004; *Neff et al*., 2006; *Guo and Macdonald*, 2006; *Guo et al*., 2007]. While our results suggest a similar source during the spring, progressive decreases in C:N ratios of dissolved OM indicate an increased contribution of OM from deeper soils during the summer and fall. Seasonal decreases in dissolved OM C:N ratios may therefore be a useful proxy for tracking landscape scale thaw. Over longer periods, a decreasing trend in late season C:N ratios of dissolved OM may signal an increase in maximum thaw depth of the active layer. Increased monitoring of dissolved OM export during the late summer and early fall merits special consideration as thawing of deeper soils, along with permafrost degradation, and permafrost subsidence, may expose previously frozen organic material to contemporary biogeochemical cycling and subsequent riverine export during this period.

Previous studies of $^{14}C$ ages of POC in Arctic rivers [e.g., *Schell*, 1983; *Guo and Macdonald*, 2006; *Guo et al*., 2007] suggest that, in contrast with DOC, the particulate fraction is composed of old, highly degraded soil material. Our C:N and $\delta^{13}C$ results from the spring are consistent with this view. In contrast to previous findings, however, the

depleted $\delta^{13}C$ values we report during the late summer and fall indicate an autochthonous (presumably modern) source becomes increasingly important. While the contribution of autochthonous production to total annual riverine particulate OM export is likely small, this relatively fresh, and presumably labile, component of the particulate pool may provide an important source of energy and nutrients to downstream ecosystems.

Recently, the fate of terrestrial-derived OM and its ecological contribution to Arctic Ocean coastal environments has received renewed attention. Early work by *Schell* [1983] using radiocarbon ages found little evidence supporting the incorporation of older terrestrial soil OM into coastal and estuarine food webs of the Alaskan Beaufort Sea. However, the results of a more recent study by *Dunton et al*. [2006] using carbon and nitrogen stable isotope ratios suggest that higher trophic organisms living in lagoons along the Alaskan Beaufort Sea coast may derive a substantial amount of their carbon requirements from terrestrial sources. The discrepancy in findings between the two studies may stem from the fact that the former did not consider the potential incorporation of terrestrial sources of dissolved OM with a predominately modern $^{14}C$ age. Similarly, although it constitutes a small portion of the total particulate OM export from rivers, it is possible that POC generated from instream production during late summer and fall contributes to the terrestrial signal in coastal food webs. In addition to providing a potential source of carbon supporting biological production in coastal systems, the flux of riverine organic nitrogen is greater than that exported as inorganic nitrogen. Subsequently, remineralization of riverine OM may be an important source of nitrogen that enhances primary productivity in nearshore and coastal Arctic ecosystems [*Tank et al*., 2012; *McClelland et al*., 2014]. Reevaluation of the potential for terrestrial OM supporting biological production in coastal Arctic ecosystems highlights that an increased

understanding of seasonal OM dynamics from Arctic rivers is essential in determining the ecological fate of exported material.

Our findings provide a direct comparison to previous investigations of OM dynamics focused on the spring and summer months from the same area as our study [e.g., *Peterson et al.*, 1986; *Townsend-Small et al.*, 2011], as well as larger river systems of the North Slope region of Alaska [*McClelland et al.*, 2014], and various pan-Arctic locations [e.g., *Raymond et al*., 2007; *Spencer et al.*, 2008; *Holmes et al.*, 2012]. While previous work on sub-Arctic catchments have focused on OM seasonality [e.g., *MacLean et al.*, 1999; *Petrone et al.*, 2006], studies with similar temporal scope are scarce in Arctic regions, specifically, those with a focus on sampling during the under-studied late summer and fall time periods. The high resolution sampling regime of our study provides a unique characterization of fluvial OM concentrations and composition from snowmelt through freeze-up in Arctic catchments. A seasonally comprehensive understanding of OM temporal trends is essential for understanding OM export dynamics of Arctic river systems, but perhaps more importantly, is critical for predicting how these systems will respond under future climate change scenarios.

Table 1.1 Watershed characteristics for Kuparuk, Imnavait, Oksrukuyik, Atigun, Roche, and Trevor basins. Latitude and longitude coordinates correspond to the locations where riverine surface water samples were collected for each basin. Area, elevation, and slope values were calculated using a digital elevation model obtained from the USGS National Elevation Dataset (ned.usgs.gov). Discharge data for Kuparuk (2009) and Imnavait (2008) provided by Douglas Kane of the Water and Environmental Research Center at the University of Alaska Fairbanks. Discharge for Oksrukuyik (2009) and Roche (2009) was calculated using site specific USGS river staff gauges and rating curves. Discharge for Atigun (2011) was obtained from the USGS at waterdata.usgs.gov (site# 15905100). Discharge for Trevor (2009) was measured using a SonTek FlowTracker (SonTek, San Diego, CA, USA).

| | **Tundra Sites** | | | **Mountain Sites** | | |
|---|---|---|---|---|---|---|
| | *Kuparuk* | *Imnavait* | *Oksrukuyik* | *Atigun* | *Roche* | *Trevor* |
| Area ($km^2$) | 134.5 | 1.7 | 71.9 | 608.3 | 83.4 | 42.4 |
| Latitude | 68° 38' 47" | 68° 37' 00" | 68° 41' 12" | 68° 27' 03" | 68° 22' 26" | 68° 17' 01" |
| Longitude | -149° 24' 34" | -149° 19' 05" | -149° 05' 50" | -149° 22' 31" | -149° 18' 45" | -149° 22' 18" |
| Mean elev. (m) | 988 | 915 | 862 | 1415 | 1542 | 1595 |
| Min. elev. (m) | 735 | 883 | 754 | 800 | 832 | 895 |
| Max elev. (m) | 1499 | 961 | 1100 | 2301 | 2286 | 2226 |
| Mean slope (%) | 11.5 | 6.9 | 5.1 | 44.6 | 51.4 | 51.8 |
| Max Q ($m^3\ s^{-1}$) | 20.9 | 0.9 | 8.6 | 103.6 | 13.6 | 2.4 |
| Mean July Q ($m^3\ s^{-1}$) | 1.9 | <0.05 | 0.2 | 22.0 | 2.3 | 0.8 |

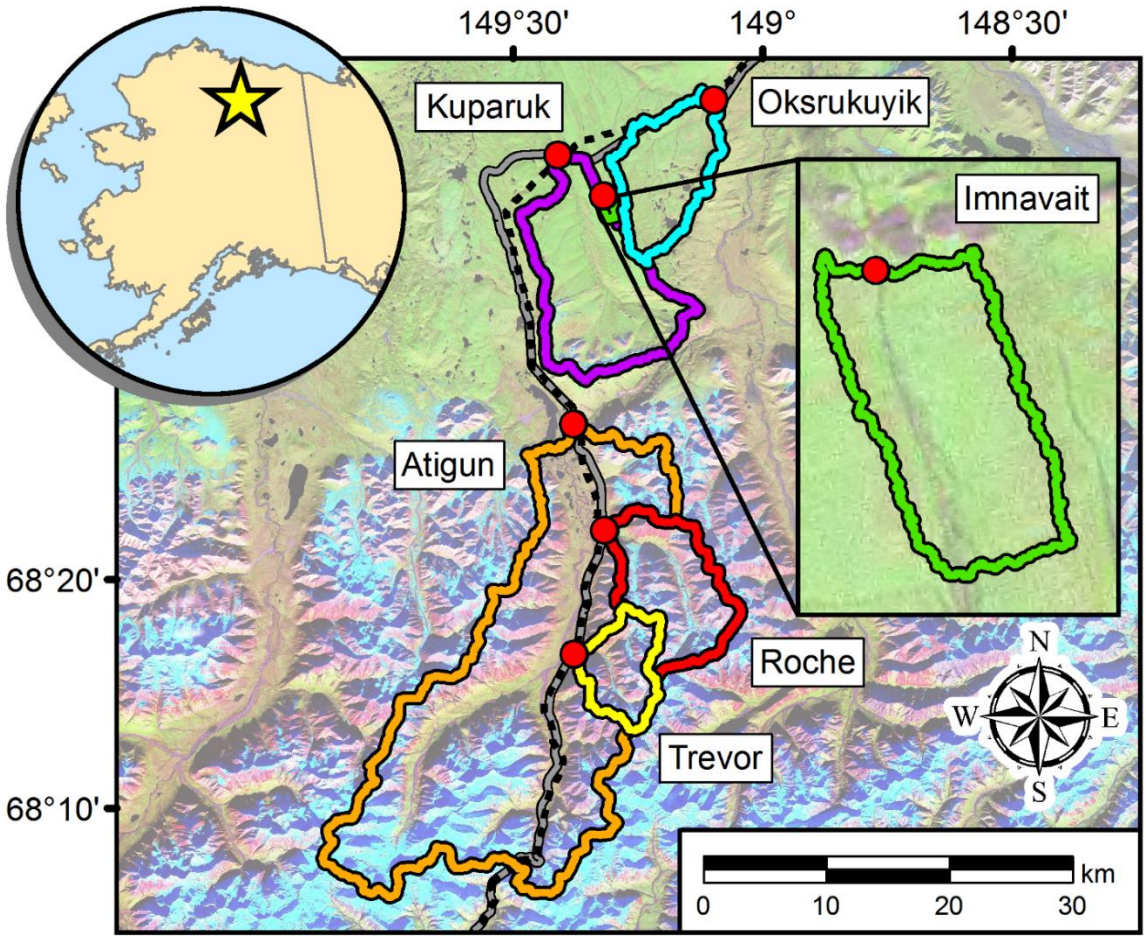


Figure 1.1 Map of the study area with delineated watershed boundaries (colored lines) and sampling locations (red circles). All watershed boundaries were delineated as the contributing area upstream from each location where river surface water samples were collected. Note that the Roche and Trevor sites are sub-catchments of the larger Atigun catchment. Map inset on the right expands the Imnavait catchment. Background imagery is a NASA multispectral Landsat false color mosaic depicting vegetation as green, bedrock and/or bare soil as pink, and snow cover as blue. The solid gray line represents the Dalton Highway and the dashed black line the Trans-Alaska Pipeline.

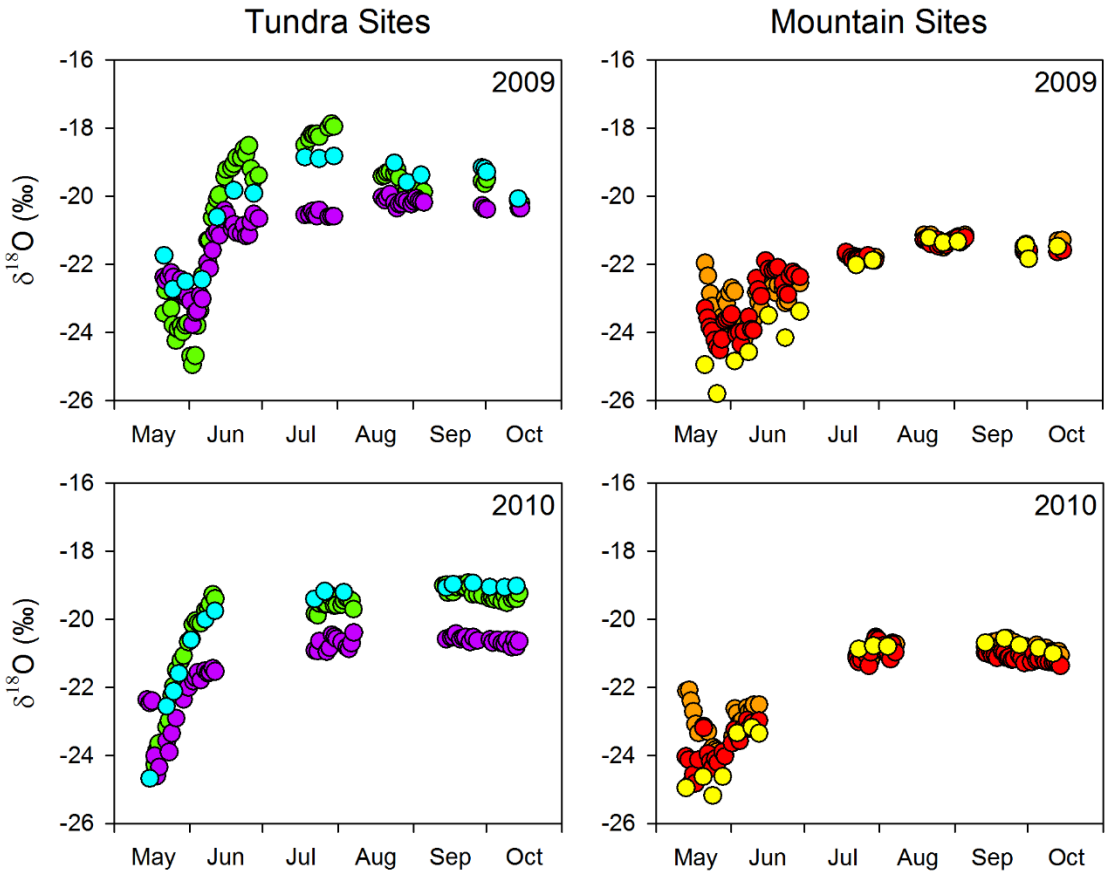


Figure 1.2. Temporal variations in $\delta^{18}O$ values of river surface waters from tundra sites and mountain sites from 2009 and 2010. Purple markers correspond to the Kuparuk, green to Imnavait, blue to Oksrukuyik, orange to Atigun, red to Roche, and yellow to Trevor.

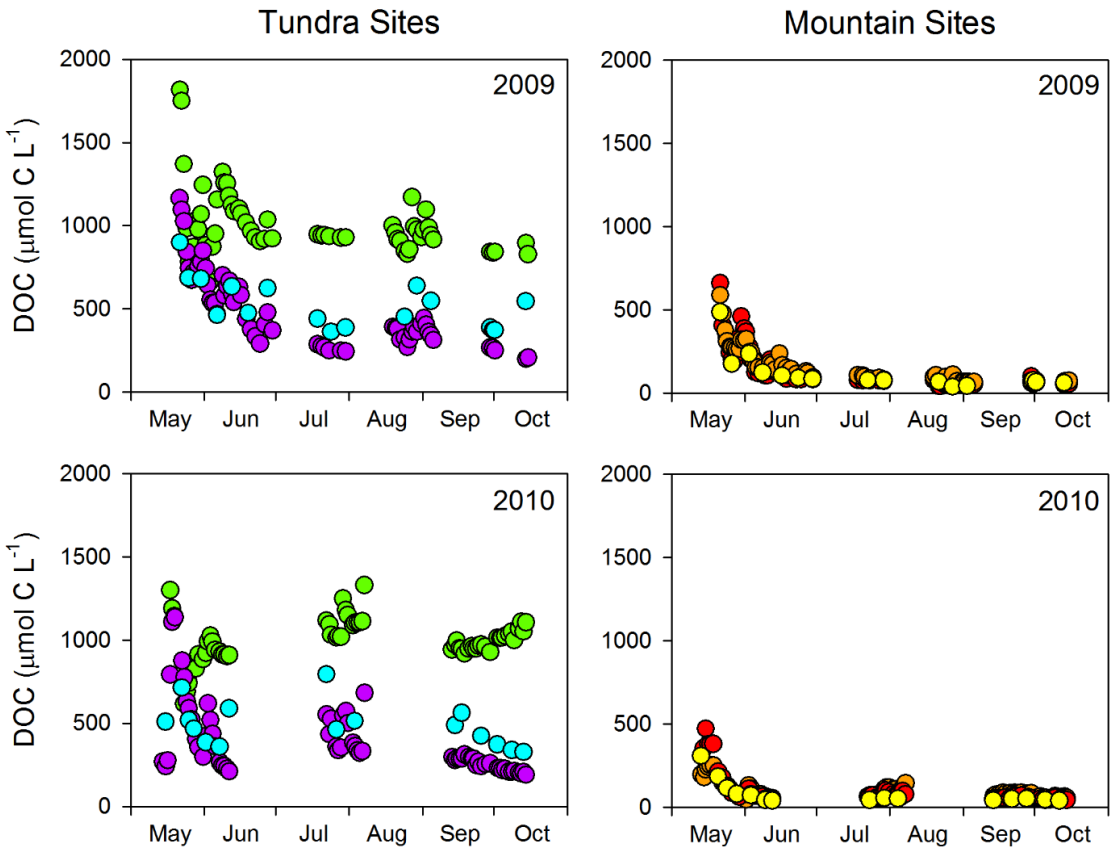


Figure 1.3. Temporal variation in DOC concentrations of riverine surface waters from tundra sites and mountain sites from 2009 and 2010. Purple markers correspond to Kuparuk, green to Imnavait, blue to Oksrukuyik, orange to Atigun, red to Roche, and yellow to Trevor.

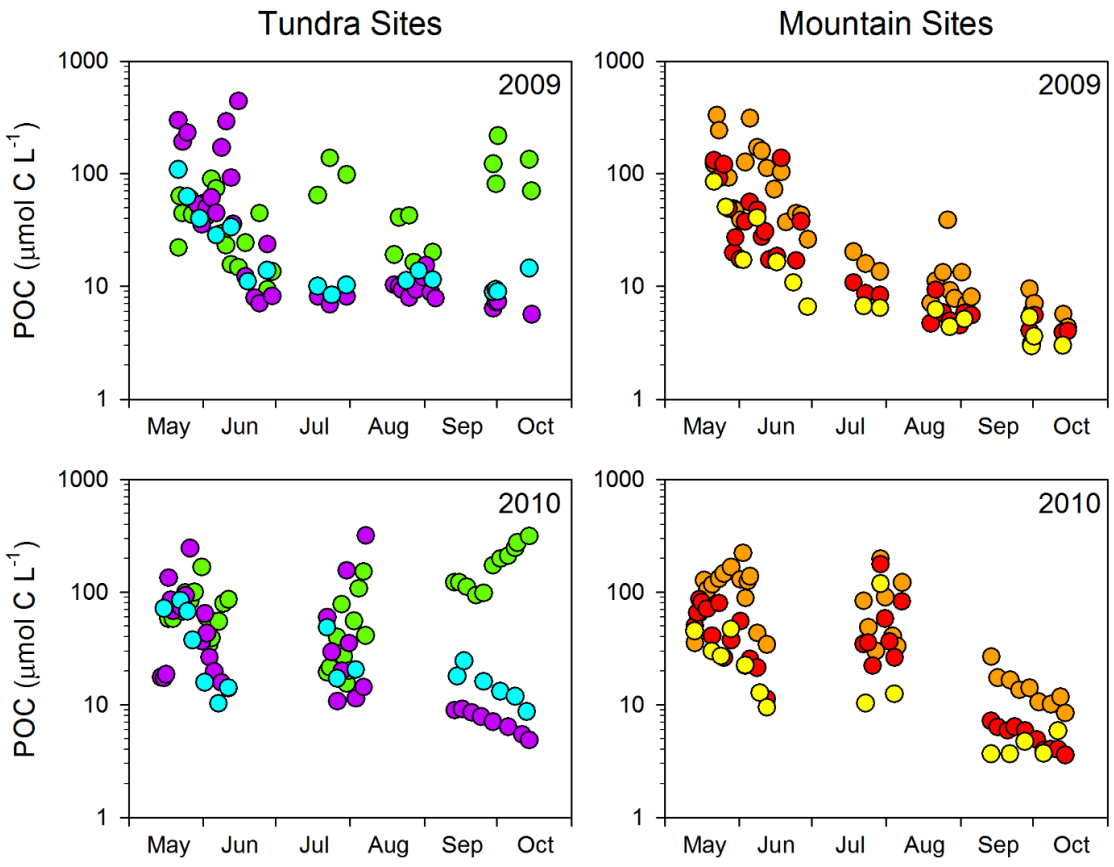


Figure 1.4. Temporal variation in POC concentrations of riverine surface waters from tundra sites and mountain sites from 2009 and 2010. Purple markers correspond to Kuparuk, green to Imnavait, blue to Oksrukuyik, orange to Atigun, red to Roche, and yellow to Trevor.

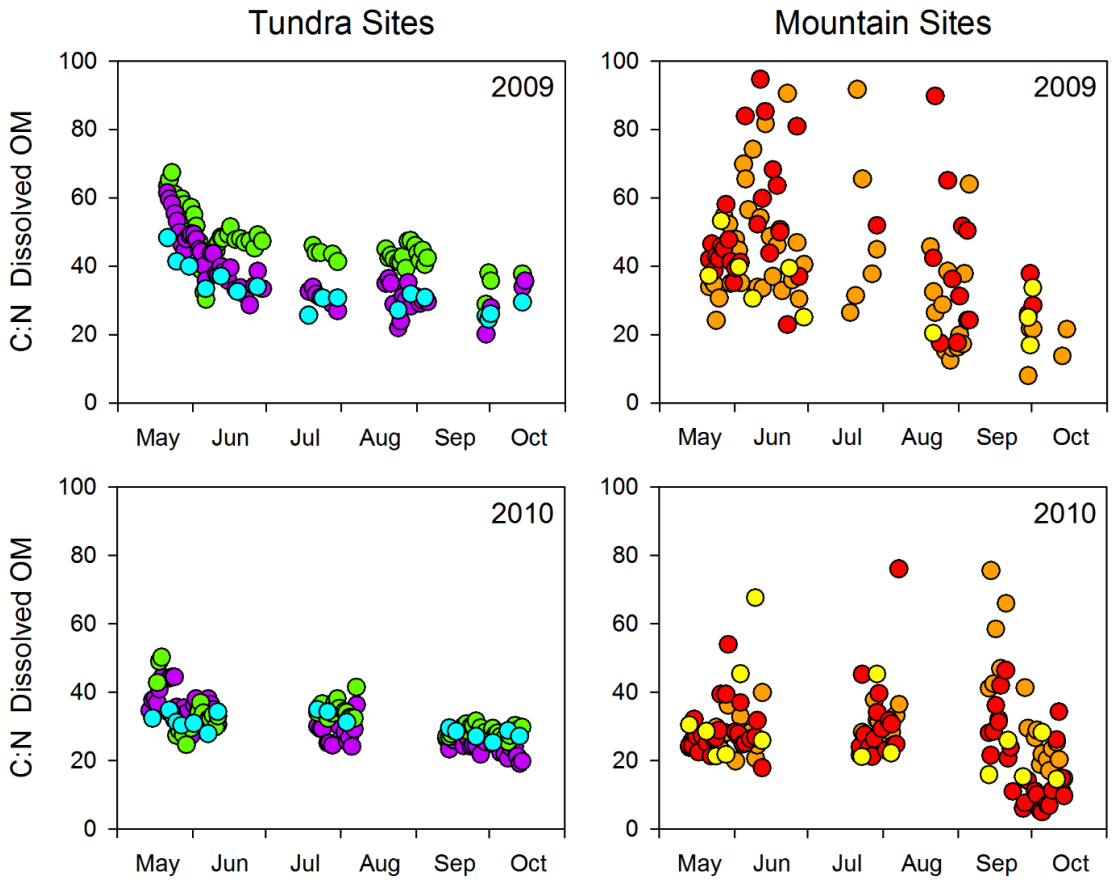


Figure 1.5. Temporal variations in C:N ratios of dissolved OM from tundra sites and mountain sites from 2009 and 2010. Purple markers correspond to the Kuparuk, green to Imnavait, blue to Oksrukuyik, orange to Atigun, red to Roche, and yellow to Trevor.

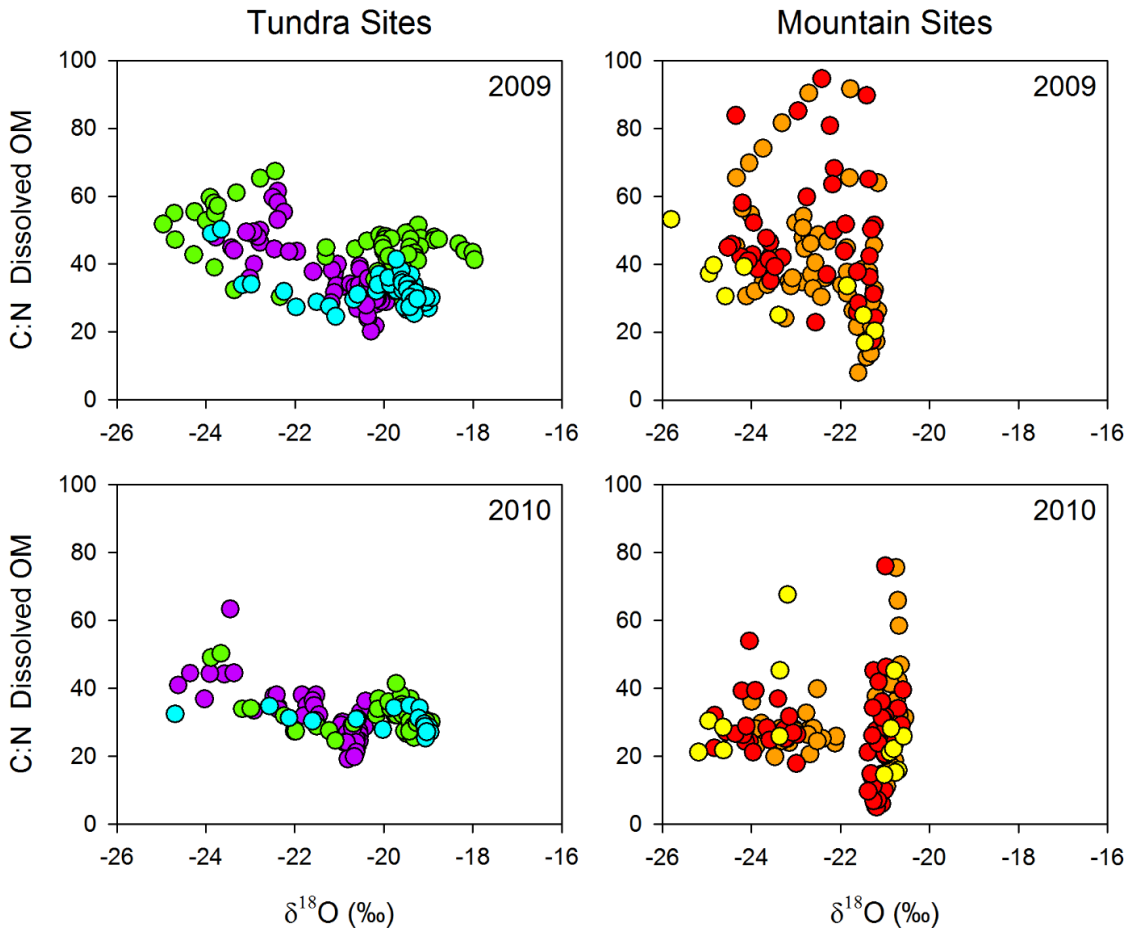


Figure 1.6. Relationship between $\delta^{18}O$ values of river surface waters and C:N ratios of dissolved OM from tundra sites and mountain sites from 2009 and 2010. Purple markers correspond to the Kuparuk, green to Imnavait, blue to Oksrukuyik, orange to Atigun, red to Roche, and yellow to Trevor.

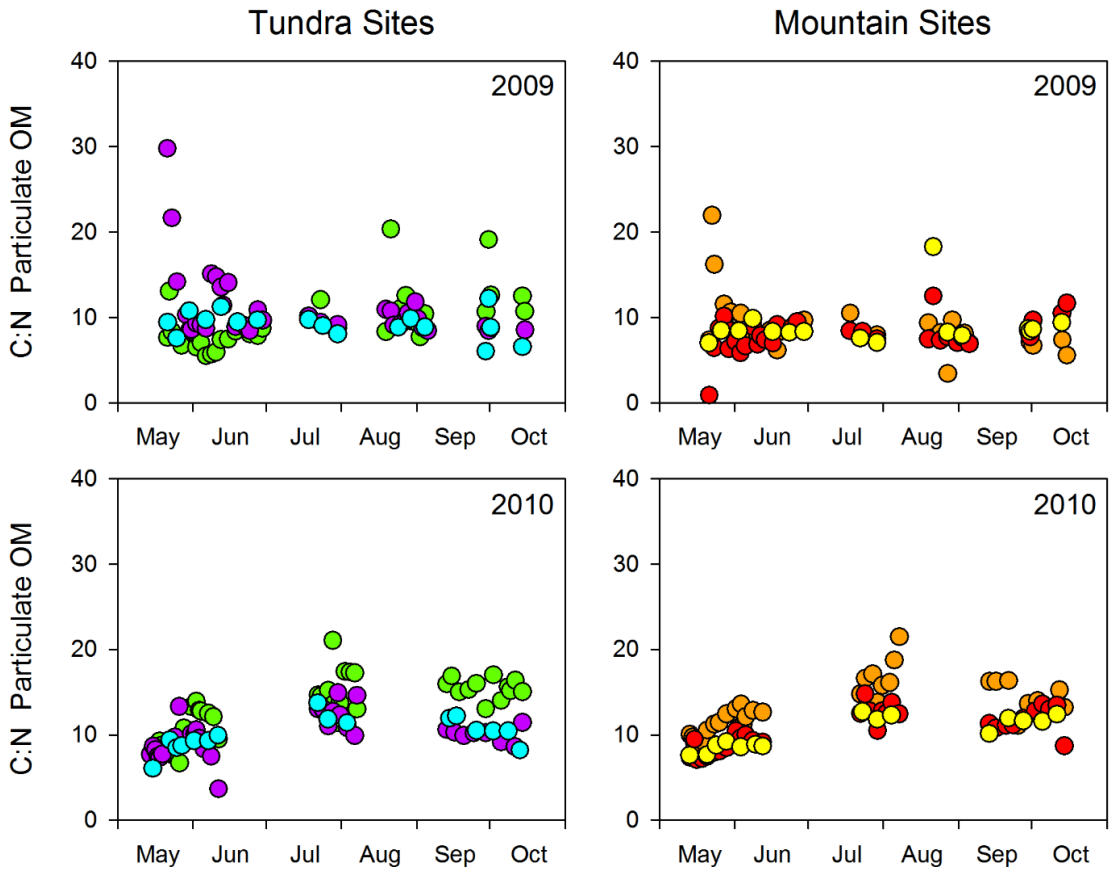


Figure 1.7. Temporal variations in C:N ratios of particulate OM from tundra sites and mountain sites from 2009 and 2010. Purple markers correspond to the Kuparuk, green to Imnavait, blue to Oksrukuyik, orange to Atigun, red to Roche, and yellow to Trevor.

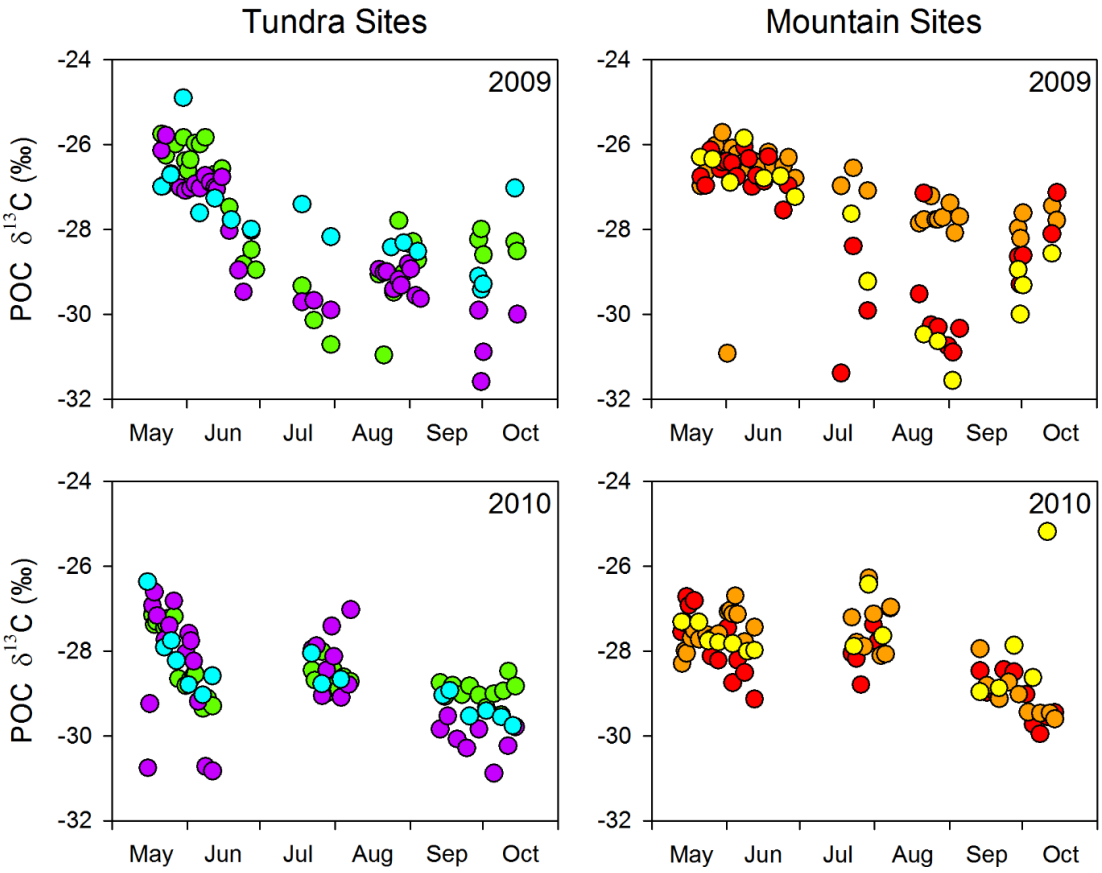


Figure 1.8. Temporal variations in $\delta^{13}C$ values of particulate OM from tundra sites and mountain sites from 2009 and 2010. Purple markers correspond to the Kuparuk, green to Imnavait, blue to Oksrukuyik, orange to Atigun, red to Roche, and yellow to Trevor.

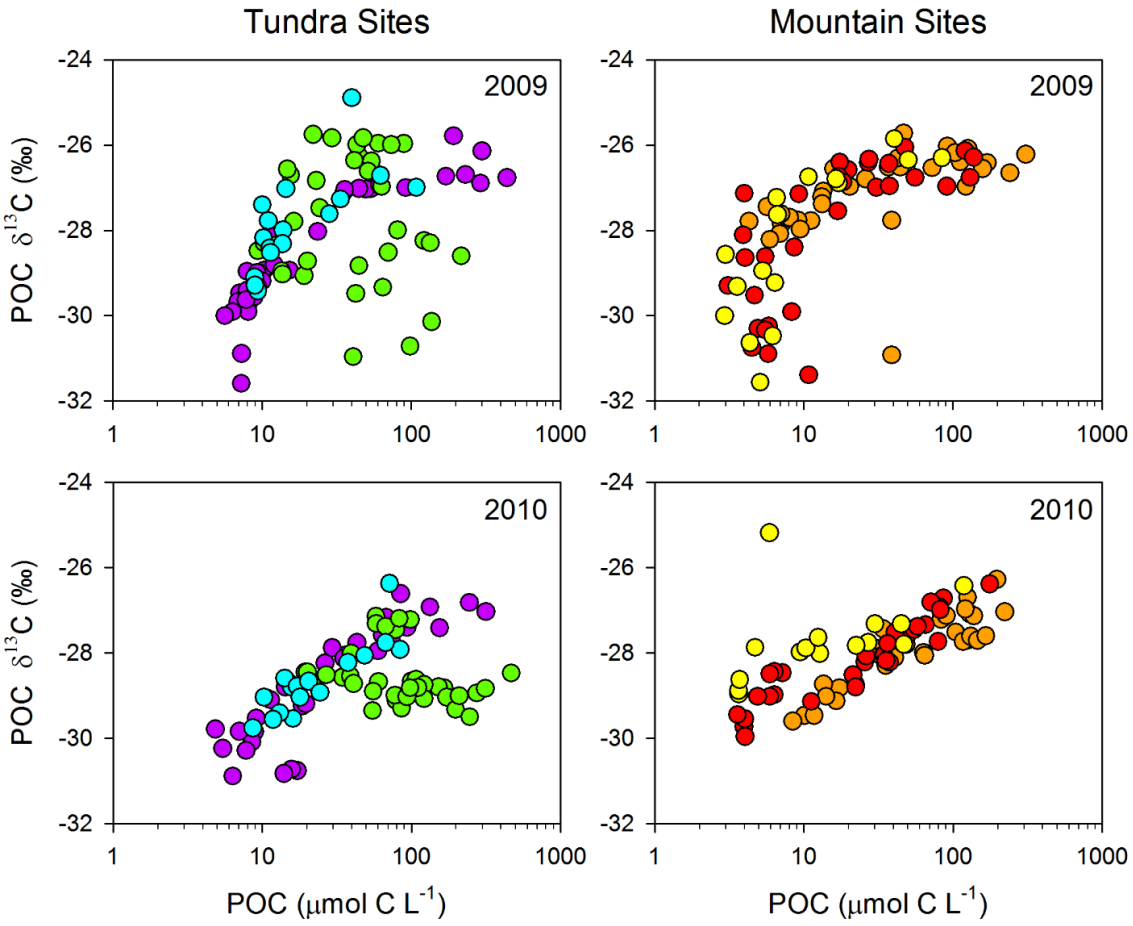


Figure 1.9. Relationship between POC concentration and $\delta^{13}C$ values of particulate OM from tundra sites and mountain sites from 2009 and 2010. Purple markers correspond to the Kuparuk, green to Imnavait, blue to Oksrukuyik, orange to Atigun, red to Roche, and yellow to Trevor.

# Chapter 2: Seasonality of dissolved nitrogen from spring melt to fall freeze-up in Alaskan Arctic tundra and mountain streams


## ABSTRACT

Predicting the response of dissolved nitrogen export from Arctic watersheds to climate change requires an improved understanding of seasonal nitrogen dynamics. Several recent studies of Arctic rivers have emphasized the importance of the spring thaw period, but studies that capture the entire hydrologic year are still rare. We examined the temporal variability of dissolved organic nitrogen (DON) and dissolved inorganic nitrogen (DIN) concentrations in six streams/rivers on the North Slope of Alaska from spring melt to fall freeze-up (May through October) in 2009 and 2010. DON concentrations were highest during peak spring melt runoff at all six sites and declined after runoff decreased. DIN concentrations were low through the spring and summer at all sites and increased markedly during the late summer and fall, primarily due to an increase in nitrate. The highest DIN concentrations occurred when the seasonally thawed active layer reached its maximum extent during the late summer and early fall. DIN-to-chloride molar ratios indicate that evaporation and/or freezing effects, as well as net increases from nitrogen sources, elevated late season DIN concentrations. Our findings suggest that penetration of water into thawed mineral soils, as well as a reduction in biological nitrogen assimilation relative to remineralization, may increase DIN export from Arctic watersheds during the late summer and fall. While this is part of a natural cycle, improved understanding of seasonal nitrogen dynamics is particularly important now because warmer temperatures in the Arctic are causing earlier spring snowmelt and later fall freeze-up in many regions.

## INTRODUCTION

Impacts of warming in the Arctic include changes to the hydrologic cycle, longer snow-and-ice free seasons, and widespread permafrost degradation [*White et al.*, 2007; *Romanovsky et al.*, 2010]. These and other responses have altered the quantity, seasonality, and flow paths of water in Arctic river catchments, and these changes are expected to intensify over the coming decades with a projected warmer climate [*Peterson et al.*, 2002; *Peterson et al.*, 2006; *Holland et al.*, 2007; *Rawlings et al.*, 2010]. Tight coupling between catchment hydrology and biogeochemistry has been observed at a variety of scales and locations throughout the Arctic [*Raymond et al.*, 2007; *McNamara et al.*, 2008; *Townsend-Small et al.*, 2011; *Holmes et al.*, 2012; *McClelland et al.*, 2014], and thus changes in hydrologic conditions are expected to cause changes in seasonal, as well as annual, fluxes of river-borne constituents from catchments [*Frey and McClelland*, 2009]. While considerable attention has been paid to how climate change will affect carbon export from high latitude river catchments [e.g., *Frey and Smith*, 2005; *Striegl et al.*, 2005; *Guo et al.*, 2007; *Raymond et al.*, 2007; *Walvoord and Striegl*, 2007], fewer studies have addressed impacts on nitrogen export from the same systems. Changes in fluvial export of particulate and dissolved nitrogen fractions, in both inorganic and organic forms, are of particular interest because they serve as important resources for downstream Arctic freshwater [e.g., *Levine and Whalen*, 2001; *MacIntyre et al.*, 2006; *Gettel et al.*, 2013] and estuarine ecosystems [e.g., *Amon and Meon*, 2004; *Tank et al.*, 2011; *McClelland et al.*, 2014].

Understanding how fluvial nitrogen export in Arctic watersheds will respond to future climate change scenarios remains uncertain, particularly in regards to the magnitude and form of nitrogen export. In rivers of Western Siberia, the results from *Frey et al*. [2007] suggest that dissolved organic nitrogen export (DON) will increase with warming and loss of permafrost. Similarly, studies in central Alaska that used space-for-time

substitution to investigate the effect of permafrost loss on nitrogen export found that watersheds with discontinuous permafrost coverage exported more nitrogen than watersheds with either continuous or low to no permafrost coverage [*Jones et al.*, 2005; *Petrone et al.*, 2006]. These results suggest that permafrost thaw and degradation may increase nitrogen export from permafrost-influenced watersheds as previously frozen material is exposed to contemporary biogeochemical processing and subsequent export. However, exposure of deeper mineral soils from a deepening of the seasonally thawed "active" layer, associated with widespread permafrost thaw and degradation, may yield decreased organic nitrogen export through adsorption and remineralization of DON [*MacLean et al.*, 1999; *Petrone et al.*, 2006], with an increase in the export of inorganic nitrogen [*Harms and Jones*, 2012].

Owing to a lack of quality-controlled long-term chemistry data from rivers in the Arctic [*Holmes et al*., 2000; *Holmes et al*., 2001], direct examination of nitrogen flux trends has been relatively limited. Data from the upper Kuparuk River that have been collected at the Arctic Long Term Ecological Research site (Arctic LTER; http://ecosystems.mbl.edu/ARC/) in Alaska since the late 1970s provide one exception. An analysis of these data found that nitrate export was relatively stable thorough the 1980s, then increased by roughly five fold between 1991 and 2001 [*McClelland et al*., 2007]. While the increase in nitrate export from the Kuparuk watershed was mainly a result of increasing nitrate concentrations from May through September, the underlying mechanism responsible for the observed concentration increases remains unresolved, but may be a result of regional warming induced changes to soils and vegetation. Although data from the Kuparuk represents one of the few long-term Arctic river water chemistry records, sampling at the Arctic LTER has, however, primarily been focused during summer months (June-August). A lack of sampling during the spring freshet and the late summer through

fall highlights a gap in knowledge pertaining to seasonal controls on fluvial nitrogen export dynamics. These seasonal transitions are critical for Arctic biogeochemical processes and nutrient exports from watersheds. The spring snowmelt period is associated with up to three quarters of the yearly annual runoff in Arctic watersheds [*Kane et al*., 1989; *Kane et al*., 1997; *McNamara et al*., 1997; *McNamara et al*., 1998; *Bowling et al*., 2003]. In addition, the timing of spring melt and fall freeze-up in the Arctic is shifting such that a longer growing season is projected in the future [*Ueyama et al*., 2003; *Pearson et al*., 2013].

An improved understanding of the seasonal dynamics of both organic and inorganic nitrogen concentrations is fundamental for determining how nitrogen export from Arctic river systems will respond to future climate change. Data from the historically under-studied shoulder seasons of spring and fall may be especially important, as the impacts to biogeochemical processes are likely most apparent during an earlier spring melt transition from winter to summer, and in the late summer to early fall when the extent of the seasonally thawed active layer reaches its maximum depth. Projections for the future Arctic indicate deeper active layers [*Jorgenson et al.*, 2006] and this could affect soil and stream biogeochemistry. While knowledge of the seasonal dynamics of water-borne constituents in Arctic rivers has improved over recent years, especially during the spring freshet as studies have made a concentrated effort to sample during snowmelt [e.g., *Raymond et al.*, 2007; *Townsend-Small et al.*, 2011; *McClelland et al.*, 2014], sampling during late summer and into fall until freeze-up has remained limited [e.g., *Cai et al.*, 2008; *Holmes et al.*, 2012].

In this study we focused on identifying seasonal patterns of DON and DIN concentrations during the entire hydrologic year from spring snowmelt through fall freeze-up (May to October) for six watersheds in Arctic Alaska. A major emphasis was placed on daily sampling during the spring snowmelt period, as well as during the late summer

and into the fall until freeze up. Nitrogen-to-chloride ratios were used to assess whether changes in late season DON and DIN concentrations reflect physical concentration of dissolved constituents (i.e., evaporation and/or freezing effects) or changes in biogeochemical processing. Additionally, we compared daily resolution water chemistry data to soil temperature data from one of our study sites in an effort to describe how seasonal variations in DON and DIN concentrations relate to seasonal thaw layer thermal dynamics. The high resolution DON and DIN concentration data presented here offer a contemporary point of comparison to earlier work conducted on these systems during the spring and summer, but more importantly, this work contributes new information about seasonal nitrogen dynamics during the historically under-sampled late summer and fall.

## MATERIALS AND METHODS

### Study Area

This study focuses on six river catchments located on the north side of the Brooks Range in Arctic Alaska approximately 250 km north of the Arctic Circle in the vicinity of Toolik Field Station (Figure 2.1). The study catchments range in size from 1.7 to 608.3 $km^2$ (Table 2.1) and all are free of major inputs from deep springs or glaciers [*Kriet et al*., 1992; *Huryn et al.*, 2005]. The region is underlain by continuous permafrost that is approximately 250 m thick and minimizes interactions between surface waters and deep groundwater [*Osterkamp and Payne*, 1981; *Hinzman et al*., 1991; *Jorgenson et al.*, 2008]. The presence of permafrost constrains subsurface flow to the seasonal surface soil thaw layer, which increases in depth over the summer typically to a maximum extent of 25-40 cm [*Hinzman et al*., 1991].

The rivers of all six study catchments are frozen for a large portion of the year; usually from river freeze-up in late September to October until snowmelt and breakup in mid- to late May or early June. Discharge from spring snowmelt is the dominant hydrologic event at these sites, often accounting for a significant proportion of total annual discharge [*McNamara et al.*, 1998]. After the spring snowmelt period, base flow decreases through the summer and into the fall until freeze-up. However, at all of the study sites, summer storms can produce high discharge events with peaks comparable in magnitude or even larger than those associated with spring snowmelt [*Kriet et al.*, 1992, *McNamara et al.*, 1998, *Kane et al.*, 2003].

Precipitation in the area is around 30 cm $year^{-1}$, with snowfall between September and May accounting for 30-50% of the total annual precipitation [*Zhang et al.*, 1996, *McNamara et al.*, 1997]. The mean annual air temperature is -8.6°C, with summer temperatures commonly ranging between 10°C and 18°C, and winter temperatures typically between -30°C and -40°C [*Zhang et al.*, 1996]. Vegetation communities are comparable at all the catchments (although the proportions of vegetated to non-vegetated area are not), with tussock-forming *Eriophorum vaginatum* dominating the vascular plant community and sphagnum mosses and lichens the non-vascular plant community. Wet sedges (e.g., *Carex spp*.) and dry heath are also common, with dwarf birch (*Betula spp.*) and willow (*Salix spp.*) found along stream banks and other low lying terrain [*Walker et al.*, 1989].

Study sites are divided into two groups of three according to the river catchment classification scheme of *Craig and McCart* [1975]. The Kuparuk, Imnavait, and Oksrukuyik watersheds are classified as "tundra sites," while the Atigun, Roche, and Trevor watersheds are classified as "mountain sites." The tundra sites are relatively lower gradient catchments (Table 2.1) located in the northern foothills of the Brooks Range.

They have a higher proportion of vegetation coverage and larger extents of organic-rich soils compared to the mountain sites, which are located within the higher gradient terrain of the Brooks Range. At lower elevations within the mountain sites, vegetation communities and soils are similar to those of the tundra sites, however there is comparatively less vegetation coverage and lower stocks of organic soils owing to the larger area of exposed rocky uplands. It should be noted that the three mountain sites are nested; the Roche and Trevor sites are separate sub-catchments within the larger Atigun watershed. The morphological and land-cover differences between the two site types can be seen visually in Figure 2.1, where green areas (vegetation) account for a much larger proportion of coverage in the tundra watersheds compared to the mountain watersheds where bedrock and bare soils (pink areas) dominate.

**Sample Collection and Analyses**

Surface water samples were collected from mid-May through mid-October in 2009 and 2010. In 2009, samples were collected during field campaigns that captured spring snowmelt, summer base flow, and late summer to fall freeze-up conditions. In 2010, sampling was also conducted in order to capture the spring snowmelt and summer base flow periods, but a greater emphasis was placed on sampling during the late summer and fall. Surface waters were collected from the Kuparuk, Imnavait, Atigun, and Roche sites on a near-daily basis during scheduled sampling periods, resulting in approximately 60 discreet samples collected from each site per year. The Oksrukuyik and Trevor sites were sampled on a weekly basis during scheduled sampling periods, yielding approximately 15 discrete samples from each site per year.

Care was taken to collect surface waters upstream from each sampling site's respective intersection with the Dalton Highway to minimize possible anthropogenic inputs from the road. However, it should be noted that the highway does run through/along upper portions of the Atigun and Oksrukuyik drainage areas (Figure 2.1). At the Kuparuk site, the point where samples were collected was well upstream of the location of the Arctic LTER experimental phosphorus addition stream reach.

Surface waters were collected at each site using MasterFlex Tygon tubing connected to a field portable peristaltic pump (Cole-Parmer, Vernon Hills, IL, USA). Water was collected from well mixed stream channel sections with precaution taken to avoid collecting from pools, backwaters, and other microenvironments that may not have been representative of bulk river water chemistry. All samples were filtered in the field using pre-cleaned 0.45 μm Versapore® membrane capsule filters (GeoTech Environmental Engineering Inc., Denver, CO, USA). Subsamples for total dissolved nitrogen (TDN), nitrate + nitrite ($NO_3^-$ + $NO_2^-$), and ammonium ($NH_4^+$) were collected into polycarbonate bottles, while chloride ($Cl^-$) subsamples were collected into high-density polyethylene (HDPE) bottles. "Nitrate" and "$NO_3^-$" are used to refer to nitrate + nitrite throughout the manuscript because nitrate is the dominant form. Samples were transported on ice to Toolik Field Station (TFS) for additional processing and storage. TDN and $NO_3^-$ samples were preserved by acidification with ultra-pure hydrochloric acid and then kept in the dark prior to analysis. $NH_4^+$ samples were filtered using 0.2 μm nylon membrane syringe tip filters into HDPE bottles and stored cold and in the dark prior to analysis.

TDN samples were analyzed at the University of Texas Marine Science Institute (UTMSI) on a Shimadzu total organic carbon analyzer fitted with a total nitrogen module for chemiluminescence detection of nitrogen (Shimadzu Corporation, Kyoto, Japan). $NO_3^-$ was measured colorimetrically at UTMSI using the cadmium reduction method described

by *Jones* [1984] modified for a BioTek μQuant microplate spectrophotometer (BioTek Instruments Inc., Winooski, VT, USA). Dissolved $NH_4^+$ concentrations were determined according to the *Holmes et al.* [1999] orthophthaldialhyde method using a Turner 10AU fluorometer (Turner Designs, Sunnyvale, CA, USA). In 2009, $NH_4^+$ measurements were made at TFS, but in 2010 $NH_4^+$ measurements were made at UTMSI. $Cl^-$ samples were analyzed on a Dionex ICS-3000 ion-chromatograph (Dionex Corporation, Sunnyvale, CA, USA) at the U.S. Army Cold Regions Research and Engineering Laboratory's Geochemistry Laboratory in Fairbanks, Alaska following methods presented in *Douglas et al*., [2013].

DIN concentrations were calculated as the sum of $NO_3^-$ and $NH_4^+$ concentrations, with DON concentrations calculated as the difference between TDN and DIN. In the latter half of 2009 (July through October), we were unable to obtain dissolved $NH_4^+$ concentrations as laboratory facilities necessary to run samples at TFS were closed by early August. When dissolved $NH_4^+$ concentration data were unavailable, DON concentrations were calculated as the difference between TDN and $NO_3^-$ alone. It is acknowledged that missing ammonium values add uncertainty to estimates of DIN and DON concentrations. However, with the exception of Imnavait in the fall of 2010 (where $NH_4^+$ concentrations approached 20 μmol N $L^{-1}$ and the DIN pool was nearly exclusively comprised of $NH_4^+$), measured concentrations of $NH_4^+$ never exceeded 1.0 μmol N $L^{-1}$ and values were typically <0.3 μmol N $L^{-1}$. DON concentrations calculated with and without $NH_4^+$ (where $NH_4^+$ data were available) resulted in only small changes to DON concentration estimates. For the tundra sites (excluding Imnavait September and October 2010 sampling dates) and mountain sites, maximum differences between DON concentrations calculated with and without $NH_4^+$ were 2.0% and 4.5% respectively. The low ammonium concentrations recorded at most sites are consistent with findings that nitrification in river channels in the

area is quite active, with $NH_4^+$ being converted to $NO_3^-$ within a few hundred meters [*Wollheim el al.*, 2001].

**Nitrogen-to-Chloride Molar Ratios**

Water discharge data can be used in combination with concentration data to elucidate whether temporal shifts in riverine constituent concentrations result from changes in mass fluxes, or dilution/concentration of temporally stable constituents due to seasonal variations in evaporation and/or freezing effects. A lack of continuous discharge measurements spanning the entire hydrologic year at any of our six study sites during either 2009 or 2010 preclude us from using this approach. As an alternative, examining nitrogen-to-chloride molar ratios ($N:Cl^-$) can help separate dilution/concentration effects from net changes in constituent source contributions associated with biogeochemical cycling. $Cl^-$ is considered conservative within aquatic environments with comparatively minimal involvement in biogeochemical and/or geochemical processes compared to most common ions [*Feth*, 1981]. Thus, shifts in dissolved $N:Cl^-$ ratios can be used as evidence of changes in dissolved nitrogen export.

**Soil Thermistor Arrays**

In April 2010 three thermistor arrays were installed in the Imnavait watershed (Figure 2.1) to record soil temperature at various depths throughout the year. On each array, four thermistors were attached to a wooden stake that was placed into a 10 cm diameter hole drilled with a SIPRE auger. Arrays 1 and 2 were installed in the floodplain of the Imnavait watershed and had individual thermistors set at 0, 28, 42, and 55 cm below the ground surface. Array 3 was installed on a hillslope within the watershed with

thermistors set at depths of 0, 12, 24, and 30 cm below the ground surface. After each thermistor array was positioned in the excavated hole, a slurry of local soil and water was used to fill the remaining air space. On each array, thermistors were connected to a battery powered ONSET-HOBO U12 data logger (Onset Computer Corporation, Bourne, MA, USA) that recorded hourly measurements in Celsius. All three thermistor arrays were deployed until September 2011.

## RESULTS

### Soil Thermal Regime

The soil thermal regime is exemplified by data from thermistor array 2 (Figure 2.2). Data from the other two thermistor arrays followed similar patterns. Temperatures at all measured soil depths were below 0°C in April, and rising air temperatures and melting of the snowpack in mid-May were reflected as an increase in temperature from the thermistor located at the soil surface (0 cm). Although thawing of surface soils was initiated in mid- to late May, soils at the 28 cm thermistor depth did not thaw until early June, and thawing of deeper soil layers at 42 and 55 cm deep did not occur until early July and mid-August, respectively. Surface soils were the first to freeze in the fall, with soils at the surface and 28 cm freezing in mid- to late September. During the fall, Arctic soils begin to freeze from the bottom up as well. The 55 cm soil layer began to freeze in early October, but soils at 42 cm remained thawed until mid-November.

### Stream Water Chemistry

DON concentrations at the three tundra sites (Figure 2.3a, c) and the three mountain sites (Figure 2.3b, d) peaked during snowmelt in mid- to late May and then decreased

following the spring melt period in both years. At the Kuparuk and Oksrukuyik sites, and all of the mountain sites, DON concentrations decreased through the spring post-snowmelt peak until reaching summer baseline values in June. DON concentrations began to decrease in the late summer (August and September) at the Kuparuk and Oksrukuyik sites, with values declining until freeze-up. DON concentrations increased slightly in late September and early October at the mountain sites, but then subsequently decreased in early to mid-October until freeze up. At Imnavait, DON concentrations gradually increased throughout the summer and into the fall, with this trend being much more pronounced in 2010 than in 2009.

Although seasonal DON concentration patterns were qualitatively similar between the two different site types, quantitative differences were observed between the mountain and tundra sites, as well as distinct differences among the three tundra catchments. Tundra sites had much higher DON concentrations compared to the mountain sites during all periods of the hydrologic year in both 2009 and 2010 (Figure 2.3). During snowmelt, DON concentrations were nearly twice as high at the tundra sites compared to the mountain sites, with the differences becoming more apparent after the spring DON peak when concentrations at the mountain sites were typically $<3.5$ μmol N $L^{-1}$ throughout the summer and fall. Among the mountain sites, DON concentrations were comparable during all seasons, whereas among the tundra sites, Imnavait had higher DON concentrations during all times of the year compared to Kuparuk and Oksrukuyik. While peak DON concentrations during spring melt were similar at Kuparuk and Oksrukuyik (Figure 2.3a, c), summer and fall concentrations were typically higher at Oksrukuyik.

Qualitatively similar seasonal trends in DIN concentrations were seen between the tundra and mountain sites; relatively low DIN concentrations were observed during the spring and early summer, with concentrations increasing during the late summer and into

the fall (Figure 2.4). With the exception of Imnavait in 2010, the observed increases in DIN concentrations reflect an increase in the $NO_3^-$ fraction of the DIN pool. The DIN concentration increase at Imnavait during the fall of 2010 was entirely attributable to an increase in $NH_4^+$, whereas both nitrate and ammonium concentrations remained relatively low throughout 2009. It is possible that we did not observe a DIN concentration increase at Imnavait during the late summer and fall in 2009 because we were unable to measure $NH_4^+$ during that sampling period. However, TDN concentrations at Imnavait did not increase in 2009 during this time. DIN concentrations may have increased concurrently with decreasing DON concentrations, resulting in no net change in TDN concentrations, but given that $NH_4^+$ was not measured, we are unable to make this distinction.

Though seasonal trends in DIN were generally similar between the two different site types, there was a noticeable distinction in the timing of DIN concentration increases, as well as a pronounced difference in the magnitude of the increases between the tundra and mountain sites during both study years (Figure 2.4). DIN concentrations at the tundra sites were typically lowest during May and June, increased gradually in July and August, and exhibited marked concentration increases in mid- to late September that continued through October (Figure 2.4a, c). As previously mentioned, the one exception to this generalized seasonal trend was Imnavait in 2009, where only a minimal increase in fall DIN concentrations from spring and summer values was observed. In 2009, late season DIN concentrations among the tundra sites were highest at Kuparuk, followed by Oksrukuyik, then Imnavait, while in 2010, DIN concentrations were highest at Imnavait, with concentrations being comparable between the Kuparuk and Oksrukuyik sites.

At all three mountain sites, increases in DIN concentrations occurred soon after sampling began in May (Figure 2.4b, d). DIN increases were similar in timing and magnitude from May through July at all three mountain sites in both years, with

concentrations increasing by approximately 10 μmol N $L^{-1}$ over the early part of the hydrologic year. From August to October, increases in DIN concentrations were much more pronounced. There were considerable differences in the magnitude of DIN increases among the mountain sites, with DIN concentrations in August, September, and October highest at Trevor, followed by Roche, and then Atigun. At all three mountain sites, late season DIN concentrations were higher in 2010 compared to 2009.

Distinct seasonal trends in DON-to-$Cl^-$ molar ratios (DON:$Cl^-$) were observed between the tundra sites and mountain sites in both sampling years (Figure 2.5). At the mountain sites, DON:$Cl^-$ ratios generally decreased over the course of the hydrologic year from maximum values observed in May and June to minimum values in September (Figure 2.5b, d). Temporal DON:$Cl^-$ trends were not as clearly defined at the tundra sites. DON:$Cl^-$ ratios generally increased from May to June, but seasonal trends were variable among sites and between years during the latter part of the hydrologic year from July through October (Figure 2.5a, c). Among the three tundra sites, DON:$Cl^-$ ratios were higher at the Kuparuk and Imnavait sites, while DON:$Cl^-$ ratios at Oksrukuyik were comparable to those observed at the mountain sites.

At both the tundra and mountain sites there were rapid increases in DIN-to-$Cl^-$ molar ratios (DIN:$Cl^-$) from May to June (Figure 2.6). From June to October, trends in DIN:$Cl^-$ ratios mirror those of DIN concentrations at the tundra sites; lower values were observed in June and July with large increases beginning in September and continuing through freeze-up in October (Figure 2.6 a, c). DIN:$Cl^-$ seasonal trends at Kuparuk and Oksrukuyik were similar in both years, while differences between study years at Imnavait were driven by late season DIN concentration increases that were observed in 2010, but not in 2009 (Figure 2.6 a, c). At the mountain sites, DIN:$Cl^-$ ratios generally increased

from June through August, with smaller changes observed in September and October (Figure 2.6 b, d).

## DISCUSSION

Our results indicate there are distinct seasonal patterns in fluvial dissolved nitrogen concentrations at each of our study sites, with generalized temporal trends observed at all six sites, as well as distinguishing qualitative and quantitative differences both between and among the tundra and mountain sites. Although a strong seasonality in fluvial nitrogen has been documented at a variety of pan-Arctic locations [e.g., *Holmes et al.*, 2012], including the North Slope of Alaska [*Peterson et al*, 1992; *McNamara et al.*, 2008; *Townsend-Small et al.*, 2011; *McClelland et al.*, 2014], the breadth and resolution of sampling during this study have provided an unprecedented opportunity to characterize the seasonal nitrogen dynamics of Arctic catchments. Detailed studies at the Bonanza Creek LTER have addressed seasonality of fluvial nitrogen in sub-Arctic catchments [e.g., *MacLean et al.*, 1999; *Jones et al.*, 2005; *Petrone et al.*, 2006], but such studies remain a rarity in the Arctic.

### Dissolved Organic Nitrogen Seasonal Dynamics

A number of studies have documented that spring snowmelt is the dominant yearly export period for dissolved organic carbon (DOC) in Arctic rivers owing to a combination of both high DOC concentrations and elevated discharge [e.g., *Peterson et al.*, 1986; *Holmes et al.*, 2012; *McClelland et al.*, 2014]. Although relatively fewer studies have documented DON export during spring snowmelt, the high DON concentrations observed during this period at our study sites are consistent with previous investigations from the

same area [*Peterson et al.*, 1992; *Townsend-Small et al.*, 2011; *McClelland et al.*, 2014], as well as those from other pan-Arctic regions [e.g., *Cai et al.*, 2008; *Holmes et al.*, 2012]. Studies that have quantified both riverine DOC and DON during the spring snowmelt from Arctic watersheds noted that export dynamics of DOC and DON are tightly coupled, with high DON concentrations accompanying high DOC concentrations [e.g., *Townsend-Small et al.*, 2011; *Holmes et al.*, 2012; *McClelland et al.*, 2014]. In 2010, high DON concentrations were noted at all six study sites prior to and concurrent with thawing of surface soils in May, but before thawing of deeper soil horizons occurred in June (Figure 2.2 and Figure 2.3). These observations are consistent with the paradigm that prior to initial runoff from snowmelt, frozen ground and the snow matrix temporarily constrain melt-water to the soil surface, and the restriction of flow facilitates leaching of dissolved organic matter from aboveground vegetation, leaf litter, and high organic matter content surface soils yielding high DON concentrations compared to other periods post snowmelt [e.g., *Guo and Macdonald*, 2006; *Spencer et al.*, 2008].

Observed decreases in DON concentrations in late spring and summer, relative to peak values associated with the spring freshet, may reflect seasonal changes in hydrologic flow paths and/or the relative contribution of various biogeochemical source/sink processes. For example, the deepening of the active layer through spring and summer facilitates water flow through deeper soils [*Keller et al.*, 2010; *Barker et al.*, 2014]. Similarly, *McNamara et al.* [1997] reported that in this region snowmelt discharge was sourced predominantly by "new" water from melting snow and ice, whereas post snowmelt increases in stream discharge following storm events were dominated by "old" water flushed from soils by "new" precipitation. As the active layer extends downward through the summer, the leaching potential of DON from soils may be reduced as water flow paths move through deeper soil horizons with lower organic matter content compared to surface

soil horizons. Likewise, DON loss may occur through increased soil mineral particle adsorption as water moves through deeper soil horizons with elevated mineral content [*MacLean at al.*, 1999; *Kawahigashi et al.*, 2006; *Petrone et al.*, 2006]. Soil bacterial remineralization of organic matter is a substantial process in the region [*Kling et al.*, 2014], and as the year progresses, deeper flow paths and longer water residence times may result in greater DON remineralization compared to earlier in the year. Our soil thermistor data from 2010 (Figure 2.2) are consistent with this explanation, showing increases in thaw depth that mirror decreases in DON. Our findings also agree with *Townsend-Small et al.* [2011] who report that DON concentrations per unit discharge were lower in July compared to May and early June at the Kuparuk site.

In addition to seasonal changes in hydrologic flow paths and soil processes, instream processing of organic matter may contribute to decreases in DON concentrations following snowmelt. Photo-oxidation of riverine DOC has been demonstrated to be a major carbon loss mechanism in lakes and rivers on the North Slope of Alaska during summer months accounting for 70-95% of total DOC processing [*Cory et al.*, 2014]. Similarly, photo-ammonification of DON [*Bushaw et al.*, 1996; *Grzybowski et al.*, 2002; *Sereda et al.*, 2012] followed by uptake or nitrification [*Peterson et al.*, 1997; *Wollheim et al.*, 2001] is likely an important DON loss mechanism in these systems as well. Moreover, partial DOC photo-oxidation stimulates additional bacterial remineralization of otherwise recalcitrant DOC [*Cory et al.*, 2013] and likely contributes to further DON remineralization. Photo-degradation mediated bacterial remineralization may be an especially important consideration following snowmelt as riverine dissolved organic matter has been demonstrated to be less labile in summer months than earlier in the year [*Holmes et al.*, 2008].

High DON concentrations observed during spring snowmelt relative to summer and fall flows at both the tundra and mountain sites (Figure 2.3) are consistent with restriction of meltwater to near-surface, organic-rich flow paths. Furthermore, overall differences in DON concentrations between the tundra (higher concentrations) and mountain (lower concentrations) sites reflect large differences in organic soil extent and vegetation coverage between the two different site types (Figure 2.1). Tundra soils contain large stores of leachable organic matter, and production and export of dissolved organic matter in the region strongly correlate with aboveground biomass [*Judd and Kling*, 2002]. In addition to distinct DON source dynamics between the two site types, the sharp decline in riverine DON concentrations at the mountain sites suggest differential seasonal variation in the strength of DON loss mechanisms compared to the tundra sites. At the mountain sites, thinner organic surface soils result in earlier thawing of mineral soil horizons, with increased DON adsorption and/or increased DON remineralization post snowmelt relative to the tundra sites. Among the mountain sites, there was little variation in seasonal DON concentration patterns, which we attribute to the similar watershed geomorphological characteristics of the three sites (Table 2.1), as each have comparable ratios of low slope vegetated terrain to exposed rocky upland.

Quantitative seasonal variations in DON concentrations at the tundra sites through most of the year (Imnavait > Oksrukuyik > Kuparuk) generally agree with differences in site mean watershed slope values (Table 2.1). The exception was Imnavait, where higher DON concentrations were observed during most times of the year. Marked differences in seasonal DON concentration patterns observed at Imnavait compared to the other tundra sites possibly relate to the site's small watershed size and distinct channel geomorphology. Large portions of the Imnavait river channel (above our sampling location) are comprised of small ponds connected by intermittently flowing water tracks; a pool-run morphology

[*Arp et al.*, 2015]. The other five study sites are all 3rd order streams or higher [*Strahler*, 1957]. This difference in watershed area and channel geomorphology may produce differential strength of landscape versus channel DON source/sink processes. Downstream reaches of the Imnavait channel may show seasonal patterns consistent with the other sites.

**Dissolved Inorganic Nitrogen Seasonal Dynamics**

The low DIN concentrations observed during the spring at all six study sites (Figure 2.4) are consistent with values previously reported for similar sized watersheds in the region [e.g., *Peterson et al.*, 1992; *MacIntyre et al.*, 2006; *McNamara et al.*, 2008; *Townsend et al.*, 2011]. Although winter microbial activity can cause net remineralization of nitrogen within soils [*Hobbie and Chapin*, 1996; *Schimel et al.*, 2004], biotic assimilation and denitrification early in the spring may limit the amount of DIN that is ultimately exported from soils to river channels during snowmelt [*Brooks and Williams*, 1999; *Schimel et al.*, 2004; *Harms and Jones*, 2012]. While we did not observe elevated DIN concentrations during the onset of snowmelt at our six study sites, elevated concentrations of $NO_3^-$ (up to 15 μmol $L^{-1}$) were measured by *McClelland et al.* [2014] at downstream sites on larger North Slope rivers (Kuparuk, Sagavanirktok, and Colville) prior to the spring freshet. $NO_3^-$deposition associated with snowfall was identified as a possible source for the elevated riverine concentrations, as $NO_3^-$ values ranging from 3-16 μmol $L^{-1}$ have been reported for snow in the region [*Jaffe and Zukowski*, 1993]. The difference between our current study and the previous findings of *McClelland et al.* [2014] may be a function of scale. Immobilization of inorganic nitrogen via plant or microbial uptake on the land surface may predominate at smaller scales [*Yano et al.*, 2010], with a $NO_3^-$ deposition/snowmelt source signal becoming increasingly apparent further downstream.

Increases in DIN concentrations during the late summer and early fall (Figure 2.4) indicate seasonal changes in source/sink processes within the watersheds, the river channels, or both. For example, *Harms and Jones* [2012] report that landscape maximum net inorganic nitrogen uptake rates in the area occur during snowmelt and decrease through the year, whereas remineralization rates are relatively consistent throughout the hydrologic year. They suggest these seasonal patterns in soil nitrogen dynamics, coupled with maximum rates of nitrogen remineralization exceeding maximum rates of net $NH_4^+$ uptake, result in the potential for inorganic nitrogen export during the summer and fall. A $^{15}NH_4^+$ tracer addition study by *Yano et al.* [2010] also found that immobilization of inorganic nitrogen was most pervasive during the spring, with high nitrogen immobilization occurring within the upper soil "green layer" and vertical flux of nitrogen to deeper soils occurring primarily during rain events. They postulate that a greater vertical flux of relatively labile nitrogen from upper peat and soil horizons to deeper soil horizons would occur during precipitation events under extended snow-free seasons. By extension, there is likely a greater vertical flux of nitrogen to deeper soils during late summer and early fall precipitation events when soil thaw depths are at or near maximum extents, with the potential for subsequent lateral export to river channels.

Because late season DIN concentrations at our study sites increased as the depth of the seasonal thaw layer extended towards maximum depths during late summer and fall, it is important to consider the role that active layer thaw dynamics play in inorganic nitrogen export from these systems. Deeper mineral soils contain large pools of inorganic nitrogen and have higher potential rates of nitrogen remineralization than overlying organic soil horizons [*Nadelhoffer et al.*, 1991; *Hobbie and Gough*, 2002], with hydrologic export possible as water flow paths move through deeper soil horizons as they thaw later in the year. As discussed above, deeper flow paths with longer water residence times during the

summer and fall may increase remineralization of organic nitrogen with a resulting increase in hydrologically exported inorganic nitrogen. Late season flow paths may also pass below the rooting zone limiting plant uptake of available inorganic nitrogen. Additionally, towards the end of the growing season plant demand for inorganic nitrogen may be lower than in the beginning of the growing season, and demand is most likely lower post senescence. There is also the possibility that within river channels, autotrophic inorganic nitrogen demand during the late summer and fall is lower compared to earlier in the hydrologic year. This "seasonal asynchrony" of lower inorganic nitrogen demand by primary producers and continued heterotrophic activity in the fall produces a net remineralization of soil organic nitrogen [*Bowden et al.*, in preparation]. Subsequently, soil DIN may be exported to river channels, with nitrification occurring within soils [*Hobbie and Gough*, 2002; *Harms and Jones*, 2012] or streams [*Wollheim et al.*, 2001].

Along with seasonal variations in soil and stream inorganic nitrogen uptake and remineralization dynamics, other sources of nitrogen may account for the observed late season riverine DIN concentration increases. Mentioned previously, snow deposition of $NO_3^-$ during winter is a source of nitrogen to the area, with rain events also a source of inorganic nitrogen. However, the limited amount of rainfall during the hydrologic year (~20 cm) and relatively low wet deposition $NO_3^-$ concentrations (1-8 μmol N $L^{-1}$) [*Everett et al.*, 1989] likely constrains total nitrogen inputs associated with precipitation during the late summer and early fall. Biological nitrogen fixation is another source of atmospheric nitrogen input that may account for 85-90% of total watershed nitrogen inputs [*Hobara et al.*, 2006]. Free living cyanobacteria of the genus *Nostoc*, associated with vegetation and particularly mosses, are the dominant nitrogen fixing organisms, with some fixation attributable to blue green algae present as phycobionts in lichens [*Alexander and Schell*, 1973]. Few direct measurements investigating the seasonality of nitrogen fixation rates in

the study area, or in the Arctic more generally, have been made, but modeling studies indicate that rates are highest between June and August, with small amounts of fixation occurring in September and negligible rates in October [*Hobara et al.*, 2006]. The inorganic nitrogen input via fixation at Imnavait has been estimated at 80 to 131 mg N $m^{-2}$ $yr^{-1}$ [*Hobara et al.*, 2006], similar to previously measured values in the region [e.g., *Alexander and Schell*, 1973; *Barsdate and Alexander*, 1975]. Although biological nitrogen fixation represents the dominant input of new nitrogen to the area, the amount of nitrogen stored in surface soil organic matter is several orders of magnitude larger (937 g N $m^{-2}$) [e.g., *Chapin et al.*, 1980], therefore large increases in late season nitrogen fixation rates would be necessary to match only small percentage changes in net soil nitrogen remineralization rates [*Shaver at al.*, 1992].

Bedrock is another source of fluvial DIN that has been identified in lower latitude watersheds and may play a significant role in localized terrestrial nitrogen cycling in variety of ecosystems [*Holloway and Dahlgren*, *1999*; *Holloway and Dahlgren*, *2002*]. Weathering of inorganic nitrogen as $NH_4^+$ from bedrock has been attributed to elevated inorganic nitrogen concentrations in soils and fresh water systems and has been shown to provide up to 30% of the nitrogen budget in streams of the Sierra Nevada mountain range in California [*Dahlgren*, 1994; *Holloway et al.*, 1999]. The regional bedrock geology of our study area on the North Slope of Alaska is dominated by shale, claystone, and sandstone conglomerate [*Irwin et al.*, 2008] and the soils of our study sites contain weathered clays and silicates [*Walker et al.*, 1989]. All of these substrates have previously been identified in other regions as containing nitrogen [*Holloway and Dahlgren*, 2002] and as possible sources of inorganic nitrogen through weathering [*Holloway et al.*, 2001]. However, the rocks in our study area have not previously been analyzed for nitrogen content and their concentration of nitrogen and the rate of nitrogen release from weathering

is currently unknown. Due to the high amounts of exposed bedrock at the mountain sites it is conceivable that geological nitrogen inputs may be important. However, the Kuparuk site has sizeable areas of exposed bedrock in the upper reaches of its catchment (Figure 2.1), yet we did not observe late season DIN concentrations comparable to the mountain sites, nor were there large quantitative differences in late season DIN concentrations between the tundra sites with and without large amounts of exposed bedrock.

Differences in the spatial extent and thickness of organic soils between the two site types may explain the variation in the observed onset, as well as the magnitude of late season DIN concentration increases between the tundra and mountain sites. The thinner organic soils of the mountain sites likely yield mineral soil horizons thawing earlier in the year compared to the tundra sites. Mineral soils may act as a source of inorganic nitrogen for export, but they may also promote remineralization over immobilization by soil microorganisms [*Nadelhoffer et al.* 1991; *Hobbie and Gough*, 2002]. Likewise, organic soils, especially the uppermost soil and peat horizons, efficiently immobilize inorganic nitrogen due to high uptake potential and competition among plants and soil microbes [*Kaye et al.*, 1996; *Yano et al.*, 2010]. The differential timing in the exposure of mineral soils to water flow and biogeochemical cycling between the two site types may contribute to the observed earlier onset and larger sustained increases in late season riverine DIN concentrations observed at the mountain sites. The lower extents of vegetation and organic soils at the mountain sites may also reduce potential uptake and immobilization during the spring, resulting in the small early season DIN concentrations increases observed post-snowmelt.

Among the mountain sites, the considerable degree of inter-site variability in the magnitude of late season DIN concentration increases during both study years (Trevor > Roche > Atigun) may be linked to differences in catchment geomorphic characteristics

(Figure 2.1 and Table 2.1). Although mean watershed slopes at all the mountain sites were similar (Table 2.1), the magnitude of late season DIN concentration increases inversely correlate to a higher areal percentage of terrain with low hydrologic slope (Atigun > Roche > Trevor). Lower slope terrain may indicate areas with higher coverage of vegetation and organic soils, which may limit landscape inorganic nitrogen export through plant uptake and microbial immobilization. Differences in the magnitude of late season DIN increases between the two study years (2010 > 2009) may be attributable to inter-annual variability in summer storm activity. In 2010, large precipitation events at the mountain sites may have caused a greater vertical movement of inorganic nitrogen from surface organic matter layers and soils to deeper thawed mineral soils [*Yano et al.*, 2010], which in turn increased lateral export of DIN to river channels.

Among the tundra sites, geomorphic characteristics do not correlate with inter-site variability in either the magnitude or timing of late season DIN concentration increases, but may have contributed to the unique dissolved nitrogen chemistry observed late in the hydrologic year at Imnavait. As previously mentioned, DIN concentration increases at all sites were attributable to increases in the $NO_3^-$ fraction of the inorganic nitrogen pool, with the exception of Imnavait in 2010, where $NH_4^+$ drove late season DIN concentration increases. It is possible that the small size of the Imnavait catchment and the beaded stream channel geomorphology, coupled with low flow post snowmelt (Table 2.1), reduced instream nitrification of available $NH_4^+$. It is also possible that an increase in the $NO_3^-$ fraction of the DIN pool may have been apparent further downstream of our Imnavait sampling site.

**Nitrogen-to-Chloride Ratios Seasonal Dynamics**

Increases in DIN:$Cl^-$ ratios from snowmelt through freeze-up at all of our study sites (Figure 2.6) point to ubiquitous increases in DIN export over the course of the hydrologic year. Although DIN:$Cl^-$ ratios increased from May to October at all sites, the differential rates and timing of the increases between the mountain and tundra sites points to mechanistic differences in DIN export during different seasons between the site types. Comparable percentage increases in 2009 and 2010 DIN concentrations and DIN:$Cl^-$ ratios from August to October at the tundra sites suggest that increases in DIN sources are driving increases in DIN concentrations during the late summer and fall. At the Imnavait site in 2010, DIN:$Cl^-$ ratios increased in mid- to late September as the depth of the active layer reached maximum yearly extents (Figure 2.2 and Figure 2.6). The concurrent increase in DIN export (as inferred from DIN:$Cl^-$ ratios) from Imnavait with thawing of deeper soil layers supports the hypothesis by *Harms and Jones* [2012] that deepening of the thaw layer increases the potential fluvial export of inorganic nitrogen from watersheds underlain by permafrost. At the mountain sites, large percentage increases in DIN concentrations during the fall were accompanied by only small percentage increases in DIN:$Cl^-$ ratios, suggesting that late season DIN concentration increases were mostly explained by evaporation and/or freezing effects. However, between May and July at the mountain sites, concurrent increases in DIN:$Cl^-$ ratios and DIN concentrations suggest that elevated early season DIN concentrations were a result of increases in DIN sources.

While DON concentrations decreased in the early spring at 5 of the 6 study sites (Imnavait excluded) (Figure 2.3), contrasting patterns in DON:$Cl^-$ ratios between the mountain sites and the remaining two tundra sites (Figure 2.5) suggests distinct differences in DON export processes. Steady decreases in DON:$Cl^-$ ratios at the mountain sites suggest that the highest DON export occurred in the spring and decreased gradually over the

hydrologic year. In contrast, increases in DON:$Cl^-$ ratios between May and July at the Kuparuk and Oksrukuyik sites suggest DON export peaked later in the year in the tundra catchments.

As previously noted, the Oksrukuyik and Atigun sites contain stretches of the Dalton Highway in their watersheds upstream of each site's respective sampling location. The Alaska Department of Transportation intermittently applies calcium chloride ($CaCl_2$) to the road surface to attract and retain moisture and reduce dusty conditions, and help keep the gravel road packed [Walker and Everett, 1987]. Although it is possible that runoff from the road resulted in elevated $Cl^-$ concentrations and contributed to the relatively lower N:$Cl^-$ ratios observed at the Oksrukuyik and Atigun compared to the other tundra and mountain sites, qualitatively the seasonal DIN:$Cl^-$ and DON:$Cl^-$ patterns are similar among each site's respective site type.

Although $Cl^-$ is considered conservative, in that it moves through soils and waters mainly as a free ion without being significantly transformed, interpretation of N-to-$Cl^-$ ratios may be complicated by mixing of multiple $Cl^-$ sources. High $Cl^-$ concentrations observed at the initiation of snowmelt suggest mobilization of $Cl^-$ ions that were left behind in soils during the previous year's freeze up. The snow itself becomes a source of $Cl^-$ as thaw accelerates and rain becomes a source of $Cl^-$ as the summer progresses. While both snow and rain are dilute sources of $Cl^-$ relative to the initial soil source, they each represent a different end-member. Snowmelt has higher concentrations of $Cl^-$ than rainwater [Jaffe and Zukowski, 1993; Pomeroy et al., 2005], so $Cl^-$ concentrations decrease as the rainwater contribution becomes more important. Thus, changes in N:$Cl^-$ ratios during early to mid-summer could reflect changes in $Cl^-$ sources. To the extent that $Cl^-$ concentrations decrease between snowmelt and rainwater, net increases in nitrogen export inferred from N:$Cl^-$ ratios may be overestimated. On the other hand, while increases in N:Cl ratios during the fall are

consistent with net N export, we may be underestimating N mobilization if there is a concomitant change in $Cl^-$ source contributions. For example, if increased $Cl^-$ concentrations during the fall are partially attributed to secondary mineral weathering [*Cooper et al*., 2002] rather than evaporation and/or freezing effects, then apparent N increases go up.

## CONCLUSIONS

As warming continues in the Arctic, it is expected to affect both biogeochemical nitrogen processes and physical export mechanisms, resulting in alterations to riverine nitrogen export. For example, experimental warming of air temperatures in wet sedge tundra in the area around Toolik Field Station increased net nitrogen mineralization [*Shaver et al.*, 1998]. Arctic climate change is also expected to cause permafrost degradation and an increase in the depth of the seasonally thawed active layer. This may result in the exposure of previously frozen higher mineral content soils to weathering and facilitate further inorganic nitrogen export [*Harms and Jones*, *2012*]. Similarly, longer snow and ice free seasons during the fall, with waters moving through deeper flow paths later in the year, would facilitate greater export of inorganic nitrogen from these watersheds.

Although discharge is low during the late summer and fall, rivers may flow until the end of October or early November before fully freezing, and it is reasonable to assume that contemporary estimates of annual DIN export would be adjusted upwards with the inclusion of late season DIN concentration measurements. While the nitrogen budget implications of elevated late season DIN concentrations merit consideration, the ecological fate of DIN exported during this time period also deserves attention. Instream utilization

of DIN during the late summer and fall is likely minimal due to decreased photosynthetic activity during this time. Additionally, streams in the region are typically phosphorus limited [*Peterson et al.*, 1983; *Bowden et al.*, 2014] and utilization of increased DIN concentrations during this period would require additional phosphorus inputs. On annual time scales, riverine supplied nitrogen from organic matter is greater than that from inorganic nitrogen, and may also play a greater role in supporting primary productivity along the Alaskan Beaufort Sea coast [*Tank et al.*, 2012; *McClelland et al.*, 2014]. However, on seasonal time scales, increased DIN export during the late summer and fall may provide an important nitrogen subsidy to estuarine ecosystems that may be utilized over winter or during the subsequent spring.

Our results demonstrate marked seasonal patterns in fluvial dissolved nitrogen concentration at each of our study sites. Similar dissolved nitrogen concentration patterns were observed across all six study sites, however, temporal variations in magnitude and timing between and among the tundra and mountain sites suggest site type, as well as site specific, differences in seasonal biogeochemical processes. Early season DON dynamics were similar to previous studies from the region, as well as those from various locations of the pan-Arctic; high DON concentrations were observed during spring snowmelt, with concentrations declining soon after and remaining lower through freeze-up. A unique finding of the present study was that late season DIN concentrations increased at all six study sites. Nitrogen-to-chloride ratios suggest that late season increases in DIN concentrations were not simply due to evaporation and/or freeze-out effects, but also a result of a seasonal shift in watershed nitrogen biogeochemical processing and export. The timing of DIN increases was consistent with a deepening of the seasonally thawed soil layer to maximum depth, along with reduced biological uptake demand in late summer and fall. As such, late season increases in DIN concentrations (or DIN:$Cl^-$) may be an important

proxy for estimating seasonal thaw at the landscape scale. Similarly, increases in late season DIN export over time may signal an expansion in maximum active layer thaw depth. While our knowledge of the seasonal dynamics of water-borne constituents in Arctic rivers has improved, the late summer and early fall remain understudied. Additional investigations during this time period when the active layer extends to maximum depths, as well as an improved understanding of the mechanisms that control the seasonal variability of water chemistry, may help us to better predict how these systems will respond to future warming.

Table 2.1. Watershed characteristics for Kuparuk, Imnavait, Oksrukuyik, Atigun, Roche, and Trevor basins. Latitude and longitude coordinates correspond to the locations where riverine surface water samples were collected for each basin. Area, elevation, and slope values were calculated using a digital elevation model obtained from the USGS National Elevation Dataset (ned.usgs.gov). Discharge data for Kuparuk (2009) and Imnavait (2008) provided by Douglas Kane of the Water and Environmental Research Center at the University of Alaska Fairbanks. Discharge for Oksrukuyik (2009) and Roche (2009) was calculated using site specific USGS river staff gauges and rating curves. Discharge for Atigun (2011) was obtained from the USGS at waterdata.usgs.gov (site# 15905100). Discharge for Trevor (2009) was measured using a SonTek FlowTracker (SonTek, San Diego, CA, USA).

| | **Tundra Sites** | | | **Mountain Sites** | | |
|---|---|---|---|---|---|---|
| | *Kuparuk* | *Imnavait* | *Oksrukuyik* | *Atigun* | *Roche* | *Trevor* |
| Area ($km^2$) | 134.5 | 1.7 | 71.9 | 608.3 | 83.4 | 42.4 |
| Latitude | 68° 38' 47" | 68° 37' 00" | 68° 41' 12" | 68° 27' 03" | 68° 22' 26" | 68° 17' 01" |
| Longitude | -149° 24' 34" | -149° 19' 05" | -149° 05' 50" | -149° 22' 31" | -149° 18' 45" | -149° 22' 18" |
| Mean elev. (m) | 988 | 915 | 862 | 1415 | 1542 | 1595 |
| Min. elev. (m) | 735 | 883 | 754 | 800 | 832 | 895 |
| Max elev. (m) | 1499 | 961 | 1100 | 2301 | 2286 | 2226 |
| Mean slope (%) | 11.5 | 6.9 | 5.1 | 44.6 | 51.4 | 51.8 |
| Max Q ($m^3\ s^{-1}$) | 20.9 | 0.9 | 8.6 | 103.6 | 13.6 | 2.4 |
| Mean July Q ($m^3\ s^{-1}$) | 1.9 | <0.05 | 0.2 | 22.0 | 2.3 | 0.8 |

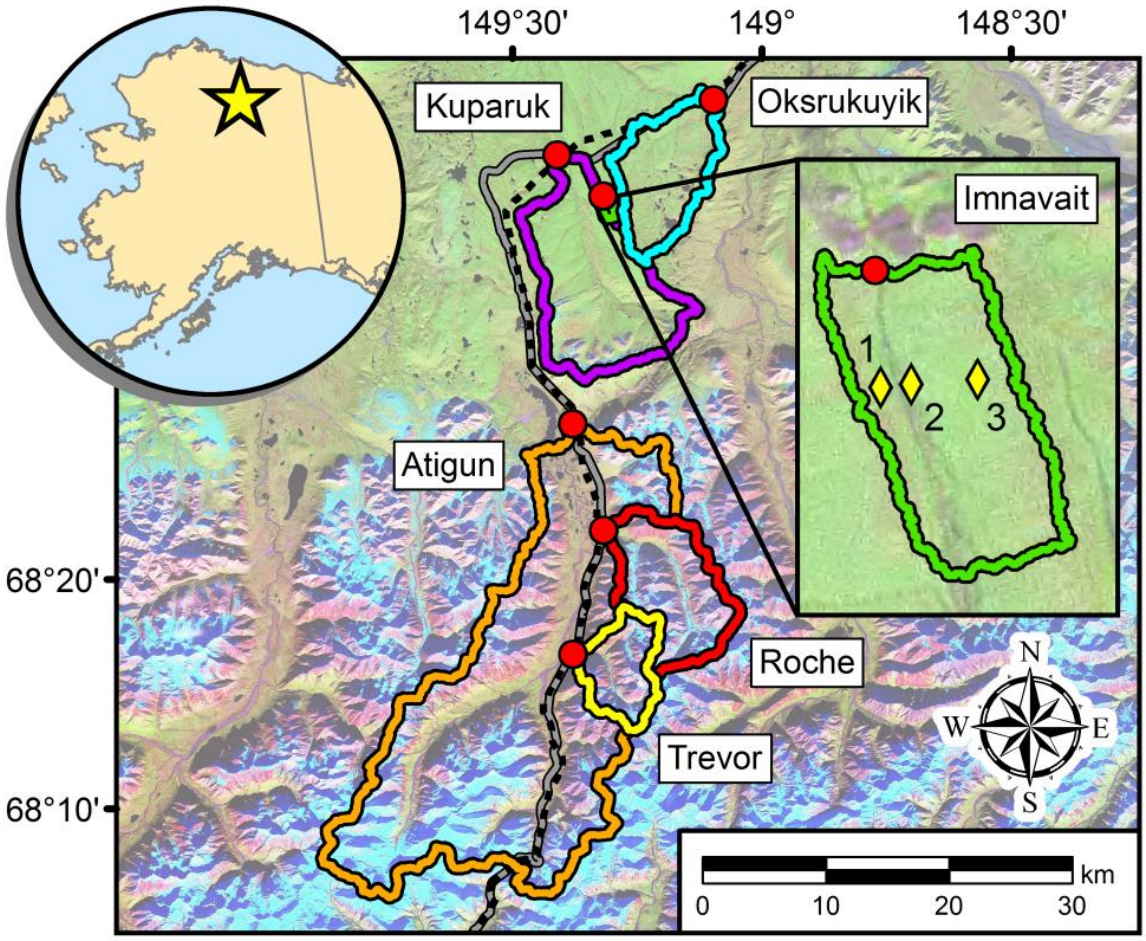


Figure 2.1. Map study area with delineated watershed boundaries (colored lines) and sample locations (red circles). All watershed boundaries were delineated as the contributing area upstream from where surface water samples were collected. Note that the Roche and Trevor sites are sub-catchments of the larger Atigun catchment. Map inset on the right expands the Imnavait catchment and shows the locations where thermistor strings were installed (yellow diamonds). Background imagery is a NASA multispectral Landsat false color mosaic depicting vegetation as green, bedrock and/or bare soil as pink, and snow cover as blue. The solid gray line represents the Dalton Highway and the dashed black line the Trans-Alaska Pipeline.

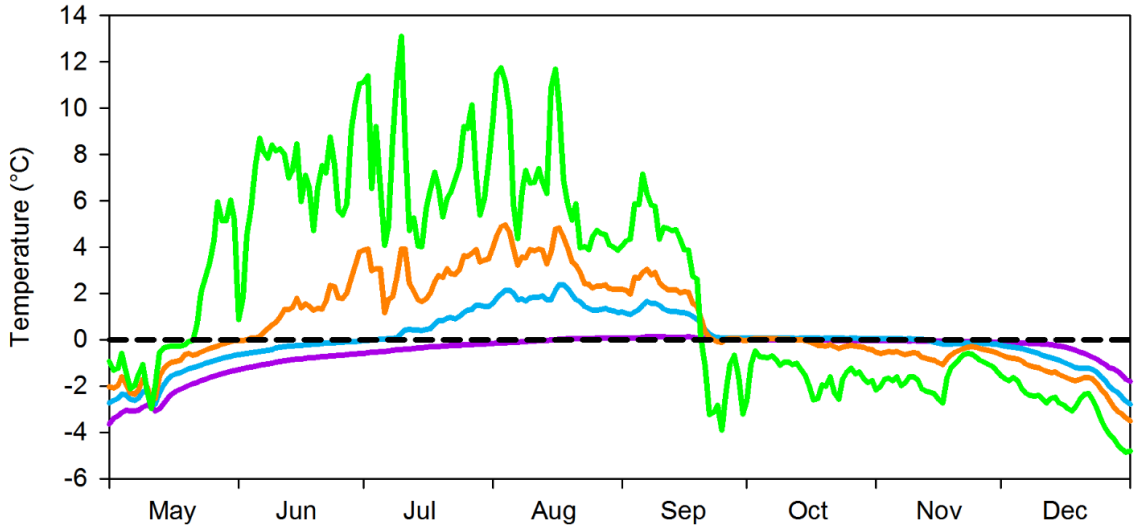


Figure 2.2. 2010 temporal variation in soil temperature from thermistor array 2 deployed in the Imnavait watershed. Solid green, orange, blue, and purple lines represent daily mean temperatures from individual thermistors deployed at depths of 0, 28, 42, and 55 cm respectively. The dashed black line indicates 0°C.

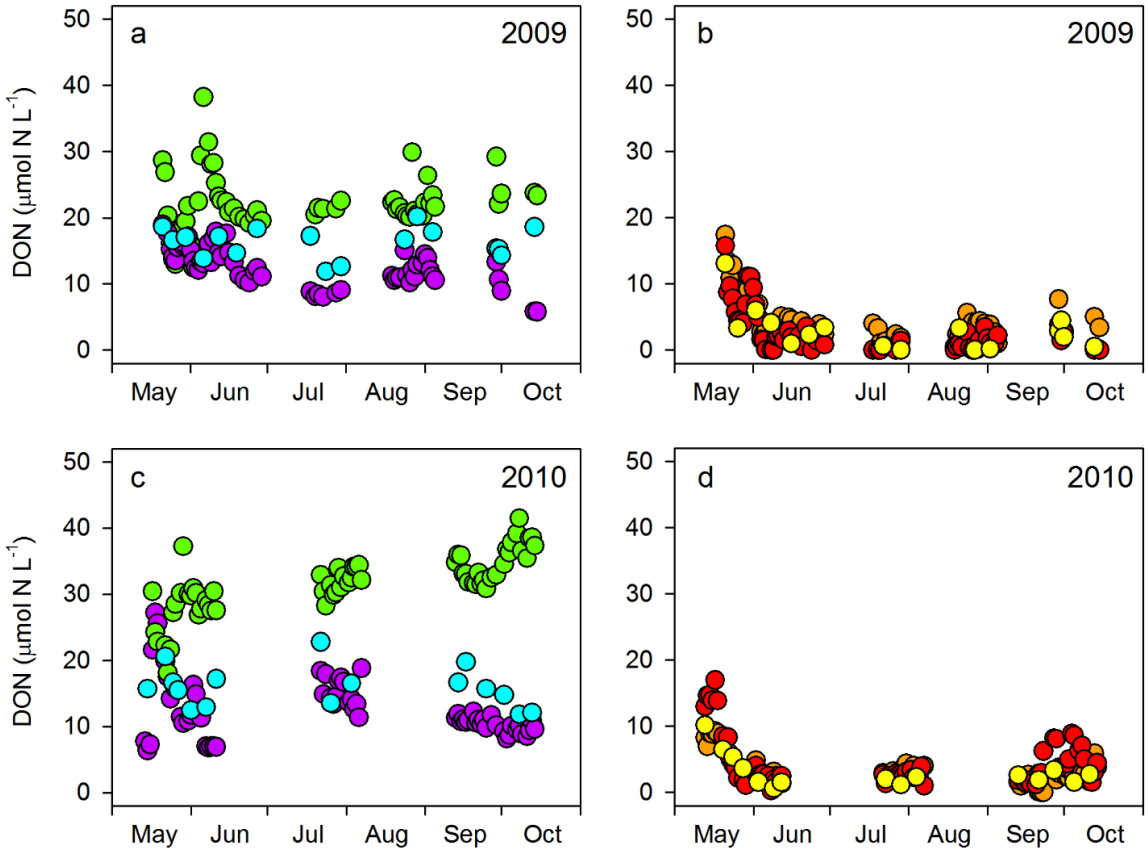


Figure 2.3. Temporal variation in DON concentrations of riverine surface waters from tundra sites (a, c) and mountain sites (b, d) from 2009 and 2010. Purple markers correspond to Kuparuk, green to Imnavait, blue to Oksrukuyik, orange to Atigun, red to Roche, and yellow to Trevor.

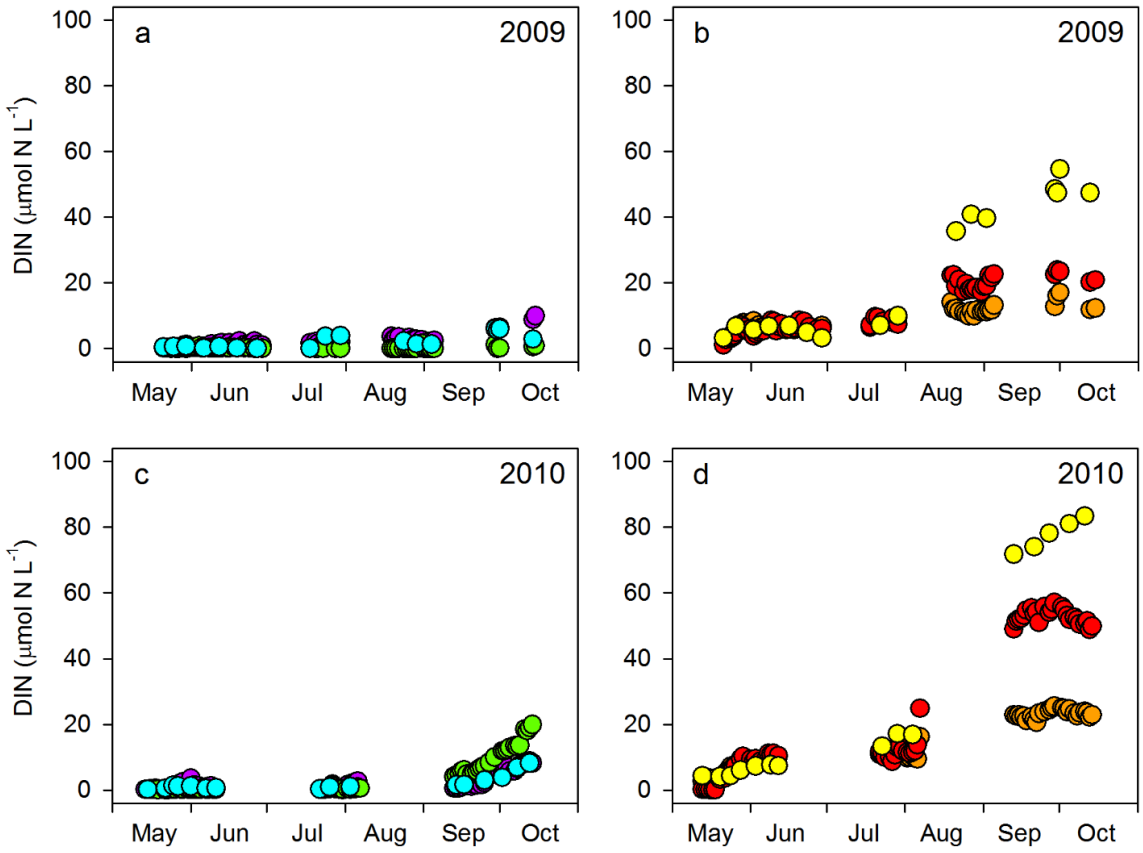


Figure 2.4. Temporal variation in DIN concentrations of riverine surface waters from tundra sites (a, c) and mountain sites (b, d) from 2009 and 2010. Purple markers correspond to Kuparuk, green to Imnavait, blue to Oksrukuyik, orange to Atigun, red to Roche, and yellow to Trevor.

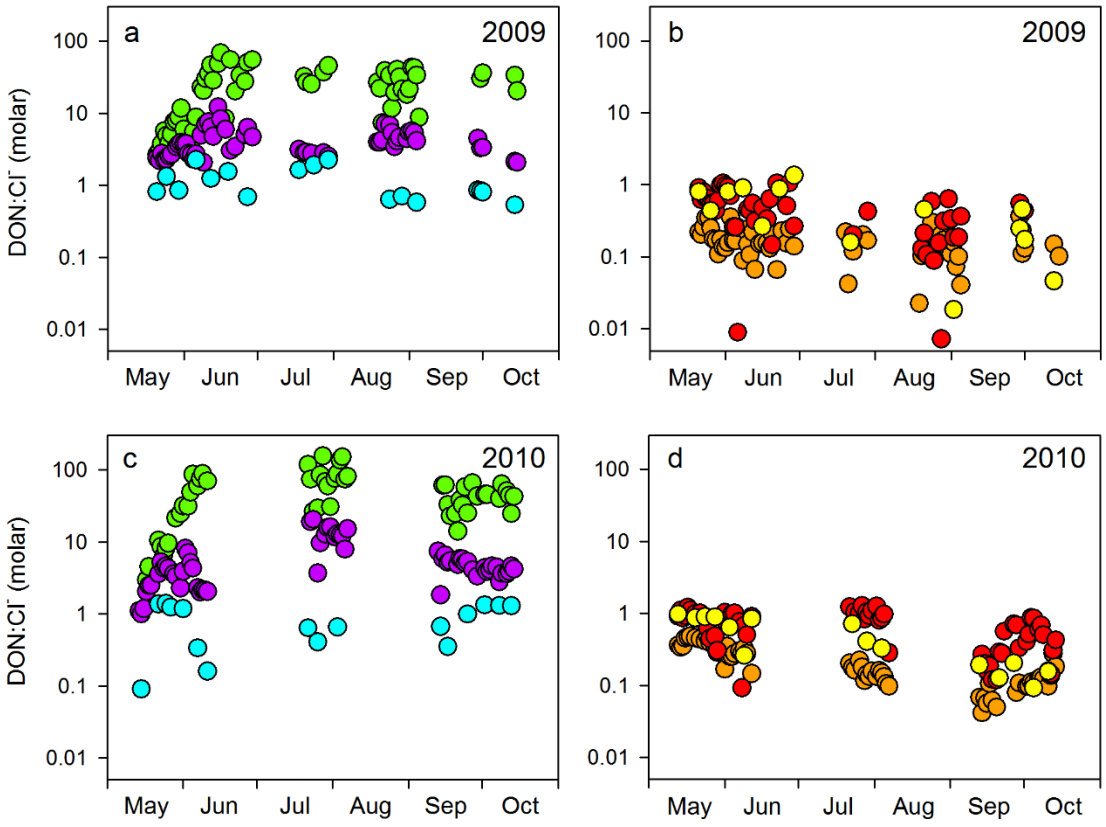


Figure 2.5. Temporal variation in DON-to-$Cl^-$ molar ratios of riverine surface waters from tundra sites (a, c) and mountain sites (b, d) from 2009 and 2010. Purple markers correspond to Kuparuk, green to Imnavait, blue to Oksrukuyik, orange to Atigun, red to Roche, and yellow to Trevor.

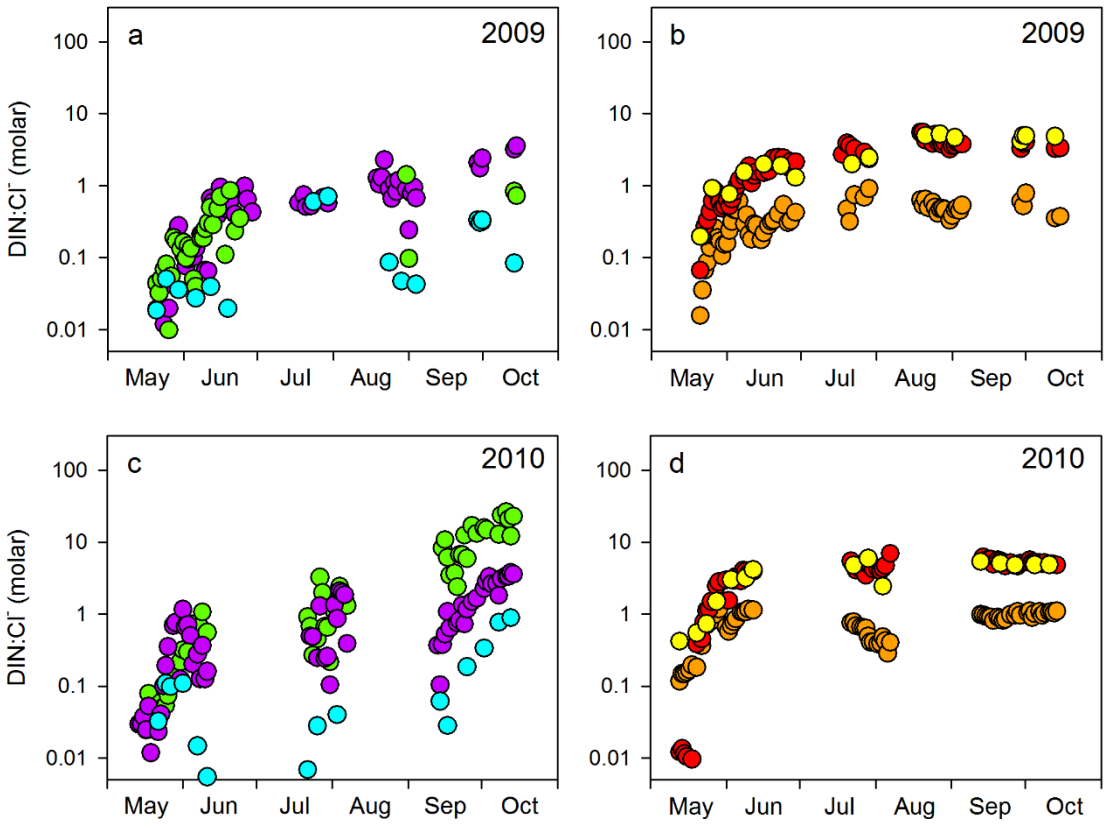


Figure 2.6. Temporal variation in DIN-to-$Cl^-$ molar ratios of riverine surface waters from tundra sites (a, c) and mountain sites (b, d) from 2009 and 2010. Purple markers correspond to Kuparuk, green to Imnavait, blue to Oksrukuyik, orange to Atigun, red to Roche, and yellow to Trevor.

# Chapter 3: DOM leaching dynamics from frozen and dried aboveground vascular plant material of the Alaskan Arctic


## ABSTRACT

Our understanding of the seasonal dynamics of fluvial dissolved organic matter (DOM) concentrations and fluxes in Arctic catchments has increased substantially during recent years, especially during the spring, which historically has been an under-sampled time period. While a number of studies have observed peaks in both DOM concentrations and fluxes during the spring freshet, our knowledge of the mechanisms that control these observations are still lacking. During the initial snowmelt phase, frozen ground constrains meltwater to the soil surface, and it is hypothesized that the restriction of flow facilitates leaching of DOM from senescent aboveground vegetation and detritus contributing to the high DOM concentrations observed during this period. This study focuses on DOM leaching dynamics from frozen and dried aboveground vegetation material from three common species of Alaskan Arctic vascular plants; *Eriophorum vaginatum, Carex bigelowii, and Salix pulchra*. Specifically we quantified leached DOM both by measuring and modeling the amount of dissolved organic carbon (DOC) and total dissolved nitrogen (TDN) released from plant material over time. Additionally, we qualified leachate composition by calculating DOC to TDN ratios (C:N) and chromophoric dissolved organic matter (CDOM) parameters $SUVA_{254}$, and $a_{250}$:$a_{365}$. Results indicate that the initial leaching rate of DOC from frozen vegetation material was higher than from dried material for all three plant species, but maximum potential DOC and TDN release was not affected by treatment. Compositionally, DOM that was leached from frozen material had higher C:N ratios than material that was only dried. Although $SUVA_{254}$, and $a_{250}$:$a_{365}$ values of vegetation leachates were similar between dried and frozen treatments, values of both parameters varied over time reflective of changes in DOM composition. Our findings

suggest the seasonal timing of freezing and drying conditions experienced by senesced plant material during the late summer and fall and over winter may impact DOM leaching characteristics on that same material the following spring during snowmelt. More importantly, these results indicate that recent aboveground vascular plant biomass has the potential to be a major source of readily leachable DOM in Arctic catchments during the spring.

## INTRODUCTION

The lateral flux of organic matter plays a significant role in the carbon and nitrogen cycles of Arctic watersheds [*McGuire et al*., 2009], with large quantities in dissolved organic matter (DOM) form being transported from terrestrial systems to ocean environments by Arctic rivers [*Dittmar and Kattner*, 2003; *Guo and Macdonald*., 2006; *McClelland et al*., 2014]. The spring freshet has been identified as a period in which a large proportion of the total annual flux of DOM is exported in Arctic rivers owing to both high concentrations and high discharge [e.g., *Finlay et al*., 2006; *Dornblaser and Striegl*, 2007; *Raymond et al*., 2007; *Holmes, et al*., 2012; *McClelland et al*., 2014]. However, climate change induced impacts to the Arctic hydrologic cycle, including altered precipitation regimes, increased discharge, and earlier snowmelt [*Peterson et al.*, 2002; *Peterson et al.*, 2006; *Holland et al.*, 2007; *White et al.*, 2007; *Rawlings et al.*, 2010], are likely already affecting DOM export from Arctic watersheds during this important seasonal transition period from winter to summer, and will most certainly impact these systems with continued warming over the coming century. While linkages between hydrology and DOM export during the spring freshet have been described at various locations and scales within the Arctic [e.g., *Finlay et al*., 2006; *McNamara et al.*, 2008; *Townsend-Small et al.*, 2011], our knowledge of the mechanisms that control seasonal DOM export dynamics lags behind.

A number of studies have observed peaks in DOM concentrations in Arctic rivers during the spring snowmelt relative to other periods during the year [e.g., *Raymond et al*., 2007; *Cai et al.*, 2008; *Holmes, et al*., 2012; *McClelland et al*., 2014]. Similarly, investigations focused on the composition of DOM report distinct qualitative seasonal shifts from spring to summer. For example, DOM has a higher proportion of vascular plant chemical markers during the spring, with the amounts decreasing through summer and fall, indicating a transition of fluvial DOM produced from surface vegetation and litter early in

the year, to that originating from deeper soil horizons as the year progresses [*Neff et al*., 2006; *Spencer et al*., 2008]. Similarly, elevated radiocarbon content of DOM during the spring points to a younger source material relative to summer and fall months [*Guo and Macdonald*, 2006; *Neff et al*., 2006; *Guo et al*., 2007; *Raymond et al*., 2007]. The shift from a young DOM pool dominated by leachates from vegetation and surface soil horizons to that of deeper soils and other highly degraded terrestrial material is also reflected in the results of incubation experiments of DOM from Arctic rivers. Microbial degradation of riverine DOM is highest during the freshet, signaling that the pool is more labile in the spring, while DOM exported during the summer is largely recalcitrant [*Holmes et al*., 2008]. The seasonal variation in DOM concentrations and composition are suggestive of a shift in DOM sources and/or export processes from spring to summer and fall.

In addition to the high DOM concentrations and fluxes observed during spring snowmelt, discharge-normalized DOM concentrations are also greater during this time compared to those in summer and fall [*Striegl et al*., 2005; *Finlay et al*., 2006; *Townsend-Small et al*., 2011]. It is hypothesized that during the initial stages of the spring thaw, frozen ground limits percolation of meltwaters into deeper soil horizons [*Woo*, 1986; *Kane et al*., 1989], facilitating leaching of aboveground vegetation, litter, and upper organic soil layers, resulting in high DOM export [*MacLean et al*., 1999; *Guo and Macdonald*, 2006; *Petrone et al*., 2006; *Spencer et al.*, 2008]. In the summer and fall, flow paths move through deeper soils with longer residence times, enhanced microbial remineralization, and mineral particle adsorption, reducing DOM export [*Striegl et al.*, 2005; *Kawahigashi et al.*, 2006]. Taken together, the results of composition and flux studies strongly indicate the influence of surface vegetation on DOM export dynamics during the spring snowmelt period. Although our knowledge of DOM seasonal export dynamics has improved considerably, a greater understanding of the mechanisms that control DOM export in Arctic

watersheds, especially during the critical spring melt period, may help us to better predict how these systems may respond to future climate change scenarios.

To date, there have been a number of studies that have examined DOM leaching from vegetation and litter and the potential export to soils and aquatic systems in temperate and tropical regions [e.g., *Tukey*, 1970; *Yavitt and Fahey*, 1986; *McDowell and Likens*, 1988; *Czech and Kappan*, 1997; *Meyer et al*., 1998; *Cleveland et al., 2004*]. However, there have been relatively few direct mechanistic investigations of DOM export from Arctic terrestrial systems [e.g., *Judd and Kling*, 2002], and limited examination of vascular plant material as a source of leachable DOM from high latitude areas [e.g., *Wickland et al*., 2007]. In this study we focused on DOM leaching dynamics from frozen and dried aboveground vegetation material (two environmental conditions experienced during the fall and winter inherently characteristic of the Arctic) from three species representing common Alaskan Arctic vascular plant genera; *Eriophorum vaginatum, Carex bigelowii, and Salix pulchra*. Specifically, we quantified DOM leached from aboveground vegetation material by measuring the amount of dissolved organic carbon (DOC) and total dissolved nitrogen (TDN) leached over time. Additionally, DOC to TDN molar ratios (C:N) and chromophoric dissolved organic matter (CDOM) parameters were calculated from vegetation leachates in an effort to quantify compositional characteristics of DOM leached from vascular plant material.

## MATERIAL AND METHODS

### Vegetation Collection and Treatment

Vegetation material of the three plant species of interest (*Eriophorum vaginatum, Carex bigelowii, and Salix pulchra*) was collected in the area of Barter Island, AK (70.123

N, 143.615 W) in late August of 2012. We collected vegetation material at the end of the growing season, but before plant material was exposed to appreciable amounts of air drying or freezing weather conditions. Collections were limited to standing aboveground plant material in an effort to collect from that year's growing season. For *Eriophorum* and *Carex*, leaf blades, leaf sheaths, partially senescent leaves (brown portions of green leaves that were alive in the current year), and inflorescences were collected, whereas for *Salix*, vegetation material collections consisted of only leaves.

Plant material from all three species was immediately subjected to one of two treatments after collection; dried or frozen. Dried treatment material was placed into a drying oven at 60°C for 24 hours and then kept in a dark desiccator cabinet. Frozen treatment material was first placed into zip-tie bags and then into a freezer. Frozen treatment material was kept between -30°C and -15°C prior to experiments.

In order to quantitatively compare the amounts of DOC and TDN leached from dried plant material and frozen plant material it was necessary to convert frozen plant material wet weights to dry weight equivalents. Frozen material sub-samples for each of the three species were weighed then dried at 60°C for 24 hours, and the resulting dry weights were used to construct species specific wet weight to dry weight conversions ($r^2$ values >0.95).

**Vegetation Leachates**

For each plant species, 1.5 to 10.5 g of treated vegetation material was added to an acid washed 10 L glass jar filled with 5 L of 0.001 N $NaHCO_3$ solution. To simulate a snowmelt thermal regime and minimize microbial activity, sample jars were placed in an ice bath within an environmental cold chamber that kept the solution in each jar between

0°C and 1°C throughout the course of the experiment. $NaHCO_3$ was used to mimic the ionic strength of melt waters from snow and to buffer against changes in pH. Each glass jar was continuously aerated to prevent anoxic conditions using a fish tank pump, acid washed pre-leached silicone tubing, and air stones. All sample jars were kept in the dark except during brief sampling periods. An experimental leaching run consisted of four jars run in parallel, with one jar for each of the three plant species of the same treatment, along with a control jar. Three individual leaching runs were conducted for each of the two experimental treatments resulting in n = 3 for each of the six plant species treatment pairs.

Vegetation material was leached for a total of 96 hours, with sample waters for DOC, TDN, and UV-Vis absorbance collected at 1, 3, 6, 12, 24, 48, 72, and 96 hours. While our measurements did not differentiate between inorganic and organic forms of dissolved nitrogen in this study, we assume that TDN was strongly dominated by organic leachates. This assumption is supported by previous studies showing that nearly all TDN leached from plant material is in the organic form [*Cleveland et al*., 2004]. Remineralization of dissolved organic nitrogen from vegetation leachates can become substantial as incubation experiments proceed [*Cleveland et al*., 2004], but the short incubation times used in this study likely minimized this effect. In any case, barring losses due to processes such as denitrification, all leached nitrogen is accounted for by measuring TDN.

Sample waters were collected from individual jars using acid washed pre-leached 140 mL polypropylene syringes and immediately filtered through 0.45 μm polyethersulfone membrane syringe filters. Samples were collected in 60 mL acid washed pre-leached polycarbonate bottles for DOC and TDN concentration analyses, and 60 mL acid washed pre-leached HDPE bottles for UV-Vis analysis. DOC and TDN samples were immediately frozen and kept cold prior to analysis, while UV-Vis samples were

refrigerated and kept cool until analysis. The sample volumes removed from each jar during sampling (120-140 mL) were immediately replaced with an equal volume of 0.001 N $NaHCO_3$ solution kept between 0°C and 1°C. The dilution effect was accounted for in the final calculation of DOC and TDN concentrations.

**DOC, TDN, and UV-Vis Analyses**

Vegetation leachate samples were analyzed for DOC and TDN concentrations at the University of Texas Marine Science Institute on a Shimadzu total organic carbon analyzer fitted with a total nitrogen module for chemiluminescence detection of nitrogen (Shimadzu Corporation, Kyoto, Japan). All DOC and TDN concentrations were converted to leached mass yields using the volume of solution in each jar, and then normalized by the amount of vegetation added to each jar using dry weights or dry weight equivalents. Final DOC and TDN values are reported as mg C or N per g of dry weight material added (mg C/N g dry $wt^{-1}$). DOC and TDN concentrations of control samples were not significantly different from measured DOC and TDN blank values so they are omitted from subsequent statistical analyses and results.

All vegetation leachate samples were analyzed for UV-Vis absorbance within 12 hours of collection. Measurements were made between 200 and 800 nm (λ) with a Perkin Elmer Lambda 35 dual beam scanning spectrophotometer using a 1 cm path length quartz cell. All samples were analyzed at ambient laboratory air temperature and were referenced to a distilled water blank. CDOM absorption coefficients (Napierian form, $m^{-1}$) of vegetation leachate samples were calculated as:

$$a(\lambda) = \frac{2.303A(\lambda)}{l}$$

where $A(\lambda)$ is the measured absorbance, and $l$ is the cell path length in meters. Values of the CDOM parameter $a_{250}$:$a_{365}$ were calculated as the ratio of absorption coefficients at 250 nm and 365 nm. Specific UV absorbance at 254 nm ($SUVA_{254}$) values were calculated as the absorbance (A) at $\lambda$ = 254 nm divided by sample DOC concentration.

**Modeling and Statistical Analyses**

All modeling and statistical analyses were performed using the statistics software program JMP Pro version 11. For each species treatment pair leaching run (n = 3) the amount of DOC and TDN leached over time was modeled using a Michaelis-Menten type equation:

$$V(t) = \frac{(V_{max}) \times (t)}{(t_{50}) + (t)}$$

where $t$ is time, $V_{max}$ is the potential maximum amount of leachable DOC or TDN, and $t_{50}$ is the time to reach half of $V_{max}$. The two parameter model was solved by minimizing the residual sum of squares error between modeled values and sampled values. Two additional leaching parameters were calculated for each leaching run using that run's solved model parameter values. The initial leaching rate ($\alpha$) of DOC and TDN was calculated as the ratio between $V_{max}$ and $t_{50}$, and a near approximation for the time to $V_{max}$ for both DOC and TDN was calculated as the time to 90% of $V_{max}$ ($t_{90}$).

Mean values for each of the four leaching yield model parameters ($V_{max}$, $t_{50}$, $t_{90}$, $\alpha$) for both DOC and TDN were analyzed separately using a 2-way ANOVA with species, treatment, and the interaction between species and treatment as fixed effects. Results were

considered significant when $p < 0.05$. Where the treatment or species effect was significant for a given ANOVA test a post-hoc analysis of model parameter mean values of all species treatment pairs was performed using a Tukey-Kramer honestly significant difference (HSD) test, with results considered significant when $p < 0.05$. The same statistical tests and post-hoc pair-wise comparisons were performed on the measured leaching yields of DOC and TDN, the C:N ratios of leached material, as well as on the CDOM optical parameters, $SUVA_{254}$ and $a_{250}$:$a_{365}$, of leached material at each sampling time point.

## RESULTS

### Measured DOC and TDN Leaching Yields

Generally, it was observed that there were similar temporal increases in measured DOC leaching yields in all plant species treatment pairs during the 96 hour experimental sampling period (Figure 3.1). In each plant species treatment pair, measured DOC yields tended to increase at a near linear rate during the first 12 to 24 hours of leaching, followed by declining DOC leaching rates and smaller increases in DOC yields. Although temporal DOC leaching yield patterns were similar among all species treatment pairs, there were distinct differences in the magnitude of measured DOC yields evident between the two different treatments as well as among the three species in each treatment. At all sampling time points DOC yields for each of the three plant species were larger in the frozen treatment compared to the dried treatment. For each of the individual ANOVA tests performed on measured DOC yields at each sampling time point, treatment had a significant effect ($p < 0.001$). Among the plant species in the frozen treatment, *Eriophorum* had the highest DOC yield at each sampling time point during the first 24 hours, while *Salix* had the largest DOC yield at the end of the 96 hour leaching period. In the dried

treatment, Carex initially had the highest DOC yields, but after 12 hours *Salix* had the largest DOC yields. In the dried treatment *Eriophorum* had the smallest DOC yields throughout the 96 hour leaching period among the three species. The largest difference in DOC yields at each sampling time point between the dried and frozen treatments was seen in *Eriophorum*, with the difference in DOC yields between treatments being similar in both *Carex* and *Salix*. For ANOVA tests performed on measured DOC yields at each sampling time point the species effect was significant ($p < 0.05$) at the 12 hour sampling point and at all subsequent sampling time points through the remainder of the 96 hour leaching period.

Similar to DOC, TDN yields increased throughout the 96 hour leaching period for all three species in both the dried and frozen treatments (Figure 3.1). The fastest rates of TDN leaching occurred during the initial 6 to 12 hour leaching period, followed by decreases in TDN leaching rates and progressively smaller increases in total TDN yields after 24 to 48 hours. Differences in TDN yields between the two treatment groups for each of the three species were typically small during the initial 24 hour leaching period, and unlike DOC there were no consistent differences in TDN yields between treatments among the three species. After 24 hours TDN yields were larger in the frozen treatment compared to the dried treatment for *Eriophorum* and *Salix*, whereas TDN yields were larger in the dried treatment for *Carex*. Only in *Eriophorum* was the difference between dried and frozen treatment TDN yields significant ($p < 0.05$) at the 48, 72, and 96 hour sampling time points. Among the three species there were distinct differences in TDN yields in both treatments. For each of the individual ANOVA tests run at each sampling time point, the species effect was significant ($p < 0.0005$) at all sampling time points during the 96 hour leaching period. In the dried treatment, *Carex* had the highest TDN yields during the initial 12 hours of leaching, but after 24 hours TDN yields were greatest in *Eriophorum*. TDN

yields in the frozen treatment were similar for *Eriophorum* and *Carex* throughout the 96 hour leaching period. In both the frozen and dried treatments, TDN yields from *Salix* were significantly less ($p < 0.05$) than yields from either *Eriophorum* or *Carex* after 12 hours.

Mean values of DOC and TDN yields for each species treatment pair at each sampling time point are reported in Appendix B (Table B.1). A summary of p-value results from individual time point two way ANOVA tests (Table B.2), and the results of Tukey Kramer HSD pair-wise comparisons performed at each sampling time point (Table B.3) are also provided.

**Modeled DOC and TDN Leaching Yields**

Modeled DOC yields generally agreed well with measured DOC yields for all three species in both the dried and frozen treatments (Figure 3.1). For individual leaching runs, the $r^2$ values of the linear regressions of modeled DOC yields to measured DOC yields during the 96 hour leaching period ranged from 0.9972 to 0.9999 (Appendix B; Table B.4). Mean values of the four modeled DOC leaching yield equation parameters for each species treatment pair are reported in Table 3.1. Among the four calculated model parameters, there were significant treatment and or species effects. For the individual ANOVA tests on $V_{max}$, $t_{50}$, and $t_{90}$ values, both the species and treatment effect were significant at the level $p < 0.01$, while for the ANOVA test on $\alpha$ only the treatment effect was significant (Appendix B; Table B.5).

In each of the three species $V_{max}$ values of modeled DOC yields were higher in the frozen treatment compared to the dried treatment, although the pair-wise comparisons of differences in treatment pairs for each species were not significant (Table 3.1). Among the three species, $V_{max}$ values of Salix were largest in the frozen and dried treatments, while

$V_{max}$ values of *Carex* were the lowest in both treatments. The $t_{50}$ and $t_{90}$ values were lower in the frozen treatment compared to the dried treatment for each of the three species, with the differences in treatment pairs significant for *Eriophorum* and *Salix*. In the frozen treatment, $t_{50}$ and $t_{90}$ values were lowest for *Eriophorum*, whereas in the dried treatment *Eriophorum* $t_{50}$ and $t_{90}$ values were significantly higher than either *Carex* or *Salix*. All $\alpha$ values were higher in the frozen treatment compared to the dried treatment for each species treatment pair and the difference between treatments was significant in all cases. Frozen treatment *Eriophorum* $\alpha$ values were significantly higher than all other species treatments pair $\alpha$ values.

Modeled TDN yields also tracked well with measured TDN yields for all species treatment pairs (Figure 3.1). The $r^2$ values of the linear regressions of modeled TDN yields to measured TDN yields during the 96 hour leaching period ranged from 0.9732 to 0.9990 for individual species treatment pair leaching runs. Mean values of the modeled TDN leaching yield equation parameters for each species treatment pair are reported in Table 3.1. For the individual ANOVA tests performed on each of the four modeled TDN leaching yield equation parameters, both species and treatment effects were significant at the level $p < 0.05$. However, like measured TDN yields, treatment did not have a consistent directional effect on modeled TDN yield parameter values for each of the three different species, but there were species specific differences in TDN leaching yield parameter values.

Dried treatment TDN $V_{max}$ values were higher than frozen $V_{max}$ values in *Eriophorum* and *Salix*, whereas in *Carex*, frozen treatment $V_{max}$ values were higher. Dried treatment *Eriophorum* had significantly higher $V_{max}$ values than all other species treatment pairs, while *Salix* had significantly lower $V_{max}$ values than the other two species in both dried and frozen treatments (Table 3.1). For *Eriophorum* and *Salix*, dried treatment $t_{50}$ and

$t_{90}$ values were higher compared to frozen treatment values, though treatment differences were only significant in *Eriophorum*. In all species $\alpha$ values were higher in the frozen treatment compared to the dried treatment.

**Vegetation Leachate Chemical Characteristics**

Temporal trends of leachate C:N ratios were qualitatively similar across all species treatment pairs during the 96 hour leaching period. C:N ratios increased during the initial 12-24 hours of leaching in all three species in both treatments, with subsequent small increases or decreases in C:N ratios during the remainder of the 96 hour leaching period (Figure 3.2). Although temporal patterns of C:N ratios were qualitatively comparable, there were significant quantitative differences in C:N ratios between treatments and among species. For each of the individual ANOVA tests performed on C:N ratios at each sampling time point, treatment and species had a significant effect ($p < 0.005$). At all sampling time points, C:N ratios were higher in the frozen treatment compared to the dried treatment in all three species, with the difference being significant for *Eriophorum* and *Salix*. Among the three species in the frozen treatment, leached material from *Salix* had significantly higher C:N ratios than leached material from either *Eriophorum* or *Carex* after 3 hours. In the dried treatment, *Salix* also leached material with higher C:N ratios than *Eriophorum* or *Carex* at all sampling points, with the difference being significant after 6 hours.

In all species treatment pairs, $SUVA_{254}$ values increased over the course of the 96 hour leaching period (Figure 3.3). There were no consistent differences in $SUVA_{254}$ values observed between treatments for each of the three species, but there were significant differences in $SUVA_{254}$ values among the three species. For each of the individual ANOVA tests performed at each sampling time point on $SUVA_{254}$ values, species had a

significant effect at the level $p < 0.0001$. In both the dried and frozen treatments, Salix had significantly higher $SUVA_{254}$ values than Eriophorum or Carex throughout the 96 hour leaching period.

Over the course of the 96 hour leaching period, $a_{250}:a_{365}$ values declined in all species treatment pairs (Figure 3.3). Similar to $SUVA_{254}$, treatment did not have a significant effect on $a_{250}:a_{365}$ values, but differences were observed in $a_{250}:a_{365}$ values among the three species. For each of the individual ANOVA tests performed at each sampling time point, species had a significant effect ($p < 0.05$) on $a_{250}:a_{365}$ values. In the frozen treatment, Salix had higher $a_{250}:a_{365}$ values than *Eriophorum* or *Carex* at all sampling points, with the difference being significant after 6 hours. *Eriophorum* initially had the highest $a_{250}:a_{365}$ values in the dried treatment among the three species, but after 24 hours *Salix* had significantly higher $a_{250}:a_{365}$ values than either *Eriophorum* or *Carex*.

Mean values of C:N ratios, $SUVA_{254}$, and $a_{250}:a_{365}$ of leached material for each species treatment pair at each sampling time point are reported in Appendix B (Table B.1) as well as p-value results for individual two way ANOVA tests performed at each sampling time point (Table B.2). The results of individual sampling time point Tukey Kramer HSD pair-wise comparisons are also provided (Table B.3).

## DISCUSSION

Comparable to previous work examining the release of DOM from foliar plant material and litter, the results from our experimental leaching runs suggest that aboveground Arctic vascular plant material from our three species of interest was a source of readily leachable water soluble DOM. The measured DOC values at the end of 96 hours ranged from $70.5 \pm 1.5$ mg C $g^{-1}$ to $120 \pm 4.6$ mg C $g^{-1}$ and measured TDN values ranged

from 1.1 ± 0.1 mg N $g^{-1}$ to 3.8 ± 0.3 mg N $g^{-1}$ (Figure 3.1). These values are similar to those reported from previous studies investigating C and N release in leachates from aboveground vegetation material from a wide range of plant species from varying ecosystems [e.g., *Cleveland et al*., 2004; *Wickland et al*., 2007]. Additionally, our modeling efforts indicate that the potential maximum amount ($V_{max}$) of leachable DOC and TDN can be as high as 22.2% and 15.8% respectively of the total C and N content of the vegetation material. These potential C and N leaching amounts represent a sizeable proportion of the C and N flux from standing vegetation to the soil surface, and of net primarily production [*Gosz et al*., 1973; *Neff and Asner*, 2001]. As the flux of DOM from vegetation to soils, followed by potential lateral transport to river channels, represents a substantial component of terrestrial C and N cycling [*Neff and Asner*, 2001; *McGuire et al*., 2009], understanding the potential environmental factors affecting leaching dynamics from plant material is of importance and may deserve increased attention in Arctic watersheds as surface vegetation and litter has been linked to the high DOM concentrations observed during spring snowmelt.

The high measured and modeled DOC and TDN release rates during the first hours after the initiation of leaching indicates that aboveground vegetation material is a source of readily available water soluble C and N (Figure 3.1). In all species treatment pairs, over 50% of modeled potential maximum ($t_{50\%}$) leachable DOC and TDN was released during the first 48 hours, and in all but three species treatment pairs it occurred during the initial 24 hours (Table 3.1). While the leaching of DOM and inorganic nutrients from litter during snowmelt has previously been considered in temperate forests [*Yavitt* and *Fahey*; 1986], the relatively quick release of DOC and TDN from vegetation material may be an important consideration in Arctic terrestrial environments where the snowmelt period can be particularly brief. In a small watershed on the North Slope of Alaska, the average snowmelt

period ranged from 7-10 days in length [*Kane et al*., 1997]. During snowmelt, frozen ground limits meltwaters from percolation into deep soil horizons, and the initial limited infiltration of meltwaters into surface soils refreezes at the colder temperatures below the soil subsurface creating ice lenses, further reducing meltwater infiltration and leading to surfacing ponding and possible leaching of aboveground vegetation, litter, and near surface soils [*Woo et al*., 1986].

As the transition from winter to spring can occur rapidly during snowmelt, snowpack water equivalent reductions of 50% can occur over a period as short as two days [*Kane et al*., 1997], the subsequent establishment of surface leaching conditions can be particularly ephemeral. While our modeling of DOC and TDN leaching indicates that there was no significant difference in the maximum amount of C or N released between frozen and dried treatments, differences in initial DOC leaching rates (α) between treatments could influence DOM leaching from plants in Arctic watersheds during the brief spring thaw and subsequently impact DOM export during the freshet (Table 3.1). Higher observed DOC leaching rates in the frozen treatment is likely a result of freezing exerting an effect on the plant material at the cellular level; ice crystal formation may perforate cell walls or membranes, and freezing can disrupt cell organization, the lipid membrane layer, and internal plant material structure, all of which may increase permeability and leaching of water soluble material [*Burke et al*., 1976]. While we observed that frozen plant material had higher DOC leaching rates compared to dried plant material, it should be noted that compared to leaching rates of fresh plant material, drying may have a positive, negative, or neutral effect on DOM release [*Tukey*, 1970; *Taylor and Bärlocher*, 1996]. As neither moisture content, leaf thickness, cuticle thickness, region of growth, or genus are an indicator of the effect of drying on leaching losses, it appears to be a species dependent property [*Taylor and Bärlocher*, 1996]. The species dependent effect may explain the inter

species variation in DOC and TDN leaching losses, as well as the variation in the difference between freezing and drying treatments among the species (Figure 3.1 and Table 3.1).

Among the three plant species there were distinct differences in C:N ratios, indicating compositional differences in DOM leachates (Figure 3.2). Although differences in leachate C:N ratios among the species is a result of the differential strength of freezing and drying effects on DOM leaching for each of the individual species, it is possible that distinct structural differences in foliar material among the species contributed to measured differences in leachate C:N ratios (*Eriophorum* and *Carex* are sedges while *Salix* is a deciduous shrub). However, with the exception of the dried *Eriophorum* species treatment pair, leachate C:N ratios of all other species treatment combinations were general >30 at all measured time points, consistent with observed fluvial DOM C:N ratios in Arctic watersheds that typically range from 30 to 50 during spring snowmelt [e.g., *Guo and Macdonald*, 2006; *Townsend-Small et al*., 2011; *Holmes et al*., 2012; *McClelland et al*., 2014]. Observed differences in C:N ratios between frozen and dried treatments for individual species was a direct result of the combined effect of treatment on DOC and TDN leaching rates. Similarly, the differential strength of treatment effect on DOC and TDN leaching resulted in temporal variations of leachate C:N ratios for individual species suggesting that qualitatively different DOM was released over the 96 hour experiment time course (Figure 3.2).

Temporal variations in CDOM parameters of individual species over the 96 hour leaching interval also reflect compositional changes in DOM leached from plant material (Figure 3.3). $SUVA_{254}$ has been previously used as a proxy for aromaticity of DOM, with higher values related to greater percent aromaticity [*Weishaar et al*., 2003]. In all species treatment pairs $SUVA_{254}$ values increased over time, consistent with initial leaching of DOM with a high percentage of amino acids and carbohydrates including sucrose, glucose,

and fructose [*Suberkropp et al*., 1976; *Hurst et al*., 1985], followed by more structurally complex compounds [*Wickland et al*., 2007]. This is also consistent with the measured decreases in $a_{250}$:$a_{365}$ values over the 96 hour leaching period, with lower values reflecting higher aromaticity and molecular size (Figure 3.3) [*Peuravuori and Pihlaja*, 1997]. Compared to natural river waters in the Yukon watershed (1.3 to 4.5 L mg $C^{-1}$ $m^{-1}$) [*Spencer et al*., 2008], the leachate $SUVA_{254}$ values we measured were comparatively low. However, our values were similar to those from vegetation leachates reported by *Wickland et al*., [2014]. Additionally, *Wickland et al*., [2014] report that their vegetation leachate $SUVA_{254}$ values were all lower than those from soil pore waters. Generally observed increases in river water $SUVA_{254}$ values during the year in the Yukon River watershed [*Spencer et al*., 2008] are consistent with a seasonal shift in the DOM pool from one dominated by vegetation leachates in the spring, to one with a higher proportion derived from soil organic matter.

## IMPLICATIONS

The measured and modeled results of our leaching experiments indicate that aboveground vegetation material from our three test species, representing common Arctic vascular plants, is a source of readily extractable water soluble DOC and TDN. Furthermore, the amounts of C and N released as leachates when immersed in water represented a sizeable percentage of plant foliar C and N content, with as much as 14% C and 8% N released as DOC and TDN in as few as 12 hours of immersion. These rates of DOC release from vegetation are considerably higher than those reported for Arctic soils which can be <1% [*Guo et al*., 2007]. As the potential amounts of C and N released as leachates from foliar material and litter represent a considerable fraction of net primary

production in terrestrial systems [*Neff and Asner*, 2001], and the prevalence of leaching conditions in permafrost influenced areas during the brief transitory spring snowmelt [*Woo et al*., 1986; *Kane et al*., 1997], leaching of previous years aboveground vegetation material and litter may likely play an important role in DOM export dynamics during the freshet in Arctic watersheds.

Upland tussock tundra represents one of two major vegetation community types of Arctic Alaska north of the Brooks Range [*Britton*, 1966], and it is widespread throughout much of the pan-Arctic as well. Of the 8 to 12 species that dominate total plant biomass and production in this community type, *Eriophorum vaginatum* is the dominant vascular species and can account for over 50% of the 60 to 80 g $m^{-2}$ of annual plant production [e.g., *Wein and Bliss*, 1973; *Wein and Bliss* 1974, *Chapin et al*., 1979; *Shaver and Chapin*, 1986]. Using an annual average production value of 20 g $m^{-2}$ for *Eriophorum* and our modeled DOC leaching parameter values, over a 24 hour leaching period we estimate potential leaching of 578 and 1582 mg DOC $m^{-2}$ from dried and frozen aboveground *Eriophorum* material respectively. Scaling up further, assuming 70 g $m^{-2}$ of total vascular plant production per year and using maximum potential leaching amounts for dried and frozen *Eriophorum*, we estimate that 4640 to 7037 mg $m^{-2}$ of DOC could be leached from the overall vegetation matrix.

Our estimated single species 24 hour DOC leaching potential per meter squared is comparable to reported average annual DOC yields calculated based on riverine export of DOC from the North Slope of Alaska [*McClelland et al*, 2014], while our potential maximum leaching yields for total vascular plant growth are considerable larger. This is not surprising given that our experimental leaching yields were determined under conditions in which vegetation material was fully immersed for four days. In any case, these calculations demonstrate that rapidly leached DOM from tundra vegetation may

account for a large proportion of the DOM that is exported from Arctic rivers during the spring freshet. Not all DOM that is leached from vegetation material during snowmelt is expected to reach the ocean, however. Decomposition of vegetation leachates on land and within stream and river channels reduces fluvial export of DOM from watersheds [*Zsolnay and Steindl*, 1991; *Bossier and Fontvieille*, 1993; *Cleveland et* al., 2004; *Wickland et al*., 2007, *Kling et al*., 2014] as does photochemical degradation [*Cory et al*., 2013; *Cory et al*., 2014]. However, rapid transport of water-borne materials from headwaters to river mouths, combined with high sediment loads that limit light penetration, minimize these loss processes during the spring freshet. Although the focus of this study was on vascular plants, non-vascular plant species, such as mosses and lichens, play an important role in terrestrial carbon and nitrogen cycles and may make up a sizeable amount of annual production in Arctic tundra communities [e.g., *Chapin et al*., 1995]. Mosses have similarly been demonstrated to leach considerable amounts of DOM when used in leaching experiments [*Wickland et al*., 2007].

While our modeling of DOM leaching dynamics indicate that frozen and dried aboveground vegetation material from our three Arctic plant species of interest have similar maximum DOC and TDN leaching potentials, our results suggest that frozen material has higher initial DOC leaching rates compared to dried material. The effects of freezing and drying on initial DOC leaching may be an important consideration in understanding the mechanisms controlling spring DOM export dynamics during the short spring snowmelt period. While previous studies have examined repeated freeze-thaw cycles on DOM release from foliar plant material of sub-Antarctic species, these investigations collected plants in the spring and their short freeze-thaw cycles (24 hours) attempted to mimic conditions in the spring [*Hurst et al*., 1985, *Melick et al*., 1992]. In Arctic watersheds, it may be appropriate to consider environmental conditions experienced

by senesced aboveground vegetation material during the late summer and fall and their potentially impacts on DOM leaching dynamics during the following spring. For example, an earlier occurrence of sub-freezing conditions, before full plant senescence at the end of the growing season when plant leaves still have available water content for ice crystal formation, could result in increased cell damage and permeability increasing DOM losses in spring. Alternatively, a longer number of days post senescence, but before sub-freezing conditions, could result in increased drying of plant material. The conditions experienced by plants over winter may also be relevant. Snow cover can act as an insulator against extreme air temperatures (-30°C) and high internal humidity within the snowpack can reduce plant desiccation [*Huryn and Hobbie*, 2012].

As freezing and drying conditions experienced by aboveground plant material post senescence may affect DOM leaching during the subsequent snowmelt, the impacts of Arctic climate change on late summer, fall, and winter climatic conditions and the resulting plant responses merits consideration. A longer snow and ice-free period [*Ueyama et al.*, 2003; *Pearson et al.*, 2013] could potentially lead to an increase in the number of days post senescence in which plants are susceptible to air drying. This may be counteracted by an increase in the length of the growing season, however, while earlier onset of spring phenology has been observed in the Arctic and the climatic factors controlling these events are well understood, there is currently limited evidence that indicates a later onset of autumnal phenological events, and these shifts are less pronounced and show more heterogeneity [*Walther et al*., 2002; *Ernakovich et al*., 2014]. Additionally, climate change is expected to result in greater amounts of winter precipitation, northward movement of the seasonal snow cover boundary, and a deeper snow cover overall in the Arctic [*White et al*., 2007]. While our understanding of seasonal DOM export dynamics in Arctic watersheds is improving, our knowledge of the mechanisms that influence DOM export remains

limited, and a greater understanding of the factors that affect these controls is essential for predicting how these systems will respond to climate change.

Table 3.1. Mean (standard error) values of model parameters $V_{max}$, $t_{50\%}$, $t_{90\%}$, and α for all species treatment pairs for both DOC and TDN. A connecting letters report format is used for the results of statistical comparisons among all species treatment combinations for each model parameter for both DOC and TDN. Cells that are not connected by the same letter have significantly different mean values. Where there are statistical differences, "A" marks the highest mean value, "B" the next highest value, "C" the next highest value, etc.

| Vegetation | Treatment | $V_{max}$ (mg C/N g dry $wt^{-1}$) | | $t_{50}$ (hours) | | $t_{90}$ (days) | | α (mg C/N g dry $wt^{-1}$ $hr^{-1}$) | |
|---|---|---|---|---|---|---|---|---|---|
| DOC | | | | | | | | | |
| *Eriophorum* | dried | 84.6 (2.1) | CD | 46.7 (3.4) | A | 17.5 (1.27) | A | 1.83 (0.15) | D |
| *Eriophorum* | frozen | 105.3 (11.0) | ABC | 7.9 (0.7) | C | 2.9 (0.27) | C | 13.41 (0.93) | A |
| *Carex* | dried | 70.5 (1.5) | D | 14.4 (0.9) | C | 5.4 (0.32) | C | 4.95 (0.42) | C |
| *Carex* | frozen | 88.5 (8.8) | BCD | 11.6 (0.4) | C | 4.4 (0.14) | C | 7.58 (0.51) | B |
| *Salix* | dried | 112.7 (1.6) | AB | 24.9 (1.0) | B | 9.3 (0.36) | B | 4.54 (0.19) | C |
| *Salix* | frozen | 120.7 (4.6) | A | 13.1 (0.1) | C | 4.9 (0.04) | C | 9.20 (0.27) | B |
| TDN | | | | | | | | | |
| *Eriophorum* | dried | 3.78 (0.25) | A | 26.2 (4.2) | A | 9.8 (1.59) | A | 0.15 (0.02) | AB |
| *Eriophorum* | frozen | 2.37 (0.20) | B | 9.3 (1.2) | B | 3.5 (0.45) | B | 0.26 (0.02) | A |
| *Carex* | dried | 2.55 (0.19) | B | 12.9 (0.7) | B | 4.8 (0.26) | B | 0.20 (0.03) | AB |
| *Carex* | frozen | 2.78 (0.16) | B | 13.0 (1.2) | B | 4.9 (0.44) | B | 0.22 (0.01) | AB |
| *Salix* | dried | 1.47 (0.07) | C | 14.2 (2.7) | B | 5.3 (1.03) | B | 0.11 (0.02) | B |
| *Salix* | frozen | 1.11 (0.03) | C | 7.2 (1.6) | B | 2.7 (0.62) | B | 0.17 (0.04) | AB |

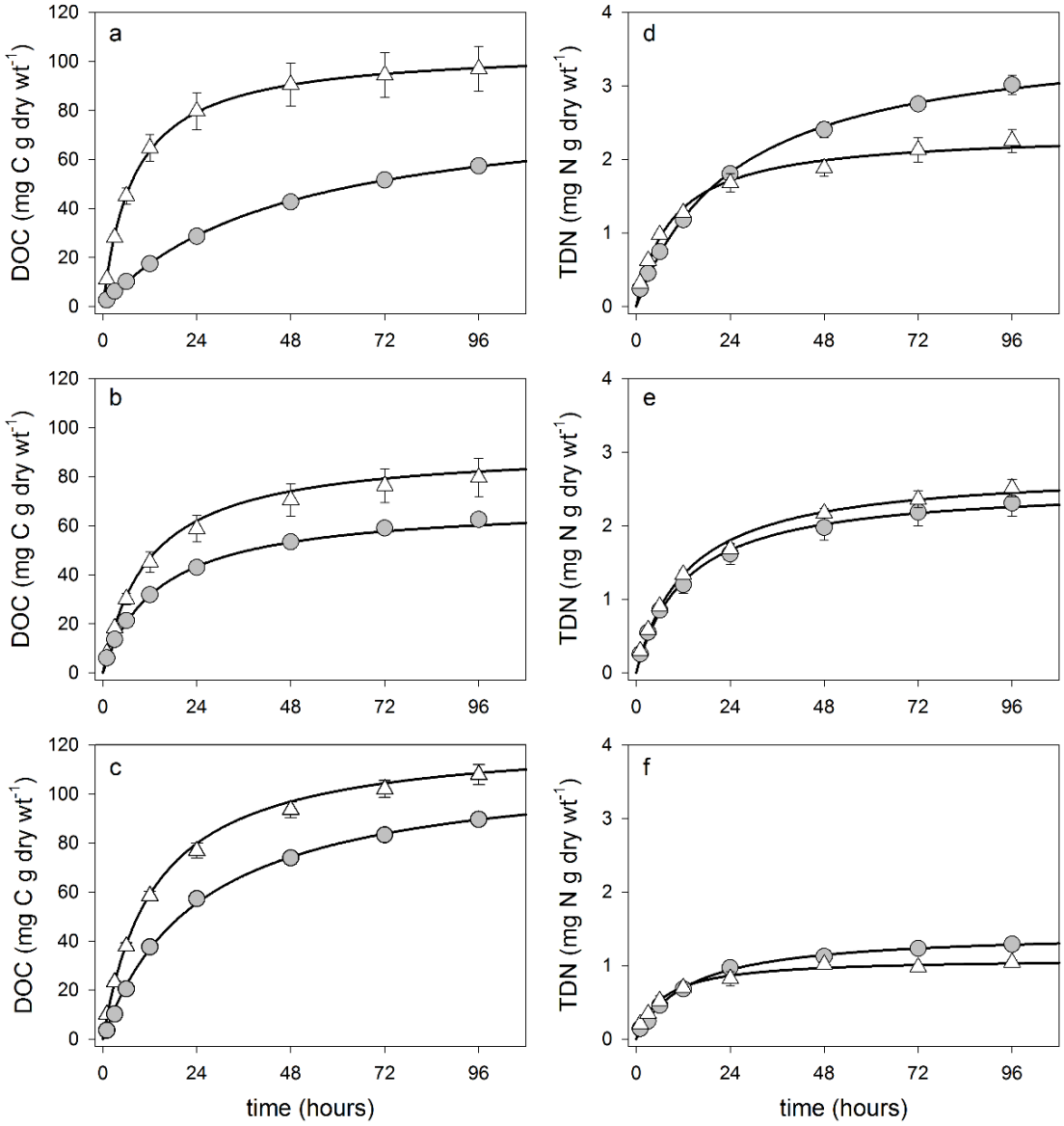


Figure 3.1. Modeled values (solid black lines) and measured mean values (symbols) of the amount of DOC and TDN leached from plant material during leaching runs for *Eriophorum* (a, d), *Carex* (b, e), and *Salix* (c, f). White triangles correspond to plant material that was frozen, while grey circles correspond to plant material that was dried. Symbol error bars represent ± standard error. Modeled values of leached DOC and TDN were calculated using the measured mean values of each species treatment pair. All values are normalized by the amount of dry weight vegetation added for each individual species treatment leaching run.

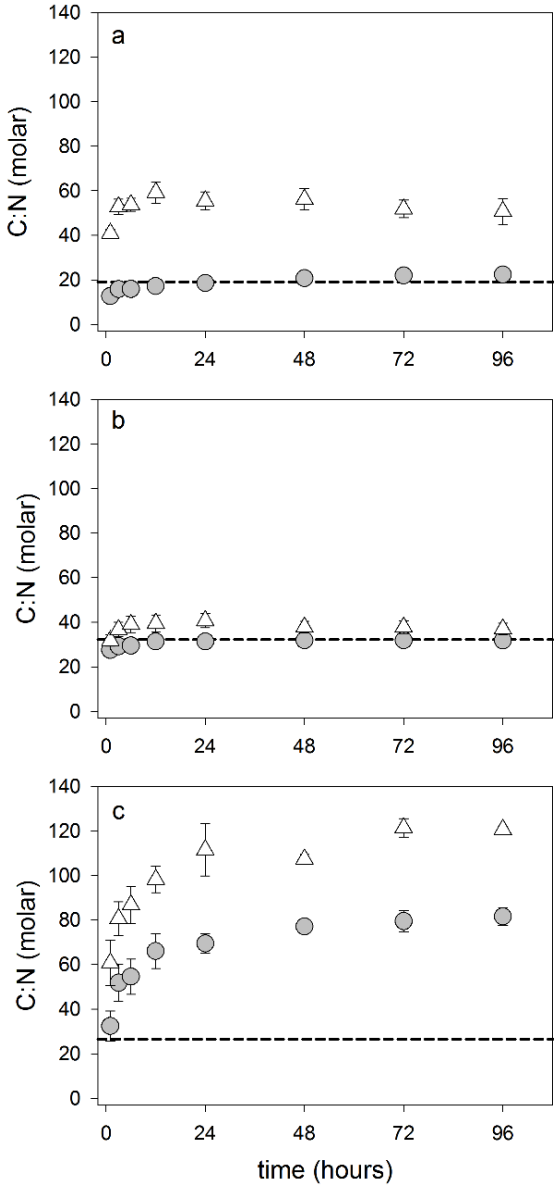


Figure 3.2. Mean C:N molar ratios of vegetation leachates at each sampling time point for *Eriophorum* (a), *Carex* (b), and *Salix* (c). White triangles correspond to plant material that was frozen, while grey circles correspond to plant material that was dried. Symbol error bars represent ± standard error. Dashed lines represent source material C:N molar ratios for each of the different plant types.

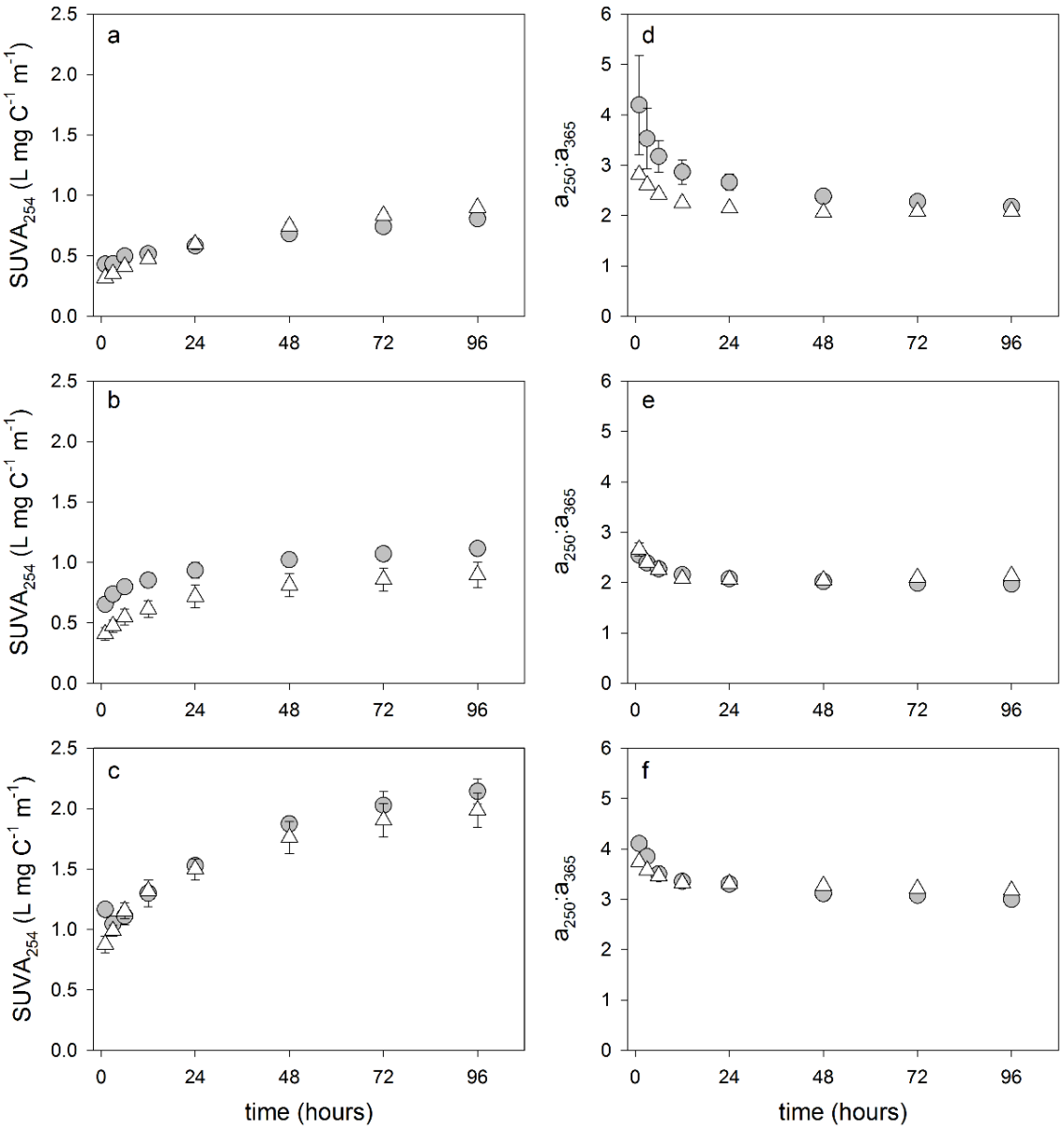


Figure 3.3. Mean values of chromophoric dissolved organic matter (CDOM) parameters of vegetation leachates at each sampling time point for *Eriophorum* (a, d), *Carex* (b, e), and *Salix* (c, f). White triangles correspond to plant material that was frozen, while grey circles correspond to plant material that was dried. Symbol error bars represent ± standard error.

# Overall Conclusions

The results of the studies contained in this dissertation provided an unprecedented characterization of organic matter (OM) and inorganic nitrogen seasonal dynamics spanning the entire hydrologic year from spring thaw through fall freeze-up in Alaskan Arctic streams and rivers (May-October). Although detailed seasonally comprehensive studies of similar scope have been carried out at sub-Arctic catchments [e.g., *MacLean et al.*, 1999; *Jones et al.*, 2005; *Petrone et al.*, 2006] the breadth and high resolution sample data sets presented in Chapter 1 and Chapter 2 are unique to Arctic environments. Additionally, the vegetation leaching experiment in Chapter 3 explores a possible mechanism influencing dissolved OM export dynamics during the spring freshet in Arctic catchments and factors that may affect dissolved OM leaching dynamics. Although there has been an increased understanding of OM and inorganic nitrogen seasonality during the spring freshet in Arctic rivers over the past decade [e.g., *McNamara et al*., 2008; *Townsend-Small et al*., 2011, *Holmes et al*., 2012; *McClelland et al*., 2014], knowledge of riverine OM and inorganic nitrogen export processes remain limited during the late summer and fall. Although absolute fluxes of OM and inorganic nitrogen during the late summer and fall may be relatively small compared to those early during the hydrologic year, the ecological fate of this material may be vastly different than that exported during the spring.

The increased understanding of OM and inorganic nitrogen seasonal variation, both in terms of quantity and quality of organic matter, in Arctic rivers is reshaping past paradigms regarding the role of river supplied material as a resource for supporting productivity in coastal ecosystems. This may be especially important in near shore estuarine environments where terrestrial inputs are likely to have the largest effect. While

studies examining the interactions of riverine inputs and productivity within Arctic estuaries are relatively limited, past investigations suggested that terrestrial inputs played a relatively minor role in supporting biological production in coastal waters. In particular, *Schell* [1983] came to this conclusion based on a large difference between the radiocarbon age of particulate OM exported by rivers (thousands of years old) and the radiocarbon age of select consumers (modern) from coastal waters of the Alaskan Beaufort Sea. Bulk radiocarbon ages of particulate OM exported by Arctic rivers are typically "old" throughout the year [e.g., *Guo et al*., 2007], however, our particulate OM $\delta^{13}C$ values indicate that some fraction of the particulate OM pool is composed of "new" autochthonous production, which would likely be highly labile and preferentially utilized in downstream ecosystems. Similarly, *Schell* [1983] only considered the transfer of particulate OM to coastal marine consumers, but did not consider dissolved OM. As dissolved OM is much younger (decades) than particulate OM [e.g., *Raymond et al*., 2007], and dissolved OM exported during the spring has been shown to be quite labile [*Holmes et al*., 2008], its potential as source of energy and nutrients is warranted. However, as reported by *Holmes et al*., [2008] dissolved OM decomposition rates may ultimately be constrained by the availability of inorganic nitrogen.

Inorganic nitrogen concentrations are generally low during the spring snowmelt period [e.g., *Townsend-Small*, 2011], and may therefore limit organic matter remineralization early in the year. However, as reported in Chapter 2, the increased DIN concentrations during the late summer and fall may provide an important nitrogen subsidy to estuarine ecosystems that can be used to support late-season production or build up and be used during the subsequent spring. During the spring snowmelt, mixing of high nutrient coastal waters with highly labile dissolved OM river waters could promote remineralization of terrestrial dissolved OM and possibly support biological production at higher trophic

levels. On the other hand, the large seasonal discharge events associated with the spring snowmelt in Arctic rivers could displace much of the nutrient rich coastal waters without an observed enhancement of decomposition. It becomes increasingly apparent that both an understanding of the seasonal variation in OM fluxes as well as inorganic nitrogen fluxes is essential in order to have a complete understanding of the potential transfer of terrestrial OM to higher trophic levels within coastal Arctic Ocean systems.

As rivers integrate biogeochemical processes throughout their watersheds the distinct seasonal trends in both OM and inorganic nitrogen concentrations may serve as valuable proxies for climate change related impacts. For example, progressive decreases in C:N ratios of dissolved OM indicate an increased source contribution from deeper soils during the summer and fall. Seasonal decreases in dissolved OM C:N ratios may be useful for tracking landscape scale thaw on an annual time scale, and over longer periods, a decreasing trend in late season dissolved OM C:N ratios may signal an increase in maximum thaw depth of the active layer or exposure of older reworked soil OM. Likewise, the timing of dissolved inorganic nitrogen increases during the fall at our six study sites corresponded with deepening of the seasonally thawed soil layer to maximum depth, and is consistent with reduced biological uptake demand in late summer and fall. As such, increases in DIN concentrations over the hydrologic year would also be a useful proxy for landscape scale thaw on seasonal scale and possible multiple year time frame. Increased monitoring of river constituents during the late summer and fall during maximum seasonal soil thaw depth could potential signal climate change induced impacts.

The results of the seasonally comprehensive studies in Chapters 1 and 2 provide a unique investigation of OM and inorganic nitrogen dynamics from streams and rivers on the North Slope of Alaska. Although our spring and summer OM and inorganic nitrogen values are comparable to previously reported values from the same study area [e.g.,

*Peterson et al.*, 1986; *Peterson et al*, 1992; *Townsend-Small et al.*, 2011] and region [e.g., *Rember and Trefry*, 2004; *McNamara et al.*, 2008; *McClelland et al.*, 2014], the paucity of studies sampling during late summer and fall through freeze-up make comparisons of late season values challenging. Further studies focused on late season sampling from other areas of Arctic Alaska would be beneficial to our understanding of seasonal dynamics. Likewise, while our experimental investigation of factors contributing to dissolved OM export during the spring freshet provides valuable mechanistic information, further investigations into end-member sources and the processes contributing to observed riverine chemistry are needed.

# Appendices

## Appendix A: Chapter 1 Supplementary Material

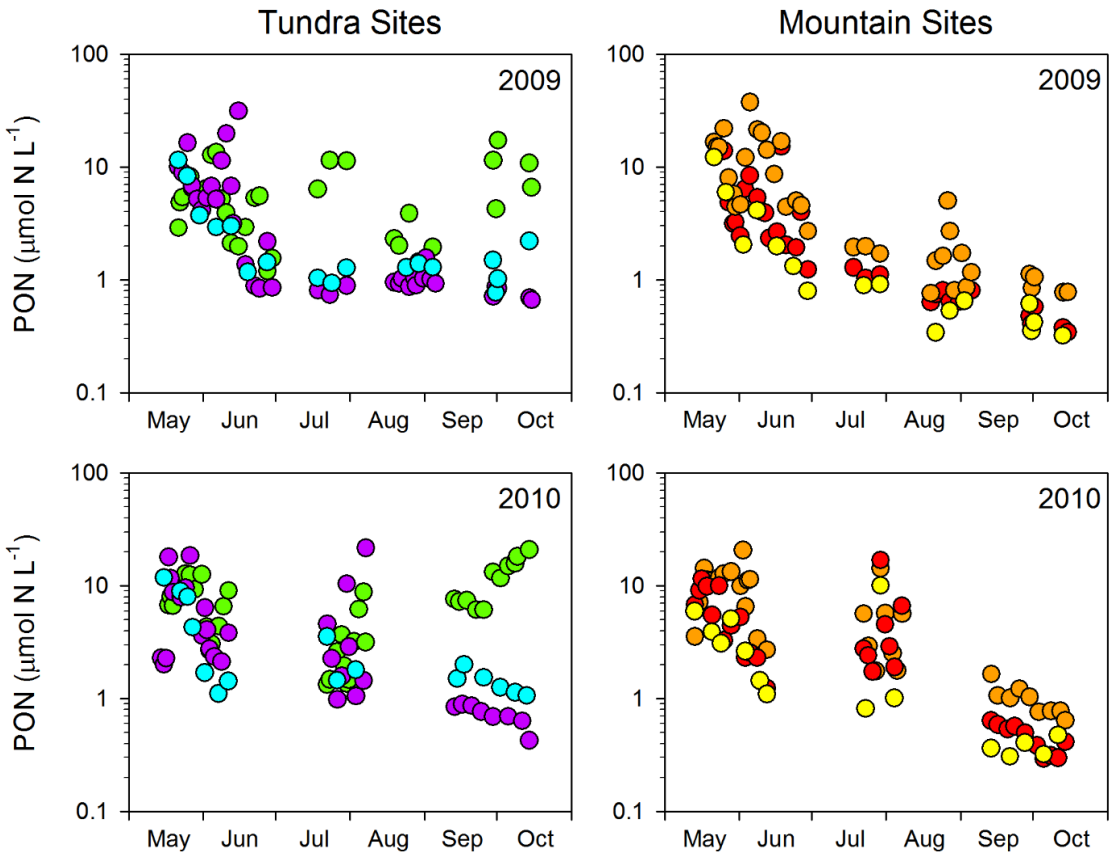


Figure A.1. Temporal variation in PON concentrations of riverine surface waters from tundra sites and mountain sites from 2009 and 2010. Purple markers correspond to Kuparuk, green to Imnavait, blue to Oksrukuyik, orange to Atigun, red to Roche, and yellow to Trevor.

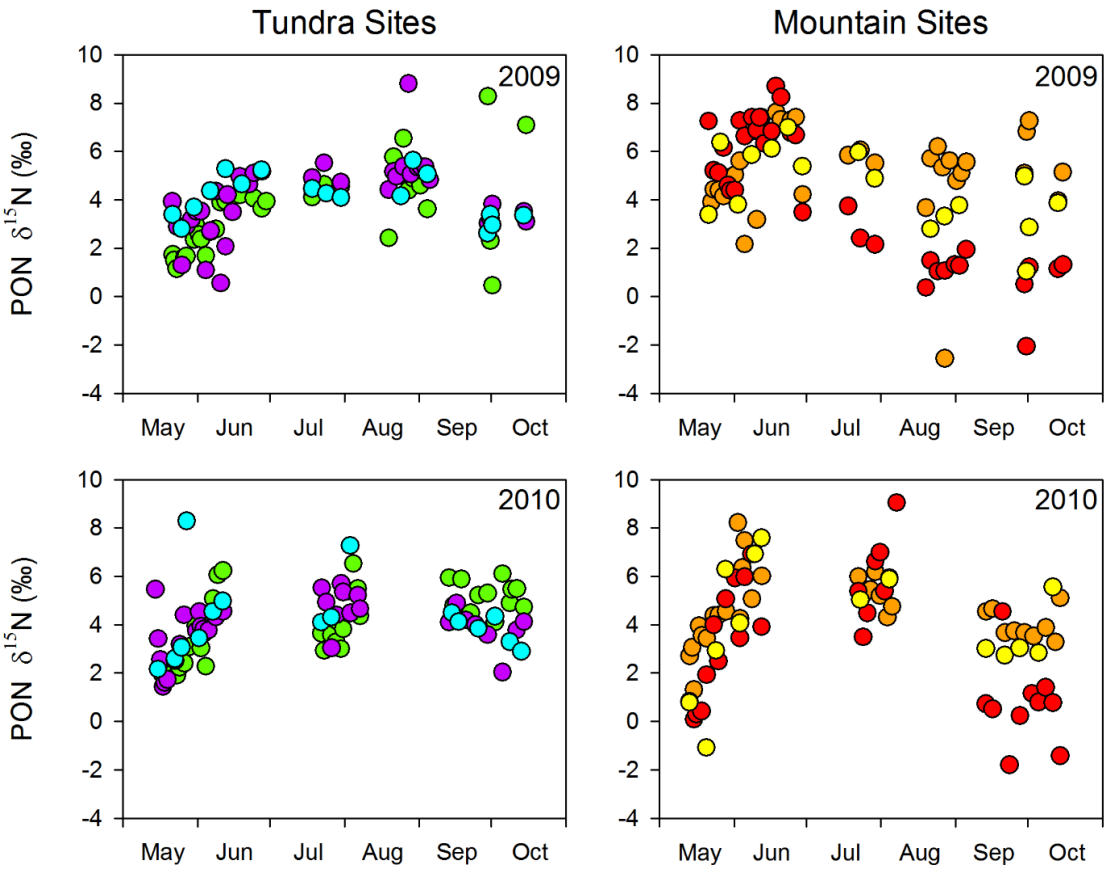


Figure A.2. Temporal variations in $\delta^{15}N$ values of particulate OM from tundra sites and mountain sites from 2009 and 2010. Purple markers correspond to the Kuparuk, green to Imnavait, blue to Oksrukuyik, orange to Atigun, red to Roche, and yellow to Trevor.

# APPENDIX B: CHAPTER 3 SUPPLEMENTARY MATERIAL

## APPENDIX B: CHAPTER 3 SUPPLEMENTARY MATERIAL

Table B.1. Mean values (standard errors) for DOC, TDN, C:N molar ratios, $SUVA_{254}$, and $\alpha_{250}:\alpha_{365}$ at each experimental sampling time point.

| Vegetation | Treatment | 1 hr | 3 hrs | 6 hrs | 12 hrs | 24 hrs | 48 hrs | 72 hrs | 96 hrs |
|---|---|---|---|---|---|---|---|---|---|
| DOC (mg C g dry $wt^{-1}$) | | | | | | | | | |
| *Eriophorum* | dried | 2.6 (0.3) | 6.1 (0.8) | 10.1 (0.7) | 17.4 (1.2) | 28.6 (1.6) | 42.6 (1.9) | 51.6 (1.9) | 57.3 (2.1) |
| *Eriophorum* | frozen | 11.2 (0.7) | 28.1 (1.5) | 45.0 (3.3) | 64.6 (5.5) | 79.6 (7.5) | 90.4 (8.7) | 94.4 (9.1) | 96.9 (9.1) |
| *Carex* | dried | 6.0 (0.4) | 13.6 (0.9) | 21.3 (1.5) | 31.8 (1.7) | 43.0 (1.6) | 53.4 (2.0) | 59.0 (1.8) | 62.4 (1.9) |
| *Carex* | frozen | 8.0 (0.3) | 18.2 (0.9) | 30.1 (2.4) | 45.1 (4.2) | 58.7 (5.4) | 70.4 (6.6) | 76.3 (6.9) | 79.6 (7.8) |
| *Salix* | dried | 3.6 (0.3) | 10.2 (0.5) | 20.4 (0.9) | 37.5 (0.2) | 57.2 (1.6) | 73.8 (2.5) | 83.2 (1.2) | 89.5 (1.2) |
| *Salix* | frozen | 10.0 (0.2) | 23.1 (0.5) | 37.8 (1.4) | 58.3 (1.8) | 76.8 (3.1) | 93.4 (3.2) | 102.0 (3.4) | 107.8 (4.1) |
| TDN (mg N g dry $wt^{-1}$) | | | | | | | | | |
| *Eriophorum* | dried | 0.24 (0.01) | 0.45 (0.03) | 0.74 (0.05) | 1.18 (0.04) | 1.80 (0.09) | 2.40 (0.11) | 2.75 (0.09) | 3.01 (0.13) |
| *Eriophorum* | frozen | 0.32 (0.01) | 0.62 (0.02) | 0.98 (0.02) | 1.27 (0.03) | 1.68 (0.12) | 1.88 (0.11) | 2.13 (0.17) | 2.25 (0.16) |
| *Carex* | dried | 0.26 (0.02) | 0.55 (0.07) | 0.85 (0.10) | 1.20 (0.12) | 1.62 (0.14) | 1.97 (0.17) | 2.18 (0.19) | 2.31 (0.18) |
| *Carex* | frozen | 0.30 (0.02) | 0.58 (0.02) | 0.90 (0.02) | 1.34 (0.06) | 1.68 (0.06) | 2.17 (0.07) | 2.36 (0.12) | 2.51 (0.12) |
| *Salix* | dried | 0.14 (0.03) | 0.24 (0.04) | 0.46 (0.08) | 0.68 (0.08) | 0.97 (0.08) | 1.12 (0.07) | 1.23 (0.09) | 1.29 (0.08) |
| *Salix* | frozen | 0.20 (0.03) | 0.34 (0.04) | 0.52 (0.06) | 0.70 (0.05) | 0.82 (0.10) | 1.02 (0.04) | 0.98 (0.0) | 1.04 (0.04) |
| C:N (molar) | | | | | | | | | |
| *Eriophorum* | dried | 12.7 (0.8) | 15.8 (1.3) | 15.9 (0.7) | 17.2 (0.8) | 18.5 (0.8) | 20.7 (1.2) | 21.9 (1.1) | 22.3 (1.6) |
| *Eriophorum* | frozen | 40.9 (1.7) | 52.8 (3.5) | 53.7 (2.9) | 59.2 (4.8) | 55.4 (4.1) | 56.1 (4.8) | 51.8 (4.0) | 50.7 (5.8) |
| *Carex* | dried | 27.6 (1.4) | 29.2 (1.5) | 29.5 (1.8) | 31.3 (1.7) | 31.3 (1.8) | 31.8 (1.8) | 31.8 (1.8) | 31.8 (1.5) |
| *Carex* | frozen | 31.8 (2.6) | 36.7 (3.3) | 39.0 (3.7) | 39.5 (3.7) | 40.7 (3.2) | 37.8 (2.6) | 37.8 (2.8) | 36.9 (2.7) |
| *Salix* | dried | 32.4 (6.7) | 51.8 (8.2) | 54.6 (7.9) | 66.1 (7.8) | 69.4 (4.4) | 77.1 (2.7) | 79.5 (4.7) | 81.5 (4.1) |
| *Salix* | frozen | 60.8 (10.1) | 80.6 (7.6) | 86.8 (8.4) | 98.2 (5.9) | 111.5 (11.7) | 107.3 (2.4) | 121.4 (4.2) | 120.7 (1.5) |

Table B.1. Continued

| Vegetation | Treatment | 1 hr | 3 hrs | 6 hrs | 12 hrs | 24 hrs | 48 hrs | 72 hrs | 96 hrs |
|---|---|---|---|---|---|---|---|---|---|
| $SUVA_{254}$ (L mg $C^{-1}$ $m^{-1}$) | | | | | | | | | |
| *Eriophorum* | dried | 0.43 (0.03) | 0.43 (0.03) | 0.50 (0.02) | 0.52 (0.02) | 0.58 (0.03) | 0.68 (0.02) | 0.74 (0.02) | 0.81 (0.03) |
| *Eriophorum* | frozen | 0.32 (0.02) | 0.35 (0.03) | 0.41 (0.04) | 0.47 (0.04) | 0.60 (0.04) | 0.74 (0.04) | 0.83 (0.03) | 0.90 (0.03) |
| *Carex* | dried | 0.65 (0.03) | 0.74 (0.05) | 0.80 (0.05) | 0.85 (0.06) | 0.93 (0.07) | 1.02 (0.06) | 1.07 (0.06) | 1.11 (0.06) |
| *Carex* | frozen | 0.41 (0.05) | 0.48 (0.05) | 0.55 (0.07) | 0.61 (0.07) | 0.72 (0.09) | 0.81 (0.10) | 0.86 (0.10) | 0.90 (0.10) |
| *Salix* | dried | 1.17 (0.02) | 1.05 (0.05) | 1.11 (0.07) | 1.30 (0.11) | 1.53 (0.05) | 1.87 (0.06) | 2.03 (0.11) | 2.14 (0.11) |
| *Salix* | frozen | 0.88 (0.07) | 0.99 (0.05) | 1.15 (0.06) | 1.32 (0.04) | 1.50 (0.09) | 1.76 (0.13) | 1.90 (0.14) | 1.99 (0.14) |
| $\alpha_{250}:\alpha_{365}$ | | | | | | | | | |
| *Eriophorum* | dried | 4.20 (0.99) | 3.53 (0.59) | 3.17 (0.31) | 2.86 (0.24) | 2.66 (0.16) | 2.38 (0.11) | 2.27 (0.11) | 2.18 (0.07) |
| *Eriophorum* | frozen | 2.81 (0.10) | 2.60 (0.06) | 2.42 (0.04) | 2.25 (0.04) | 2.14 (0.03) | 2.06 (0.03) | 2.07 (0.04) | 2.08 (0.04) |
| *Carex* | dried | 2.55 (0.14) | 2.39 (0.09) | 2.27 (0.10) | 2.15 (0.09) | 2.07 (0.06) | 2.02 (0.06) | 1.98 (0.05) | 1.97 (0.04) |
| *Carex* | frozen | 2.66 (0.14) | 2.40 (0.07) | 2.26 (0.09) | 2.08 (0.06) | 2.06 (0.06) | 2.05 (0.06) | 2.10 (0.02) | 2.14 (0.05) |
| *Salix* | dried | 4.10 (0.04) | 3.85 (0.11) | 3.50 (0.04) | 3.36 (0.06) | 3.30 (0.09) | 3.11 (0.14) | 3.07 (0.09) | 2.99 (0.07) |
| *Salix* | frozen | 3.74 (0.05) | 3.57 (0.04) | 3.46 (0.03) | 3.32 (0.05) | 3.31 (0.03) | 3.27 (0.03) | 3.21 (0.03) | 3.17 (0.02) |

Table B.2. Summary of p-values for individual two way ANOVA tests performed at each sampling time point on the leaching yields of DOC and TDN, the C:N molar ratios of leached dissolved material, and the CDOM optical parameters $SUVA_{254}$ and $a_{250}$:$a_{365}$. Values in bold are below the p = 0.05 threshold.

| Effect | 1 hr | 3 hrs | 6 hrs | 12 hrs | 24 hrs | 48 hrs | 72 hrs | 96 hrs |
|---|---|---|---|---|---|---|---|---|
| DOC | | | | | | | | |
| *species* | 0.8499 | 0.4443 | 0.2437 | **0.0244** | **0.0052** | **0.002** | **0.0008** | **0.0006** |
| *treatment* | **<0.0001** | **<0.0001** | **<0.0001** | **<0.0001** | **<0.0001** | **<0.0001** | **<0.0001** | **<0.0001** |
| *species*treatment* | **<0.0001** | **<0.0001** | **<0.0001** | **0.0003** | **0.002** | **0.015** | **0.0444** | 0.1001 |
| TDN | | | | | | | | |
| *species* | **0.0004** | **<0.0001** | **<0.0001** | **<0.0001** | **<0.0001** | **<0.0001** | **<0.0001** | **<0.0001** |
| *treatment* | **0.0048** | **0.0083** | **0.0421** | 0.165 | 0.4222 | 0.116 | **0.0401** | **0.0225** |
| *species*treatment* | 0.6478 | 0.2618 | 0.3095 | 0.674 | 0.5392 | **0.0158** | **0.0244** | **0.0081** |
| C:N (molar) | | | | | | | | |
| *species* | **0.0048** | **<0.0001** | **<0.0001** | **<0.0001** | **<0.0001** | **<0.0001** | **<0.0001** | **<0.0001** |
| *treatment* | **0.0004** | **<0.0001** | **<0.0001** | **<0.0001** | **<0.0001** | **<0.0001** | **<0.0001** | **<0.0001** |
| *species*treatment* | 0.0583 | **0.0328** | **0.0397** | **0.0112** | **0.0272** | **0.0005** | **0.0006** | **0.0007** |
| $SUVA_{254}$ | | | | | | | | |
| *species* | **<0.0001** | **<0.0001** | **<0.0001** | **<0.0001** | **<0.0001** | **<0.0001** | **<0.0001** | **<0.0001** |
| *treatment* | **<0.0001** | **0.0027** | 0.0518 | 0.1226 | 0.1758 | 0.1926 | 0.2743 | 0.2146 |
| *species*treatment* | 0.1226 | 0.0664 | 0.0601 | 0.1534 | 0.2091 | 0.2383 | 0.2359 | 0.2123 |
| $a_{250}$:$a_{365}$ | | | | | | | | |
| *species* | **0.0222** | **0.0009** | **<0.0001** | **<0.0001** | **<0.0001** | **<0.0001** | **<0.0001** | **<0.0001** |
| *treatment* | 0.1328 | 0.0801 | **0.0371** | **0.0215** | **0.0258** | 0.5224 | 0.7576 | 0.0722 |
| *species*treatment* | 0.2222 | 0.2082 | **0.0343** | **0.0432** | **0.0122** | **0.0373** | **0.0396** | **0.0402** |

Table B.3. Connecting letters report for the results of statistical comparisons among all species/treatment combinations for DOC, TDN, C:N molar ratios, $SUVA_{254}$, and $\alpha_{250}$:$\alpha_{365}$ at each experimental sampling time point. Cells that are not connected by the same letter have significantly different mean values. Where there are statistical differences, "A" marks the highest mean value, "B" the next highest value, "C" the next highest value, etc.

| Vegetation | Treatment | 1 hr | 3 hrs | 6 hrs | 12 hrs | 24 hrs | 48 hrs | 72 hrs | 96 hrs |
|---|---|---|---|---|---|---|---|---|---|
| DOC | | | | | | | | | |
| *Eriophorum* | dried | D | E | E | D | D | C | D | C |
| *Eriophorum* | frozen | A | A | A | A | A | A | AB | AB |
| *Carex* | dried | C | D | CD | CD | CD | BC | CD | C |
| *Carex* | frozen | B | C | BC | BC | BC | AB | BC | BC |
| *Salix* | dried | D | DE | D | C | BC | AB | AB | AB |
| *Salix* | frozen | A | B | AB | AB | AB | A | A | A |
| TDN | | | | | | | | | |
| *Eriophorum* | dried | ABC | AB | AB | A | A | A | A | A |
| *Eriophorum* | frozen | A | A | A | A | A | B | B | B |
| *Carex* | dried | AB | A | A | A | A | AB | AB | B |
| *Carex* | frozen | AB | A | A | A | A | AB | AB | AB |
| *Salix* | dried | C | C | B | B | B | C | C | C |
| *Salix* | frozen | BC | BC | B | B | B | C | C | C |
| C:N (molar) | | | | | | | | | |
| *Eriophorum* | dried | C | C | D | D | D | E | D | D |
| *Eriophorum* | frozen | AB | B | BC | BC | BC | C | C | C |
| *Carex* | dried | BC | BC | CD | D | CD | DE | D | D |
| *Carex* | frozen | BC | BC | BCD | CD | CD | D | CD | CD |
| *Salix* | dried | BC | B | B | B | B | B | B | B |
| *Salix* | frozen | A | A | A | A | A | A | A | A |

Table B.3. Continued

| Vegetation | Treatment | 1 hr | 3 hrs | 6 hrs | 12 hrs | 24 hrs | 48 hrs | 72 hrs | 96 hrs |
|---|---|---|---|---|---|---|---|---|---|
| $SUVA_{254}$ | | | | | | | | | |
| *Eriophorum* | dried | D | C | C | C | C | B | B | B |
| *Eriophorum* | frozen | D | C | C | C | C | B | B | B |
| *Carex* | dried | C | B | B | B | B | B | B | B |
| *Carex* | frozen | D | C | BC | BC | BC | B | B | B |
| *Salix* | dried | A | A | A | A | A | A | A | A |
| *Salix* | frozen | B | A | A | A | A | A | A | A |
| a250:a365 | | | | | | | | | |
| *Eriophorum* | dried | A | AB | A | A | B | B | B | B |
| *Eriophorum* | frozen | A | B | B | B | C | B | B | B |
| *Carex* | dried | A | B | B | B | C | B | B | B |
| *Carex* | frozen | A | B | B | B | C | B | B | B |
| *Salix* | dried | A | A | A | A | A | A | A | A |
| *Salix* | frozen | A | AB | A | A | A | A | A | A |

Table B.4. Modeled outputs of equation parameters for individual species treatment pair leaching runs for DOC and TDN. The $r^2$ values are from the linear regressions of measured DOC and TDN yields against modeled DOC and TDN yields for individual leaching runs.

| Vegetation | Treatment | $V_{max}$ (mg C g dry $wt^{-1}$) | $t_{50\%}$ (hours) | $t_{90\%}$ (days) | $\alpha$ (mg C g dry $wt^{-1}$ $hr^{-1}$) | $r^2$ |
|---|---|---|---|---|---|---|
| DOC | | | | | | |
| *Eriophorum* | dried | 88.3 | 49.5 | 18.5 | 1.79 | 0.9999 |
| *Eriophorum* | dried | 81.1 | 50.6 | 19.0 | 1.60 | 0.9994 |
| *Eriophorum* | dried | 84.5 | 39.9 | 15.0 | 2.12 | 0.9990 |
| *Eriophorum* | frozen | 85.4 | 7.2 | 2.7 | 11.85 | 0.9997 |
| *Eriophorum* | frozen | 123.4 | 9.3 | 3.5 | 13.28 | 0.9991 |
| *Eriophorum* | frozen | 107.1 | 7.1 | 2.7 | 15.08 | 0.9992 |
| *Carex* | dried | 69.2 | 14.8 | 5.5 | 4.68 | 0.9979 |
| *Carex* | dried | 68.8 | 15.7 | 5.9 | 4.39 | 0.9989 |
| *Carex* | dried | 73.5 | 12.7 | 4.8 | 5.77 | 0.9978 |
| *Carex* | frozen | 104.3 | 12.3 | 4.6 | 8.49 | 0.9992 |
| *Carex* | frozen | 87.5 | 11.6 | 4.3 | 7.55 | 0.9995 |
| *Carex* | frozen | 73.7 | 11.0 | 4.1 | 6.71 | 0.9984 |
| *Salix* | dried | 110.3 | 26.2 | 9.8 | 4.20 | 0.9972 |
| *Salix* | dried | 115.8 | 25.5 | 9.5 | 4.55 | 0.9992 |
| *Salix* | dried | 112.0 | 23.1 | 8.7 | 4.85 | 0.9984 |
| *Salix* | frozen | 123.9 | 13.2 | 5.0 | 9.36 | 0.9993 |
| *Salix* | frozen | 126.5 | 13.2 | 5.0 | 9.56 | 0.9990 |
| *Salix* | frozen | 111.7 | 12.9 | 4.8 | 8.67 | 0.9988 |

Table B.4. Continued

| Vegetation | Treatment | $V_{max}$ (mg N g dry wt $^{-1}$) | $t_{50\%}$ (hours) | $t_{90\%}$ (days) | α (mg N g dry wt$^{-1}$ hr$^{-1}$) | $r^2$ |
|---|---|---|---|---|---|---|
| TDN | | | | | | |
| *Eriophorum* | dried | 4.0 | 26.1 | 9.8 | 0.15 | 0.9990 |
| *Eriophorum* | dried | 4.0 | 33.7 | 12.6 | 0.12 | 0.9971 |
| *Eriophorum* | dried | 3.3 | 19.0 | 7.1 | 0.17 | 0.9981 |
| *Eriophorum* | frozen | 2.4 | 9.9 | 3.7 | 0.24 | 0.9753 |
| *Eriophorum* | frozen | 2.7 | 11.0 | 4.1 | 0.25 | 0.9906 |
| *Eriophorum* | frozen | 2.0 | 6.9 | 2.6 | 0.29 | 0.9929 |
| *Carex* | dried | 2.3 | 14.1 | 5.3 | 0.16 | 0.9941 |
| *Carex* | dried | 2.4 | 12.9 | 4.9 | 0.19 | 0.9982 |
| *Carex* | dried | 2.9 | 11.7 | 4.4 | 0.25 | 0.9961 |
| *Carex* | frozen | 3.1 | 15.3 | 5.7 | 0.20 | 0.9968 |
| *Carex* | frozen | 2.6 | 12.3 | 4.6 | 0.21 | 0.9929 |
| *Carex* | frozen | 2.7 | 11.3 | 4.2 | 0.24 | 0.9909 |
| *Salix* | dried | 1.4 | 19.0 | 7.1 | 0.07 | 0.9974 |
| *Salix* | dried | 1.6 | 14.0 | 5.2 | 0.12 | 0.9904 |
| *Salix* | dried | 1.4 | 9.5 | 3.6 | 0.15 | 0.9936 |
| *Salix* | frozen | 1.1 | 10.1 | 3.8 | 0.11 | 0.9758 |
| *Salix* | frozen | 1.1 | 4.4 | 1.6 | 0.26 | 0.9732 |
| *Salix* | frozen | 1.1 | 7.1 | 2.7 | 0.15 | 0.9877 |

Table B.5. Summary of p-values of two way ANOVA tests performed on parameters of modeled DOC and TDN yields. Values in bold are below the p = 0.05 threshold.

| Effect | $V_{max}$ | $t_{50}$ | $t_{90}$ | $\alpha$ |
|---|---|---|---|---|
| DOC | | | | |
| *species* | **0.0002** | **<0.0001** | **<0.0001** | 0.0515 |
| *treatment* | **0.0095** | **<0.0001** | **<0.0001** | **<0.0001** |
| *species*treatment* | 0.5713 | **<0.0001** | **<0.0001** | **<0.0001** |
| TDN | | | | |
| *species* | **<0.0001** | **0.0269** | **0.0269** | **0.0367** |
| *treatment* | **0.0027** | **0.0011** | **0.0011** | **0.0097** |
| *species*treatment* | **0.0013** | **0.0098** | **0.0098** | 0.1936 |

## APPENDIX C: ORGANIC MATTER AND NUTRIENT CONCENTRATIONS IN RIVER SURFACE WATERS OF THE NORTH SLOPE, ALASKA, USA

### Introduction

The high resolution observational data sets presented in Chapter 1 and Chapter 2 of this dissertation are unique in that they provide a seasonally comprehensive investigation of riverine organic matter and inorganic nitrogen dynamics in Arctic watersheds. Chapter 1 focused on organic matter (OM) seasonal dynamics; specifically we quantified dissolved organic carbon (DOC) and particulate organic carbon (POC) concentrations, and used carbon to nitrogen molar ratios (C:N) to characterize both the dissolved and particulate OM pools, while also using stable carbon isotope ratios ($\delta^{13}C$) to identify potential sources of POC. Chapter 2 examined the seasonality of dissolved nitrogen species, focusing on dissolved organic nitrogen (DON) and dissolved inorganic nitrogen (DIN) concentrations. While the breadth our sampling regime in these studies provides a rare examination of OM and inorganic nitrogen dynamics during the historically under-sampled late summer and fall in Arctic watersheds, our spring and summer data offers a point of comparison to previous studies in the immediate area in addition to other rivers on The North Slope, Alaska.

The results from both Chapter 1 and Chapter 2 are consistent with previous studies that measured the same OM and inorganic nitrogen constituents from the study area around Toolik Lake Research Station [e.g., *Peterson et al*., 1986; *Peterson et al*., 1992; *Townsend-Small et al.*, 2011], the north slope region [e.g., *Rember and Trefry*, 2004; *Guo et al*., 2007; *McNamara et al*., 2008; *McClelland et al.*, 2014], as well as those from other pan-Arctic locations [e.g., *Cai et al.*, 2008; *Holmes et al.*, 2012]. While our results are similar both quantitatively and qualitatively to those reported by *McClelland et al*., [2014] a more robust analysis of the data sets from these two different studies could help establish generalized

seasonal trends in water-borne materials from rivers of The North Slope and potentially resolve factors controlling inter-site differences. For example, differences in scale among watersheds may influence seasonal patterns of riverine constituents. The large range is size between the study catchments of this dissertation (1.7 to 608.3 $km^2$) and the three rivers studied by *McClelland et al*., [2014] (8,107 to 59,756 $km^2$) would offer an interesting point of comparison. Similarly, the catchment classification scheme used by this current study of grouping study sites as "tundra" or "mountain" sites [*Craig and McCart* 1975] could be expanded upon as the three catchments examined by *McClelland et al*., [2014] also had varying proportions of mountain, foothill, and coastal plain terrain.

In addition to comparing results of this dissertation with previously published studies investigation larger rivers of The North Slope, watersheds draining eastern portions of the Brook's Range also merit inclusion in a regional comparison. Some of these large river catchments east of the Sagavanirktok include the Canning, Okpilak, Hulahula, Jago, and Kongakut, which collectively drain a large proportion of the eastern North Slope and are located within the Arctic National Wildlife Refuge (ANWR). Several of the rivers draining this area have been documented to have significant glacial contribution to river flow, which may alter the relative importance of the spring snowmelt period with regards to annual water discharge. Instead of a large water flux period during the spring snowmelt that dominates total annual discharge, there is a shift towards increased summer and fall discharge relative to non-glaciated catchments. This shift in hydrology will likely affect the export dynamics of OM and inorganic nitrogen as well, with a similar shift from spring snowmelt dominance to significant summer and fall fluxes likely to be observed. Additionally, as you move east across the North Slope, the Arctic tundra coastal plain becomes narrower and the proportions of upland tundra and mountainous terrain shift.

These two factors may also be important when considering regional differences in river water chemistry.

Using data sets from Chapters 1 and 2 of this dissertation, combined with the data set from the three largest rivers draining the North Slope of Alaska from *McClelland et al*., [2014], and sample collections from rivers draining the eastern portion of The North Slope, may allow for a North Slope region wide analysis. The primary questions of this regional comparison of river chemistry from watersheds on the North Slope of Alaska are: 1) are there broad scale, seasonal patterns in organic matter concentrations and composition and inorganic nitrogen concentrations on the North Slope of Alaska and 2) what are the factors controlling the inter-site differences in water chemistry. Specifically, we propose a regional comparison of seasonal DOC, DON, POC, PON, $\delta^{13}C$ of POC, and DIN concentrations using the data sets from the six rivers in Chapters 1 and 2 of this dissertation, data from the Colville, Kuparuk, and Sagavanirktok form *McClelland et al*., [2014], and data from collections made on various river systems in ANWR. An improved understanding of general OM and inorganic nitrogen concentration patterns and the watershed basin characteristics and mechanisms that control fluvial constituent export, may help us to better project how export processes in watersheds of this region may respond to climate change.

**Methods and Results**

As there is currently a lack of water chemistry data sets from river systems east of the Sagavanirktok for inclusion in a North Slope regional comparison, this necessitated the collection of river surface water samples from these sites. However, due to the lack of pre-existing logistical support for working in this highly remote area, we could not commit to

a sampling regime nearly as intensive compared to those in Chapters 1 and 2 or by *McClelland et al*., [2014]. Collection of riverine surface water samples from these systems was generally accomplished in one of two ways. In 2011, samples were collected as part of a two week intensive collaborative scientific meeting/river float trip on the Hulahula. During this river float trip, biotic samples were also collected for use as isotopic terrestrial endmembers. Additionally, opportunistic samples were made between 2011 and 2014 by colleagues, who happened to be conducting other research on The North Slope, and by citizen scientists adventure traveling in ANWR. Spatial coverage of samples collected as part of these two collection regimes is seen in Figure C.1.

***Water chemistry sample collection and analyses***

Water sample collections often took place in remote field sites that were only accessible by bush plane, and collections were often performed by citizen scientists and researchers without prior experience collecting water samples. This necessitated the development of a light weight, portable, easily operable sampling procedure.

In the field, river surface water samples for dissolved constituents were collected using acid washed pre-leached 140 mL polypropylene syringes. Samples were immediately filtered using 33 mm diameter 0.45 μm polyethersulfone membrane syringe tip filters into two 60 mL acid washed pre-leached polycarbonate bottles. Immediately after filtration, each 60 mL sample bottle was acidified for preservation using 0.48 mL of ultra-pure hydrochloric acid diluted to 1.5 N. Acid was diluted to avoid hazmat travel and shipping restrictions associated with full strength acid. Each aliquot of 0.48 mL of 1.5 N HCl was sufficient to acidify each sample to a final pH <2, but was small enough to make

any dilution effects insignificant. After collection samples were kept in the dark prior to analysis.

At a subset of sampling locations, whole water collections were made for POC and PON concentrations and stable isotope analyses. Waters were collected using 2 L polycarbonate bottles and field filtered through pre-combusted glass fiber filter discs (nominal pore size 0.7 μm) using either acid washed 60 mL polypropylene syringes with polycarbonate syringe tip filter holders, or a field portable peristaltic pump with MasterFlex Tygon tubing (Cole-Parmer, Vernon Hills, IL, USA) and an inline polycarbonate filter holder. Two filters were collected at each sub-sampling site; one filter for C analysis and one filter for N analysis. After filtration, filters were air-dried in the field before transport back to the lab (1-2 weeks) where they were immediately oven dried at 60°C for 24 hours and stored in a desiccator cabinet prior to analysis.

DOC and TDN samples were analyzed at the University of Texas Marine Science Institute on a Shimadzu total organic carbon analyzer fitted with a total nitrogen module for chemiluminescence detection of nitrogen (Shimadzu Corporation, Kyoto, Japan). $NO_3^-$ was measured colorimetrically at UTMSI using a cadmium reduction method modified for a microplate spectrophotometer [*Jones*, 1984].

POC and PON concentrations and $\delta^{13}C$ and $\delta^{15}N$ values were measured at the University of Texas Marine Science Institute using a Carlo Erba 1500 elemental analyzer coupled to a Finnigan MAT Delta Plus continuous flow isotope ratio mass spectrometer (EA-IRMS). Filters for POC and $\delta^{13}C$ were acidified prior to analysis to remove inorganic carbon using sulfurous acid ($H_2SO_3$, ACS 6% $SO_2$ minimum). Filters were triple acidified with a 20 minute drying period in a 60°C oven between the first two acid applications, and a 24 hour drying period after the third acid application.

***Biota sample collection and analyses***

In the summer of 2011, biota samples from rivers, streams, and riparian areas were collected in the Hulahula watershed. All invertebrate, plant, and detritus samples were collected and identified in the field and stored in plastic petri dishes. Samples were air dried in the field before returning to the lab (1-2 weeks) where they were immediately oven dried at 60°C for 24 hours and then stored in a desiccator cabinet prior to analysis. Fish tissue samples were collected by Jason Stolarski of the University of Alaska Fairbanks. Fish tissue samples consisted of tail muscle from juvenile (approximately 1 year) Arctic. In the summer of 2012 vegetation samples from three species representative of common vascular plants were collected from the area of Barter Island, Alaska. Plants were identified and in the field, and immediately brought back to the lab where they were oven dried at 60°C for 24 hours and then stored in a desiccator cabinet prior to analysis.

Samples for C and N content and $\delta^{13}C$ and $\delta^{15}N$ values were measured at the University of Texas Marine Science Institute using a Carlo Erba 1500 elemental analyzer coupled to a Finnigan MAT Delta Plus continuous flow isotope ratio mass spectrometer (EA-IRMS). Additionally, sub-samples for radiocarbon content ($\Delta^{14}C$) were sent to the National Ocean Sciences Accelerator Mass Spectrometry (NOSAMS) facility at the Woods Hole Oceanographic Institute. Prior to analysis, invertebrate and fish samples were acidified using 1 N HCl to remove calcium carbonate hard structures and then dried in an oven at 60°C for 24 hours. All samples were manually ground for C and N content, as well as all isotopic analyses.

**Results**

Water chemistry sample data is provided in Table C.1. Metadata for all water chemistry sample collections is located in Table C.2 and a water chemistry data dictionary is provided in Table C.3.

Biota sample data, including C and N content, and isotopic values, is reported in Table C.4. Metadata for all biota samples is located in Table C.5 and a biota sample data dictionary is provided in Table C.6.

Table C.1. Chemistry data from surface waters collected from rivers of the North Slope, Alaska, USA.

| Site Name | DOC (µM C) | TDN (µM N) | $NO_3^-$ (µM N) | POC (µM C) | PON (µM N) | $\delta^{13}C$ POC (‰) | $\delta^{15}N$ PON (‰) |
|---|---|---|---|---|---|---|---|
| HH 01 | 45.9 | 5.1 | 1.1 | | | | |
| HH 02 | 59.6 | 4.8 | 0.0 | | | | |
| HH-HP | 88.8 | 11.0 | 1.9 | | | | |
| HH 03 | 49.4 | 4.3 | 0.8 | | | | |
| HH-OWC 01 | 111.9 | 17.4 | 12.7 | | | | |
| HH-OMC 01 | 158.0 | 8.0 | 0.6 | | | | |
| HH 04 | 59.8 | 4.2 | 0.9 | | | | |
| HH 05 | 53.4 | 4.4 | 0.4 | | | | |
| JAGO 01 | 53.3 | 3.6 | 0.0 | | | | |
| JAGO 01 | 60.3 | 7.9 | 3.8 | | | | |
| JAGO 03 | 59.8 | 5.8 | 2.0 | | | | |
| JAGO 06 | 55.1 | 5.3 | 1.8 | | | | |
| JAGO-ST 01 | 441.7 | 18.0 | 1.4 | | | | |
| JAGO 03 | 56.7 | 7.0 | 3.5 | | | | |
| JAGO 05 | 59.5 | 8.0 | 2.0 | | | | |
| JAGO 06 | 50.4 | 6.8 | 2.1 | | | | |
| JAGO-ST 02 | 622.5 | 24.9 | 0.0 | | | | |
| SAG 01 | 59.5 | 8.6 | 6.1 | | | | |
| JAGO 03 | 44.0 | 10.4 | 7.3 | | | | |
| JAGO-UC 01 | 39.1 | 3.7 | 0.1 | | | | |
| JAGO- MC 01 | 32.0 | 6.5 | 4.3 | | | | |
| JAGO- MC 01 | 23.5 | 5.9 | 3.6 | | | | |
| JAGO- MC 05 | 139.3 | 13.5 | 11.7 | | | | |
| HH 06 | 130.0 | 7.1 | 1.9 | | | | |

Table C.1. Continued.

| Site Name | DOC (µM C) | TDN (µM N) | $NO_3^-$ (µM N) | POC (µM C) | PON (µM N) | $\delta^{13}C$ POC (‰) | $\delta^{15}N$ PON (‰) |
|---|---|---|---|---|---|---|---|
| HH-OWC 01 | 126.9 | 12.1 | 8.1 | 5.4 | 0.4 | -32.0 | 3.2 |
| HH-OMC 01 | 142.2 | 7.2 | 1.4 | 8.1 | 0.8 | -30.0 | 2.5 |
| HH-ES 01 | 83.0 | 15.4 | 10.8 | 71.0 | 2.7 | -29.6 | 10.1 |
| HH-MTA 01 | 1017.8 | 32.9 | 0.0 | | | | |
| HH-MTB 01 | 80.2 | 7.8 | 4.8 | 6.1 | 0.3 | -30.1 | 4.8 |
| HH-PS | 106.6 | 20.8 | 12.7 | | | | |
| HH 07 | 78.5 | 7.6 | 4.1 | | | | |
| HH 08 | 77.4 | 7.1 | 3.3 | | | | |
| HH 09 | 84.7 | 6.2 | 3.2 | | | | |
| HH-VT 01 | 1647.1 | 47.0 | 0.0 | | | | |
| HH-FH1T-01 | 1246.0 | 41.5 | 0.0 | 8.5 | 0.8 | -29.9 | 2.7 |
| HH 10 | 98.2 | 7.1 | 3.0 | 8.9 | 0.7 | -29.1 | 4.4 |
| HH 11 | 77.4 | 5.2 | 1.4 | 8.9 | 0.8 | -28.7 | 3.8 |
| HH 12 | 79.9 | 5.0 | 1.3 | | | | |
| JAGO 07 | 105.8 | 8.8 | 2.0 | | | | |
| CAN 01 | 88.5 | 6.5 | 0.6 | | | | |
| OKP 01 | 144.6 | 9.6 | 0.2 | | | | |
| HH 13 | 73.8 | 6.8 | 1.3 | | | | |
| OKP 01 | 158.9 | 12.3 | 0.0 | | | | |
| ACK 01 | 44.0 | 9.0 | 5.7 | | | | |
| ACK 02 | 44.2 | 7.1 | 8.6 | | | | |
| ACK 03 | 65.0 | 12.5 | 10.9 | | | | |
| JAGO 08 | 95.5 | 9.5 | 5.0 | 40.7 | 2.6 | -26.7 | 3.1 |
| JAGO-B 08 | 256.5 | 147.5 | 6.0 | 16.5 | 2.0 | -28.2 | 3.9 |
| JAGO 08 | 165.2 | 30.9 | 6.6 | 13.6 | 1.1 | -29.2 | 2.6 |
| JAGO 08 | 55.5 | 13.1 | 8.2 | 32.3 | 4.0 | -27.8 | 3.5 |
| JAGO 08 | 51.5 | 20.8 | 7.4 | 23.7 | 2.7 | -28.7 | 4.3 |

Table C.1. Continued.

| Site Name | DOC (µM C) | TDN (µM N) | $NO_3^-$ (µM N) | POC (µM C) | PON (µM N) | $\delta^{13}C$ POC (‰) | $\delta^{15}N$ PON (‰) |
|---|---|---|---|---|---|---|---|
| DB-T | 358.1 | 17.9 | 3.5 | | | | |
| OKP 02 | 61.0 | 8.3 | 5.3 | | | | |
| SAG 02 | 99.3 | 11.6 | 7.5 | | | | |
| CAN 02 | 107.0 | 9.4 | 4.1 | 52.6 | 4.7 | -28.0 | 3.9 |
| JAGO 09 | 551.7 | 23.4 | 4.4 | 27.5 | 2.4 | -28.4 | 2.6 |
| JAGO 09 | 58.4 | 12.7 | 7.9 | 92.6 | 8.0 | -28.6 | 2.5 |
| JAGO 09 | 56.6 | 11.9 | 7.8 | 62.6 | 9.0 | -27.7 | 3.1 |
| JAGO 09 | 430.0 | 43.0 | 4.7 | 44.6 | 3.7 | -27.8 | 1.6 |
| JAGO 09 | 87.8 | 11.7 | 4.2 | 21.2 | 2.3 | -28.2 | 3.1 |
| JAGO 09 | 81.7 | 9.8 | 3.3 | 18.5 | 1.3 | -28.8 | 2.2 |
| CAN 03 | 36.1 | 6.3 | 2.9 | | | | |
| CAN 04 | 57.0 | 4.9 | 1.1 | | | | |
| CAN 05 | 127.5 | 7.2 | 1.0 | | | | |
| CAN-T01 | 1021.8 | 44.2 | 0.0 | | | | |
| CAN 06 | 182.4 | 8.4 | 1.6 | | | | |
| CAN 07 | 104.7 | 7.0 | 2.4 | | | | |
| CAN-T02 | 479.6 | 27.2 | 0.7 | | | | |
| KVK 01 | 339.8 | 12.9 | 0.2 | | | | |
| BCL Cornerin | 137.7 | 6.3 | 0.0 | | | | |
| Trough Runoff | 382.5 | 13.7 | 0.0 | | | | |
| CHP 01 | 721.5 | 18.4 | 0.5 | | | | |
| KONG 01 | 155.7 | 9.9 | 4.8 | | | | |
| KONG 02 | 131.4 | 9.1 | 5.7 | | | | |
| KONG 03 | 105.5 | 8.1 | 5.2 | | | | |
| KONG 04 | 98.5 | 8.8 | 13.2 | | | | |
| CHP 02 | 1077.6 | 29.1 | | | | | |
| KONG 05 | 252.1 | 9.4 | | | | | |

Table C.1. Continued.

| Site Name | DOC (µM C) | TDN (µM N) | $NO_3^-$ (µM N) | POC (µM C) | PON (µM N) | $\delta^{13}C$ POC (‰) | $\delta^{15}N$ PON (‰) |
|---|---|---|---|---|---|---|---|
| KONG 06 | 293.8 | 8.5 | | | | | |
| KONG 07 | 251.7 | 9.2 | | | | | |
| KONG 08 | 246.3 | 7.5 | | | | | |
| KONG 09 | 239.5 | 6.2 | | | | | |
| HH 14 | 43.3 | 6.8 | | | | | |
| HH 14 | 122.0 | 7.9 | | | | | |
| CAN 08 | 82.5 | 4.4 | | | | | |
| CAN 09 | 80.5 | 3.8 | | | | | |
| CAN 10 | 91.1 | 2.3 | | | | | |
| CAN 11 | 85.2 | 3.0 | | | | | |
| CAN 12 | 78.2 | 2.8 | | | | | |
| CAN 13 | 100.2 | 2.7 | | | | | |
| CAN 14 | 91.6 | 3.1 | | | | | |
| CAN 15 | 92.2 | 3.7 | | | | | |
| CAN 16 | 90.6 | 3.3 | | | | | |
| CAN 17 | 148.6 | 5.4 | | | | | |
| CAN 18 | 198.4 | 7.2 | | | | | |
| CAN 19 | 237.4 | 7.3 | | | | | |
| CAN 20 | 219.8 | 6.7 | | | | | |
| CAN 21 | 250.1 | 8.7 | | | | | |
| JAGO-B 08 | 561.7 | 18.4 | | | | | |
| KOGO-T01 | 767.1 | 31.2 | | | | | |
| KOGO | 420.7 | 18.8 | | | | | |
| BL-T01 | 895.8 | 40.3 | | | | | |

Table C.2. Metadata for surface water samples collected from rivers of the North Slope, Alaska, USA.

| Sample ID | Site Name | Site Description | Main Stem Watershed | Date | Latitude | Longitude | Collected By | Collector Affiliation |
|---|---|---|---|---|---|---|---|---|
| HH 01 | Hulahula | Hulahula main stem | Hulahula | 6/10/11 | 69.09308 | -144.62746 | Greta Burkart | United States Fish and Wildlife Service |
| HH 02 | Hulahula | Hulahula main stem | Hulahula | 6/11/11 | 69.17529 | -144.59282 | Greta Burkart | United States Fish and Wildlife Service |
| HH-EPC | East Patuk Creek | Hulahula tributary | Hulahula | 6/12/11 | 69.17527 | -144.58128 | Greta Burkart | United States Fish and Wildlife Service |
| HH 03 | Hulahula | Hulahula main stem | Hulahula | 6/13/11 | 69.48917 | -144.38861 | Greta Burkart | United States Fish and Wildlife Service |
| HH-OWC 01 | Old Woman Creek | Hulahula tributary | Hulahula | 6/13/11 | 69.48972 | -144.39833 | Greta Burkart | United States Fish and Wildlife Service |
| HH-OMC 01 | Old Man Creek | Hulahula tributary | Hulahula | 6/13/11 | 69.49375 | -144.36497 | Greta Burkart | United States Fish and Wildlife Service |
| HH 04 | Hulahula | Hulahula main stem | Hulahula | 6/14/11 | 69.47400 | -144.38100 | Greta Burkart | United States Fish and Wildlife Service |
| HH 05 | Hulahula | Hulahula main stem | Hulahula | 6/14/11 | 69.47100 | -144.37900 | Greta Burkart | United States Fish and Wildlife Service |
| JAGO 01 | Jago | Jago main stem | Jago | 6/16/11 | 69.44861 | -143.71972 | Greta Burkart | United States Fish and Wildlife Service |
| JAGO 01 | Jago | Jago main stem | Jago | 6/17/11 | 69.44861 | -143.71972 | Greta Burkart | United States Fish and Wildlife Service |
| JAGO 03 | Jago | Jago main stem | Jago | 6/17/11 | 69.44185 | -143.69810 | Greta Burkart | United States Fish and Wildlife Service |
| JAGO 06 | Jago | Jago main stem | Jago | 6/17/11 | 69.44168 | -143.69903 | Greta Burkart | United States Fish and Wildlife Service |
| JAGO-ST 01 | n/a | Jago tributary | Jago | 6/18/11 | 69.43368 | -143.72252 | Greta Burkart | United States Fish and Wildlife Service |
| JAGO 03 | Jago | Jago main stem | Jago | 6/18/11 | 69.44185 | -143.69810 | Greta Burkart | United States Fish and Wildlife Service |
| JAGO 05 | Jago | Jago main stem | Jago | 6/18/11 | 69.44238 | -143.69590 | Greta Burkart | United States Fish and Wildlife Service |

Table C.2. Continued.

| Sample ID | Site Name | Site Description | Main Stem Watershed | Date | Latitude | Longitude | Collected By | Collector Affiliation |
|---|---|---|---|---|---|---|---|---|
| JAGO 06 | Jago | Jago main stem | Jago | 6/18/11 | 69.44168 | -143.69903 | Greta Burkart | United States Fish and Wildlife Service |
| JAGO-ST 02 | n/a | Jago tributary | Jago | 6/19/11 | 69.44639 | -143.72583 | Greta Burkart | United States Fish and Wildlife Service |
| SAG 01 | Sagavanirktok | Sagavanirktok main stem | Sagavanirktok | 7/29/11 | 69.14694 | -148.82623 | Greta Burkart | United States Fish and Wildlife Service |
| JAGO 03 | Jago | Jago main stem | Jago | 7/31/11 | 69.44185 | -143.69810 | Greta Burkart | United States Fish and Wildlife Service |
| JAGO-UC 01 | McCall Creek | McCall Creek at glacier terminus | Jago | 8/5/11 | 69.29585 | -143.79144 | Greta Burkart | United States Fish and Wildlife Service |
| JAGO-MC 01 | McCall Creek | McCall Creek at glacier terminus | Jago | 8/8/11 | 69.33435 | -143.83641 | Greta Burkart | United States Fish and Wildlife Service |
| JAGO-MC 01 | McCall Creek | McCall Creek at glacier terminus | Jago | 8/8/11 | 69.33435 | -143.83641 | Greta Burkart | United States Fish and Wildlife Service |
| JAGO-MC 05 | McCall Creek | McCall Creek below Jaeger Pass | Jago | 8/10/11 | 69.38183 | -143.77606 | Greta Burkart | United States Fish and Wildlife Service |
| HH 06 | Hulahula | Hulahula main stem | Hulahula | 8/11/11 | 69.48804 | -144.39080 | Greta Burkart | United States Fish and Wildlife Service |
| HH-OWC 01 | Old Woman Creek | Hulahula tributary | Hulahula | 8/12/11 | 69.48953 | -144.40069 | Matt Khosh | University of Texas Marine Science Institute |
| HH-OMC 01 | Old Man Creek | Hulahula tributary | Hulahula | 8/13/11 | 69.49375 | -144.36497 | Matt Khosh | University of Texas Marine Science Institute |
| HH-ES 01 | Esetuk Creek | Hulahula tributary | Hulahula | 8/14/11 | 69.42988 | -144.42000 | Matt Khosh | University of Texas Marine Science Institute |
| HH-MTA 01 | n/a | Hulahula tributary | Hulahula | 8/14/11 | 69.44628 | -144.38734 | Matt Khosh | University of Texas Marine Science Institute |
| HH-MTB 01 | n/a | Hulahula tributary | Hulahula | 8/14/11 | 69.45757 | -144.35659 | Matt Khosh | University of Texas Marine Science Institute |
| HH-PS | n/a | Hulahula tributary | Hulahula | 8/14/11 | 69.46873 | -144.37111 | Matt Khosh | University of Texas Marine Science Institute |

Table C.2. Continued.

| Sample ID | Site Name | Site Description | Main Stem Watershed | Date | Latitude | Longitude | Collected By | Collector Affiliation |
|---|---|---|---|---|---|---|---|---|
| HH 07 | Hulahula | Hulahula main stem | Hulahula | 8/15/11 | 69.48804 | -144.39080 | Matt Khosh | University of Texas Marine Science Institute |
| HH 08 | Hulahula | Hulahula main stem | Hulahula | 8/15/11 | 69.60969 | -144.22443 | Matt Khosh | University of Texas Marine Science Institute |
| HH 09 | Hulahula | Hulahula main stem | Hulahula | 8/16/11 | 69.65505 | -144.19608 | Matt Khosh | University of Texas Marine Science Institute |
| HH-VT 01 | n/a | Hulahula tributary | Hulahula | 8/16/11 | 69.65598 | -144.19472 | Matt Khosh | University of Texas Marine Science Institute |
| HH-FH1T-01 | n/a | Hulahula tributary | Hulahula | 8/17/11 | 69.76147 | -144.13015 | Matt Khosh | University of Texas Marine Science Institute |
| HH 10 | Hulahula | Hulahula main stem | Hulahula | 8/17/11 | 69.76059 | -144.15851 | Matt Khosh | University of Texas Marine Science Institute |
| HH 11 | Hulahula | Hulahula main stem | Hulahula | 8/19/11 | 69.98425 | -144.02254 | Matt Khosh | University of Texas Marine Science Institute |
| HH 12 | Hulahula | Hulahula main stem | Hulahula | 8/19/11 | 70.03716 | -144.02974 | Matt Khosh | University of Texas Marine Science Institute |
| JAGO 07 | Jago | Jago main stem | Jago | 8/12/11 | 70.11658 | -143.34462 | Roy Churchwell | University of Alaska Fairbanks |
| CAN 01 | Canning | Canning main stem | Canning | 8/18/11 | 70.05937 | -145.56938 | Roy Churchwell | University of Alaska Fairbanks |
| OKP 01 | Okpilak | Okpilak main stem | Okpilak | 8/20/11 | 70.07966 | -144.00860 | Roy Churchwell | University of Alaska Fairbanks |
| HH 13 | Hulahula | Hulahula main stem | Hulahula | 8/20/11 | 70.05573 | -144.12226 | Roy Churchwell | University of Alaska Fairbanks |
| OKP 01 | Okpilak | Okpilak main stem | Okpilak | 8/23/11 | 70.07966 | -144.00860 | Roy Churchwell | University of Alaska Fairbanks |
| ACK 01 | Aichilik | Aichilik main stem | Aichilik | 6/24/12 | 69.51955 | -143.03625 | Beverly Boynton | Citizen Scientist |
| ACK 02 | Aichilik | Aichilik main stem | Aichilik | 6/27/12 | 69.67352 | -142.78740 | Beverly Boynton | Citizen Scientist |

Table D.2. Continued.

| Sample ID | Site Name | Site Description | Main Stem Watershed | Date | Latitude | Longitude | Collected By | Collector Affiliation |
|---|---|---|---|---|---|---|---|---|
| ACK 03 | Aichilik | Aichilik main stem | Aichilik | 6/28/12 | 69.81983 | -142.14906 | Beverly Boynton | Citizen Scientist |
| JAGO 08 | Jago | Jago main stem | Jago | 6/14/12 | 69.71653 | -143.60370 | Matt Nolan | University of Alaska Fairbanks |
| JAGO-B 08 | Jago | Jago main stem | Jago | 6/15/12 | 69.71653 | -143.60370 | Matt Nolan | University of Alaska Fairbanks |
| JAGO 08 | Jago | Jago main stem | Jago | 6/15/12 | 69.71653 | -143.60370 | Matt Nolan | University of Alaska Fairbanks |
| JAGO 08 | Jago | Jago main stem | Jago | 6/16/12 | 69.71653 | -143.60370 | Matt Nolan | University of Alaska Fairbanks |
| JAGO 08 | Jago | Jago main stem | Jago | 6/16/12 | 69.71653 | -143.60370 | Matt Nolan | University of Alaska Fairbanks |
| DB-T | Turner | Turner main stem | Turner | 8/1/12 | 69.63572 | -141.40805 | Tim Robertson | Nuka Research & Planning Group, LLC. |
| OKP 02 | Okpilak | Okpilak main stem | Okpilak | 8/3/12 | 70.06080 | -144.01915 | Tim Robertson | Nuka Research & Planning Group, LLC. |
| SAG 02 | Sagavanirktok | Sagavanirktok main stem | Sagavanirktok | 8/6/12 | 70.21323 | -148.38872 | Tim Robertson | Nuka Research & Planning Group, LLC. |
| CAN 02 | Canning | Canning main stem | Canning | 8/9/12 | 70.05752 | -145.56435 | Roy Churchwell | University of Alaska Fairbanks |
| JAGO 09 | Jago | Jago main stem | Jago | 8/12/12 | 70.12001 | -143.26859 | Roy Churchwell | University of Alaska Fairbanks |
| JAGO 09 | Jago | Jago main stem | Jago | 8/5/12 | 69.71653 | -143.60370 | Matt Nolan | University of Alaska Fairbanks |
| JAGO 09 | Jago | Jago main stem | Jago | 8/6/12 | 69.71653 | -143.60370 | Matt Nolan | University of Alaska Fairbanks |
| JAGO 09 | Jago | Jago main stem | Jago | 8/7/12 | 69.71653 | -143.60370 | Matt Nolan | University of Alaska Fairbanks |
| JAGO 09 | Jago | Jago main stem | Jago | 8/22/12 | 69.71653 | -143.60370 | Matt Nolan | University of Alaska Fairbanks |

Table C.2. Continued.

| Sample ID | Site Name | Site Description | Main Stem Watershed | Date | Latitude | Longitude | Collected By | Collector Affiliation |
|---|---|---|---|---|---|---|---|---|
| JAGO 09 | Jago | Jago main stem | Jago | 8/23/12 | 69.71653 | -143.60370 | Matt Nolan | University of Alaska Fairbanks |
| CAN 03 | Canning | Canning main stem | Canning | 8/24/12 | 69.28164 | -146.02247 | Greta Burkart | United States Fish and Wildlife Service |
| CAN 04 | Canning | Canning main stem | Canning | 8/26/12 | 69.67772 | -146.24975 | Greta Burkart | United States Fish and Wildlife Service |
| CAN 05 | Canning | Canning main stem | Canning | 8/29/12 | 69.86696 | -146.41178 | Greta Burkart | United States Fish and Wildlife Service |
| CAN-T01 | n/a | Canning tributary | Canning | 8/29/12 | 69.87811 | -146.38264 | Greta Burkart | United States Fish and Wildlife Service |
| CAN 06 | Canning | Canning main stem | Canning | 9/1/12 | 69.97164 | -146.27611 | Greta Burkart | United States Fish and Wildlife Service |
| CAN 07 | Canning | Canning main stem | Canning | 9/4/12 | 70.04269 | -146.07452 | Greta Burkart | United States Fish and Wildlife Service |
| CAN-T02 | n/a | Canning tributary | Canning | 9/5/12 | 70.10815 | -145.83966 | Greta Burkart | United States Fish and Wildlife Service |
| KVK 01 | Kavik | Kavik main stem | Kavik | 9/6/12 | 69.67253 | -146.90167 | Greta Burkart | United States Fish and Wildlife Service |
| BCL Cornerin | Chipp | n/a | Chipp | 6/12/13 | 70.68758 | -155.28774 | Josh Koch | United States Geological Survey |
| Trough Runoff | n/a | n/a | Alaktak | 6/12/13 | 70.68375 | -155.19335 | Josh Koch | United States Geological Survey |
| CHP 01 | n/a | n/a | Chipp | 6/16/13 | 70.67466 | -155.42444 | Josh Koch | United States Geological Survey |
| KONG 01 | Kongakut | Kongakut main steam | Kongakut | 6/25/13 | 69.45570 | -141.46928 | Larry Lynn | Arctic Wild, LLC |
| KONG 02 | Kongakut | Kongakut main steam | Kongakut | 6/26/13 | 69.56842 | -141.886617 | Larry Lynn | Arctic Wild, LLC |
| KONG 03 | Kongakut | Kongakut main steam | Kongakut | 6/27/13 | 69.58852 | -141.87165 | Larry Lynn | Arctic Wild, LLC |

Table C.2. Continued.

| Sample ID | Site Name | Site Description | Main Stem Watershed | Date | Latitude | Longitude | Collected By | Collector Affiliation |
|---|---|---|---|---|---|---|---|---|
| KONG 04 | Kongakut | Kongakut main steam | Kongakut | 6/28/13 | 69.73005 | -141.75700 | Larry Lynn | Arctic Wild, LLC |
| CHP 02 | Chipp | n/a | Chipp | | 70.67466 | -155.42444 | Josh Koch | United States Geological Survey |
| KONG 05 | Kongakut | Kongakut main steam | Kongakut | 8/25/13 | 69.14773 | -141.86903 | Bill Mohrwinkel | Arctic Wild, LLC |
| KONG 06 | Kongakut | Kongakut main steam | Kongakut | 8/27/13 | 69.24958 | -141.73282 | Bill Mohrwinkel | Arctic Wild, LLC |
| KONG 07 | Kongakut | Kongakut main steam | Kongakut | 8/28/13 | 69.36600 | -141.55868 | Bill Mohrwinkel | Arctic Wild, LLC |
| KONG 08 | Kongakut | Kongakut main steam | Kongakut | 8/29/13 | 69.45040 | -141.47170 | Bill Mohrwinkel | Arctic Wild, LLC |
| KONG 09 | Kongakut | Kongakut main steam | Kongakut | 8/30/13 | 69.46303 | -141.48777 | Bill Mohrwinkel | Arctic Wild, LLC |
| HH 14 | Hulahula | Hulahula main steam | Hulahula | 6/24/14 | 69.70390 | -144.20114 | Mathew Schellekens | United States Geological Survey |
| HH 14 | Hulahula | Hulahula main steam | Hulahula | 9/5/14 | 69.70390 | -144.20114 | Mathew Schellekens | United States Geological Survey |
| CAN 08 | Canning | Canning main stem | Canning | 8/20/14 | 69.88174 | -146.38873 | Randy Brown | United States Fish and Wildlife Service |
| CAN 09 | Canning | Canning main stem | Canning | 8/21/14 | 69.88174 | -146.38873 | Randy Brown | United States Fish and Wildlife Service |
| CAN 10 | Canning | Canning main stem | Canning | 8/22/14 | 69.88174 | -146.38873 | Randy Brown | United States Fish and Wildlife Service |
| CAN 11 | Canning | Canning main stem | Canning | 8/23/14 | 69.88174 | -146.38873 | Randy Brown | United States Fish and Wildlife Service |
| CAN 12 | Canning | Canning main stem | Canning | 8/24/14 | 69.88174 | -146.38873 | Randy Brown | United States Fish and Wildlife Service |
| CAN 13 | Canning | Canning main stem | Canning | 8/25/14 | 69.88174 | -146.38873 | Randy Brown | United States Fish and Wildlife Service |

Table C.2. Continued.

| Sample ID | Site Name | Site Description | Main Stem Watershed | Date | Latitude | Longitude | Collected By | Collector Affiliation |
|---|---|---|---|---|---|---|---|---|
| CAN 14 | Canning | Canning main stem | Canning | 8/26/14 | 69.88174 | -146.38873 | Randy Brown | United States Fish and Wildlife Service |
| CAN 15 | Canning | Canning main stem | Canning | 8/27/14 | 69.88174 | -146.38873 | Randy Brown | United States Fish and Wildlife Service |
| CAN 16 | Canning | Canning main stem | Canning | 8/28/14 | 69.88174 | -146.38873 | Randy Brown | United States Fish and Wildlife Service |
| CAN 17 | Canning | Canning main stem | Canning | 8/29/14 | 69.88174 | -146.38873 | Randy Brown | United States Fish and Wildlife Service |
| CAN 18 | Canning | Canning main stem | Canning | 8/30/14 | 69.88174 | -146.38873 | Randy Brown | United States Fish and Wildlife Service |
| CAN 19 | Canning | Canning main stem | Canning | 8/31/14 | 69.88174 | -146.38873 | Randy Brown | United States Fish and Wildlife Service |
| CAN 20 | Canning | Canning main stem | Canning | 9/1/14 | 69.88174 | -146.38873 | Randy Brown | United States Fish and Wildlife Service |
| CAN 21 | Canning | Canning main stem | Canning | 9/2/14 | 69.88174 | -146.38873 | Randy Brown | United States Fish and Wildlife Service |
| JAGO-B 08 | Jago | Jago main stem | Jago | 7/31/14 | 69.74280 | -143.60748 | Greta Burkart | United States Fish and Wildlife Service |
| KOGO-T01 | n/a | Kogotpak tributary | Kogotpak | 8/5/14 | 69.86420 | -142.29033 | Greta Burkart | United States Fish and Wildlife Service |
| KOGO | Kogotpak | Kogotpak main stem | Kogotpak | 8/5/14 | 69.85813 | -142.28261 | Greta Burkart | United States Fish and Wildlife Service |
| BL-T01 | n/a | Beaufort Lagoon tributary | Beaufort Lagoon | 8/6/14 | 69.87681 | -142.31580 | Greta Burkart | United States Fish and Wildlife Service |

Table C.3. Data dictionary for water chemistry data and metadata tables.

| Field Name | Data Type | Units/Format | Definition |
|---|---|---|---|
| DOC (μM C) | numeric | micromoles carbon per liter | Numeric representation of the measure of the dissolved organic carbon concentration of the sample |
| TDN (μM N) | numeric | micromoles nitrogen per liter | Numeric representation of the measure of the total dissolved nitrogen concentration of the sample |
| $NO_3^-$ (μM N) | numeric | micromoles nitrogen per liter | Numeric representation of the measure of the dissolved nitrate concentration of the sample |
| POC (μM C) | numeric | micromoles carbon per liter | Numeric representation of the measure of the particulate organic carbon concentration of the sample |
| PON (μM N) | numeric | micromoles nitrogen per liter | Numeric representation of the measure of the particulate organic nitrogen concentration of the sample |
| $\delta^{13}$C POC (‰) | numeric | parts per thousand relative to Pee Dee Belemnite | Numeric representation of the measure of the ratio of carbon stable isotopes $^{13}C$:$^{12}C$ from the particulate organic carbon fraction of the whole water sample compared to the ratio of carbon stable isotopes $^{13}C$:$^{12}C$ of a standard reported in parts per thousand |
| $\delta^{15}$N PON (‰) | numeric | parts per thousand relative to atmosphere | Numeric representation of the measure of the ratio of nitrogen stable isotopes $^{15}N$:$^{14}N$ from the particulate organic nitrogen fraction of the whole water sample compared to the ratio of carbon stable isotopes $^{15}N$:$^{14}N$ of a standard reported in parts per thousand |
| Sample ID | text | n/a | Identifying value given to each sample |
| Site Name | text | n/a | Name of site (if listed name available) |
| Site Description | text | n/a | Brief description of site; tributary or main stem |
| Main stem Watershed | text | n/a | Name of the main stem river watershed that sampling site is located within |
| Date | date | M/DD/YY | The date that sample was collected in M/DD/YY format |
| Latitude | numeric | decimal degrees | Latitude of where sample was collected in decimal degrees |
| Longitude | numeric | decimal degrees | longitude of where sample was collected in decimal degrees |
| Collected By | text | n/a | Name of individual who collected sample |
| Collector Affiliation | text | n/a | Sample collector's professional association |

Table C.4. Carbon and nitrogen content, and isotope data from biota samples collected from rivers and terrestrial sites of the North Slope, Alaska, USA.

| Sample ID | $\delta^{13}C$ (‰) | $\delta^{15}N$ (‰) | C Content | N Content | C:N (molar) | $\Delta^{14}C$ | Radiocarbon Age | NOSAMS $\delta^{13}C$ (‰) |
|---|---|---|---|---|---|---|---|---|
| HH-OWC Invert 01 | | | | | | -231.75 | 2,060 | -45.04 |
| HH-OWC peri 01 | -43.4 | 2.6 | 25.4% | 3.2% | 9.3 | | | |
| HH-OWC bryo 01 | -28.4 | 0.6 | 39.9% | 1.3% | 37.0 | | | |
| HH-OWC detritus 01 | -43.6 | 1.9 | 34.6% | 4.5% | 9.0 | | | |
| HH-OWC veg 01 | -28.7 | 10.2 | 34.7% | 2.0% | 19.8 | | | |
| HH-OWC invert 01 | -31.2 | 2.2 | 43.8% | 8.9% | 5.7 | | | |
| HH-OWC invert 02 | -25.9 | 10.3 | 47.1% | 7.2% | 7.6 | | | |
| HH fish 01 | -27.7 | 5.7 | 43.78% | 12.37% | 4.1 | -179.17 | 1,530 | -28.39 |
| HH-OMC fish 02 | -28.2 | 6.1 | 46.64% | 11.79% | 4.6 | -169.39 | 1,430 | -29.53 |
| HH-OMC Invert 01 | | | | | | -129.75 | 1,060 | -32.73 |
| HH-OMC det 01 | -29.6 | 1.4 | 20.8% | 1.5% | 18.0 | | | |
| HH-FH1T Invert 01 | | | | | | -187.28 | 1,610 | -29.83 |
| HH-FH1T bryo 01 | -32.1 | 1.1 | 24.7% | 1.5% | 19.3 | | | |
| HH-FH1T det 01 | -28.9 | -1.1 | 33.1% | 1.1% | 35.5 | | | |
| HH-FH1T Invert 02 | -30.9 | 1.6 | 42.9% | 6.7% | 7.5 | | | |
| BI Veg 01 | -28.6 | 3.4 | 43.7% | 2.7% | 19.0 | | | |
| BI Veg 02 | -29.1 | 0.3 | 43.7% | 2.7% | 32.6 | | | |
| BI Veg 03 | -28.5 | -0.7 | 43.9% | 1.6% | 26.7 | | | |

Table C.5. Metadata for biota collected from rivers and terrestrial sties of the North Slope, Alaska, USA.

| Sample ID | Site Name | Date | Latitude | Longitude | Main Stem Watershed | Sample Description |
|---|---|---|---|---|---|---|
| HH-OWC Invert 01 | Old Woman Creek | 8/12/11 | 69.48953 | -144.40069 | Hulahula | Chironomidae |
| HH-OWC peri 01 | Old Woman Creek | 8/12/11 | 69.48953 | -144.40069 | Hulahula | stream periphyton |
| HH-OWC bryo 01 | Old Woman Creek | 8/12/11 | 69.48953 | -144.40069 | Hulahula | bryophytes from stream bank |
| HH-OWC detritus 01 | Old Woman Creek | 8/12/11 | 69.48953 | -144.40069 | Hulahula | Instream detritus/periphyton |
| HH-OWC veg 01 | Old Woman Creek | 8/12/11 | 69.48953 | -144.40069 | Hulahula | *Equisetum sp.* |
| HH-OWC invert 01 | Old Woman Creek | 8/12/11 | 69.48953 | -144.40069 | Hulahula | unidentified aquatic invertebrate |
| HH-OWC invert 02 | Old Woman Creek | 8/12/11 | 69.48953 | -144.40069 | Hulahula | unidentified aquatic invertebrate |
| HH fish 01 | Hulahula | 8/13/11 | 69.48804 | -144.39080 | Hulahula | juvenile (approx.. 1 year) Arctic char; 5 fish composite |
| HH-OMC fish 02 | Old Man Creek | 8/13/11 | 69.49375 | -144.36497 | Hulahula | juvenile (approx.. 1 year) Arctic char; 5 fish composite |
| HH-OMC Invert 01 | Old Man Creek | 8/13/11 | 69.49375 | -144.36497 | Hulahula | stoneflies |
| HH-OMC det 01 | Old Man Creek | 8/13/11 | 69.49375 | -144.36497 | Hulahula | Instream detritus |
| HH-FH1T Invert 01 | Hulahula FH1 tributary | 8/17/11 | 69.76059 | -144.15851 | Hulahula | stoneflies |
| HH-FH1T bryo 01 | Hulahula FH1 tributary | 8/17/11 | 69.76059 | -144.15851 | Hulahula | bryophytes from stream bank |
| HH-FH1T det 01 | Hulahula FH1 tributary | 8/17/11 | 69.76059 | -144.15851 | Hulahula | Instream detritus |
| HH-FH1T Invert 02 | Hulahula FH1 tributary | 8/17/11 | 69.76059 | -144.15851 | Hulahula | unidentified aquatic invertebrate |
| BI Veg 01 | Barter Island | 8/20/12 | 70.12211 | -143.66716 | n/a | *Eriophorum vaginatum* |
| BI Veg 02 | Barter Island | 8/20/12 | 70.12211 | -143.66716 | n/a | *Carex bigelowii* |
| BI Veg 03 | Barter Island | 8/20/12 | 70.12211 | -143.66716 | n/a | *Salix pulchra* |

Table C.6. Data dictionary for biota sample data and metadata tables.

| Field Name | Data Type | Units/Format | Definition |
|---|---|---|---|
| $\delta^{13}C$ (‰) | numeric | parts per thousand relative to Pee Dee Belemnite | Numeric representation of the measure of the ratio of carbon stable isotopes $^{13}C$:$^{12}C$ of the sample relative to Pee Dee Belemnite standard. Measured at UTMSI |
| $\delta^{15}N$ (‰) | numeric | parts per thousand relative to atmosphere | Numeric representation of the measure of the ratio of carbon stable isotopes $^{15}N$: $^{14}N$ of the sample relative to atmosphere. Measured at UTMSI |
| Carbon Content | numeric | percent | numeric representation of the carbon content of the sample calculated as the percentage of the carbon mass to total sample dry mass |
| Nitrogen Content | numeric | percent | numeric representation of the nitrogen content of the sample calculated as the percentage of the nitrogen mass to total sample dry mass |
| C:N (molar) | numeric | | numeric representation of the molar ratio of carbon to nitrogen content of the sample |
| $\Delta^{14}C$ | numeric | parts per thousand | Numeric representation of the delta carbon-13 normalized radiocarbon depletion in the sample normalized to 1950 |
| Radiocarbon Age | numeric | years | Numeric representation of the radiocarbon age calculated using the Libby half-life and reported without reservoir corrections or calibration to calendar year |
| NOSAMS $\delta^{13}C$ (‰) | numeric | | Numeric representation of the measure of the ratio of carbon stable isotopes $^{13}C$:$^{12}C$ of the sample relative to Pee Dee Belemnite standard. Measured at NOSAMS |
| Sample ID | text | | The identifying name assigned to the sample collected |
| Site Name | text | | The name of the site where the sample was collected |
| Date | date | M/DD/YYYY | The date that sample was collected in M/DD/YYYY format |
| Latitude | numeric | decimal degrees | Latitude of where sample was collected in decimal degrees |
| Longitude | numeric | decimal degrees | longitude of where sample was collected in decimal degrees |
| Main stem Watershed | text | | Name of the main stem river watershed |
| Sample Description | text | | description of collected sample |

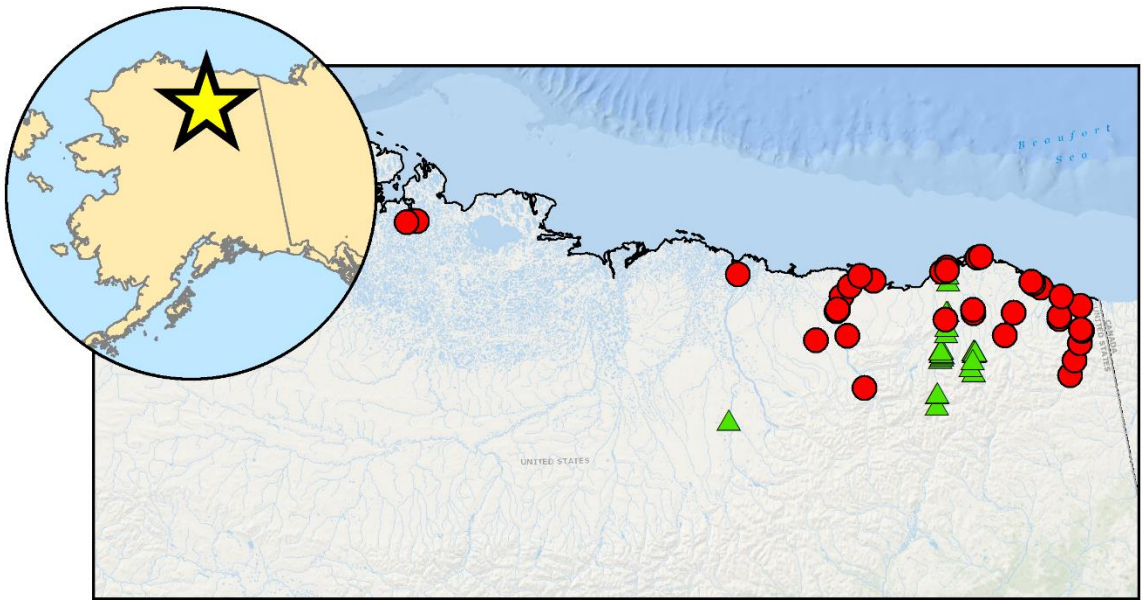


Figure C.1. Map of the North Slope of Alaska displaying the locations of river surface water samples and biota samples collected between 2011 and 2014. Green triangles correspond to samples collected during the Hulahula float trip in 2011, while red circles correspond to samples collected by colleagues at various academic institutes and government agencies, as well as volunteer citizen scientists between 2011 and 2014.

# References


Aagaard, K., and E. C. Carmack (1989), The role of sea ice and other fresh water in the Arctic circulation, *J. Geophys. Res.*, *94*(C10), 14485, doi:10.1029/JC094iC10p14485.

Alexander, V., and D. M. Schell (1973), Seasonal and Spatial Variation of Nitrogen Fixation in the Barrow, Alaska, Tundra, *Arct. Alp. Res.*, *5*(2), 77–88.

Amon, R. M. W., and B. Meon (2004), The biogeochemistry of dissolved organic matter and nutrients in two large Arctic estuaries and potential implications for our understanding of the Arctic Ocean system, *Mar. Chem.*, *92*(1-4), 311–330, doi:10.1016/j.marchem.2004.06.034.

Arctic Climate Impact Assessment (2005), *Arctic Climate Impact Assessment*, Cambridge University Press: New York.

Arp, C. D., M. S. Whitman, B. M. Jones, G. Grosse, B. V. Gaglioti, and K. C. Heim (2014), Beaded streams of Arctic permafrost landscapes, *Biogeosciences Discuss.*, *11*(7), 11391–11441, doi:10.5194/bgd-11-11391-2014.

Barker, A. J., T. A. Douglas, A. D. Jacobson, J. W. McClelland, A. G. Ilgen, M. S. Khosh, G. O. Lehn, and T. P. Trainor (2014), Late season mobilization of trace metals in two small Alaskan arctic watersheds as a proxy for landscape scale permafrost active layer dynamics, *Chem. Geol.*, *381*, 180–193, doi:10.1016/j.chemgeo.2014.05.012.

Barsdate, R. J., and V. Alexander (1975), The Nitrogen Balance of Arctic Tundra: Pathways, Rates, and Environmental Implications, *J. Environ. Qual.*, *4*(1), 111, doi:10.2134/jeq1975.00472425000400010025x.

Bekku, Y. S., T. Nakatsubo, A. Kume, M. Adachi, and H. Koizumi (2003), Effect of warming on the temperature dependence of soil respiration rate in arctic, temperate and tropical soils, *Appl. Soil Ecol.*, *22*(3), 205–210, doi:10.1016/S0929-1393(02)00158-0.

Benner, R. (2004), Export of young terrigenous dissolved organic carbon from rivers to the Arctic Ocean, *Geophys. Res. Lett.*, *31*(5), L05305, doi:10.1029/2003GL019251.

Billings, W. D., J. O. Luken, D. a. Mortensen, and K. M. Peterson (1983), Increasing atmospheric carbon dioxide: possible effects on arctic tundra, *Oecologia*, *58*(3), 286–289, doi:10.1007/BF00385225.

Bowden, W. B., B. J. Peterson, L. A. Deegan, A. D. Huryn, J. P. Benstead, H. Golden, M. Kendrick, S. M. Parker, E. Schuett, and J. E. Hobbie (2014), *Alaska's Changing Arctic: Ecological Consequences for Tundra, Streams, and Lakes*, edited by J. E. Hobbie and G. W. Kling, Oxford University Press, New York.

Bowden, W. B., M. S. Khosh, M. N. Gooseff, W. M. Wollheim, K. Whittnghill, A. Wlostkowski, T. A. Douglas, A. D. Jacobson, G. O. Lehn, and A. J. Barker (2015), Seasonality of nitrate concentrations and loads in arctic headwater streams: potential mechanisms and implications given a warming arctic climate, *Prep.*

Bowling, L. C., D. L. Kane, R. E. Gieck, L. D. Hinzman, and D. P. Lettenmaier (2003), The role of surface storage in a low-gradient Arctic watershed, *Water Resour. Res.*, *39*(4), 1–13, doi:10.1029/2002WR001466.

Britton, M. E. (1966), *Vegetation of the arctic tundra*, Oregon State University Press.

Brooks, P. D., and M. W. Williams (1999), Snowpack controls on nitrogen cycling and export in seasonally snow-covered catchments, *Hydrol. Process.*, *13*, 2177–2190.

Burke, M. J., L. V. Gusta, H. A. Quamme, C. J. Weiser, and P. Li (1976), Freezing and Injury in Plants, *Annu. Rev. Plant Physiol.*, *27*(1), 507–528, doi:10.1146/annurev.pp.27.060176.002451.

Bushaw, K. L., R. G. Zepp, M. A. Tarr, D. Schulz-Jander, R. A. Bourbonniere, R. E. Hodson, W. L. Miller, D. A. Bronk, and M. A. Moran (1996), Photochemical release of biologically available nitrogen from aquatic dissolved organic matter, *Nature*, *381*, 381–407.

Cai, Y., L. Guo, T. A. Douglas, and T. E. Whitledge (2008), Seasonal variations in nutrient concentrations and speciation in the Chena River, Alaska, *J. Geophys. Res.*, *113*(3), 1–11, doi:10.1029/2008JG000733.

Chapin, F. Stuart, I., K. Van Cleve, and M. C. Chapin (1979), Soil temperature and nutrient cycling in the tussock growth form of Eriophorum vaginatum, *J. Ecol.*, *67*(1), 169–189.

Chapin, F. Stuart, I., P. C. Miller, W. D. Billings, and P. I. Coyne (1980), *An Arctic ecosystem: The Coastal Tundra at Barrow, Alaska*, edited by J. Brown, P. C. Miller, L. L. Tieszan, and F. L. Bunnell, Dowden, Hutchinson & Ross, Stroudsburg, Pennsylvania, United States of America.

Chapin, F. Stuart, I., G. R. Shaver, A. Giblin, K. Nadelhoffer, and J. Laundre (1995), Responses of Arctic Tundra to Experimental and Observed Changes in Climate, *Ecology*, *76*(3), 694–711, doi:10.2307/1939337.

Cleveland, C. C., J. C. Neff, A. R. Townsend, and E. Hood (2004), Composition, Dynamics, and Fate of Leached Dissolved Organic Matter in Terrestrial Ecosystems: Results from a Decomposition Experiment, *Ecosystems*, *7*(3), 275–285, doi:10.1007/s10021-003-0236-7.

Cooper, R. J. J., J. L. L. Wadham, M. Tranter, R. Hodgkins, and N. E. E. Peters (2002), Groundwater hydrochemistry in the active layer of the proglacial zone, Finsterwalderbreen, Svalbard, *J. Hydrol.*, *269*(3-4), 208–223, doi:10.1016/S0022-1694(02)00279-2.

Cory, R. M., B. C. Crump, J. A. Dobkowski, and G. W. Kling (2013), Surface exposure to sunlight stimulates CO2 release from permafrost soil carbon in the Arctic., *Proc. Natl. Acad. Sci. U. S. A.*, *110*(9), 3429–34, doi:10.1073/pnas.1214104110.

Cory, R. M., C. P. Ward, B. C. Crump, and G. W. Kling (2014), Sunlight controls water column processing of carbon in arctic fresh waters, *Science (80-. ).*, *345*(6199), 925–928, doi:10.1126/science.1253119.

Craig, P. C., and P. J. McCart (1975), Classification of stream types in Beaufort sea drainages between Prudhoe Bay, Alaska, and the Mackenzie Delta, N.W.T. Canada, *Arct. Alp. Res.*, *7*(2), 183–198.

Czech, D., and L. Kappen (1997), Field measurement of carbon leaching from leaves in beech and alder forests of northern Germany, *Flora Morphol. Geobot. Oekophysiologie*, *192*(3).

Dahlgren, R. A. (1994), Soil acidification and nitrogen saturation from weathering of ammonium-bearing rock, *Nature*, *368*, 838–841.

Dittmar, T., and G. Kattner (2003), The biogeochemistry of the river and shelf ecosystem of the Arctic Ocean: a review, *Mar. Chem.*, *83*(3-4), 103–120, doi:10.1016/S0304-4203(03)00105-1.

Dornblaser, M. M., and R. G. Striegl (2007), Nutrient (N, P) loads and yields at multiple scales and subbasin types in the Yukon River basin, Alaska, *J. Geophys. Res. Biogeosciences*, *112*(4), 1–10, doi:10.1029/2006JG000366.

Douglas, T. A., J. D. Blum, L. Guo, K. Keller, and J. D. Gleason (2013), Hydrogeochemistry of seasonal flow regimes in the Chena River, a subarctic watershed draining discontinuous permafrost in interior Alaska (USA), *Chem. Geol.*, *335*, 48–62, doi:10.1016/j.chemgeo.2012.10.045.

Dunton, K. H., T. Weingartner, and E. C. Carmack (2006), The nearshore western Beaufort Sea ecosystem: Circulation and importance of terrestrial carbon in arctic coastal food webs, *Prog. Oceanogr.*, *71*(2-4), 362–378, doi:10.1016/j.pocean.2006.09.011.

Ernakovich, J. G., K. A. Hopping, A. B. Berdanier, R. T. Simpson, E. J. Kachergis, H. Steltzer, and M. D. Wallenstein (2014), Predicted responses of arctic and alpine ecosystems to altered seasonality under climate change, *Glob. Chang. Biol.*, *20*(10), 3256–3269, doi:10.1111/gcb.12568.

Everett, K. R., G. M. Marion, D. L. Kane, A. K. R. Everett, G. M. Marion, D. L. Kane, and K. R. Everett (1989), Seasonal geochemistry of an arctic tundra drainage basin, *Holarct. Ecol.*, *12*(3), 279–289, doi:10.1111/j.1600-0587.1989.tb00847.x.

Feth, J. H. (1981), Chloride in Natural Continental Water-A Review, *U.S. Geol. Surv. Water Supply Papp. 2176*.

Finlay, J. C. (2001), Stable-carbon-isotope ratios of river biota: Implications for energy flow in lotic food webs, *Ecology*, *82*(4), 1052–1064, doi:10.1890/0012-9658(2001)082[1052:SCIROR]2.0.CO;2.

Finlay, J. C., J. C. Neff, S. A. Zimov, A. Davydova, and S. Davydov (2006), Snowmelt dominance of dissolved organic carbon in high-latitude watersheds: Implications for characterization and flux of river DOC, *Geophys. Res. Lett.*, *33*(10), n/a–n/a, doi:10.1029/2006GL025754.

Freeman, C., C. D. Evans, D. T. Monteith, B. Reynolds, and N. Fenner (2001), Export of organic carbon from peat soils., *Nature*, *412*(6849), 785, doi:10.1038/35090628.

Freeman, C., N. Fenner, N. J. Ostle, H. Kang, D. J. Dowrick, B. Reynolds, M. a Lock, D. Sleep, S. Hughes, and J. Hudson (2004), Export of dissolved organic carbon from peatlands under elevated carbon dioxide levels., *Nature*, *430*(6996), 195–8, doi:10.1038/nature02707.

Frey, K. E., and J. W. McClelland (2009), Impacts of permafrost degradation on arctic river biogeochemistry, *Hydrogeol. J.*, *23*, 169–182, doi:10.1002/hyp.

Frey, K. E., and L. C. Smith (2005), Amplified carbon release from vast West Siberian peatlands by 2100, *Geophys. Res. Lett.*, *32*(9), L09401, doi:10.1029/2004GL022025.

Frey, K. E., D. I. Siegel, and L. C. Smith (2007), Geochemistry of west Siberian streams and their potential response to permafrost degradation, *Water Resour. Res.*, *43*(3), n/a–n/a, doi:10.1029/2006WR004902.

Gersper, P. L., V. Alexander, S. A. Barkley, R. J. Barsdate, and P. S. Flint (1980), *An Arctic ecosystem: The Coastal Tundra at Barrow, Alaska*, edited by J. Brown, P. C. Miller, L. L. Tieszan, and F. L. Bunnell, Dowden, Hutchinson & Ross, Stroudsburg, Pennsylvania, United States of America.

Gettel, G. M., A. E. Giblin, and R. W. Howarth (2013), Controls of Benthic Nitrogen Fixation and Primary Production from Nutrient Enrichment of Oligotrophic, Arctic Lakes, *Ecosystems*, *16*(8), 1550–1564, doi:10.1007/s10021-013-9701-0.

Gosz, J. R., G. E. Likens, and F. H. Bormann (1973), Nutrient release from decomposing leaf and branch litter in the Hubbard Brook Forest, New Hampshire, *Ecol. Monogr.*, *43*(2), 173–191, doi:10.2307/1942193.

Grzybowski, W. (2002), The significance of dissolved organic matter photodegradation as a source of ammonium in natural waters, *Oceanologia*, *44*(3), 355–365.

Guo, L., and R. W. Macdonald (2006), Source and transport of terrigenous organic matter in the upper Yukon River: Evidence from isotope (δ 13 C, Δ 14 C, and δ 15 N) composition of dissolved, colloidal, and particulate phases, *Global Biogeochem. Cycles*, *20*(2), doi:10.1029/2005GB002593.

Guo, L., C.-L. Ping, and R. W. Macdonald (2007), Mobilization pathways of organic carbon from permafrost to arctic rivers in a changing climate, *Geophys. Res. Lett.*, *34*(13), 1–5, doi:10.1029/2007GL030689.

Harms, T. K., and J. B. Jones (2012), Thaw depth determines reaction and transport of inorganic nitrogen in valley bottom permafrost soils, *Glob. Chang. Biol.*, *18*(9), 2958–2968, doi:10.1111/j.1365-2486.2012.02731.x.

Hillebrand, H., and U. Sommer (1999), The nutrient stoichiometry of benthic microalgal growth: Redfield proportions are optimal, *Limnol. Oceanogr.*, *44*(2), 440–446, doi:10.4319/lo.1999.44.2.0440.

Hinzman, L. D., D. L. Kane, R. E. Gieck, and K. R. Everett (1991), Hydrologic and thermal-properties of the active layer in the Alaskan Arctic, *Cold Reg. Sci. Technol.*, *19*(2), 95–110, doi:10.1016/0165-232X(91)90001-W.

Hobara, S., C. McCalley, K. Koba, A. E. Giblin, M. S. Weiss, G. M. Gettel, and G. R. Shaver (2006), Nitrogen Fixation in Surface Soils and Vegetation in an Arctic Tundra Watershed: A Key Source of Atmospheric Nitrogen, *Arctic, Antarct. Alp. Res.*, *38*(3), 363–372, doi:10.1657/1523-0430(2006)38[363:NFISSA]2.0.CO;2.

Hobbie, S. E., and F. S. Chapin (1996), Winter regulation of tundra litter carbon and nitrogen dynamics, *Biogeochemistry*, *35*(2), 327–338, doi:10.1007/BF02179958.

Hobbie, S. E., and L. Gough (2002), Foliar and soil nutrients in tundra on glacial landscapes of contrasting ages in northern Alaska, *Oecologia*, *131*(3), 453–462, doi:10.1007/s00442-002-0892-x.

Holland, M. M., J. Finnis, A. P. Barrett, and M. C. Serreze (2007), Projected changes in Arctic Ocean freshwater budgets, *J. Geophys. Res. Biogeosciences*, *112*(4), 1–13, doi:10.1029/2006JG000354.

Holloway, J. M., and R. A. Dahlgren (1999), Geologic nitrogen in terrestrial biogeochemical cycling, *Geology*, *27*(6), 567, doi:10.1130/0091-7613(1999)027<0567:GNITBC>2.3.CO;2.

Holloway, J. M., and R. A. Dahlgren (2002), Nitrogen in rock: Occurrences and biogeochemical implications, *Global Biogeochem. Cycles*, *16*(4), 65–1–65–17, doi:10.1029/2002GB001862.

Holloway, J. M., R. A. Dahlgren, and W. H. Casey (2001), Nitrogen release from rock and soil under simulated field conditions, *Chem. Geol.*, *174*(4), 403–414, doi:10.1016/S0009-2541(00)00290-4.

Holmes, R. M., A. Aminot, R. Kérouel, B. A. Hooker, and B. J. Peterson (1999), A simple and precise method for measuring ammonium in marine and freshwater ecosystems, *Can. J. Fish. Aquat. Sci.*, *56*(10), 1801–1808, doi:10.1139/f99-128.

Holmes, R. M., B. J. Peterson, V. V. Gordeev, and A. V. Zhulidov (2000), Flux of nutrients from Russian rivers to the Arctic Ocean: Can we establish a baseline against which to judge future changes?, *Water Resour. Res.*, *36*(8), 2309–2320.

Holmes, R. M., B. J. Peterson, A. V. Zhulidov, V. V. Gordeev, P. N. Makkaveev, P. A. Stunzhas, L. S. Kosmenko, G. H. Köhler, and A. I. Shiklomanov (2001), Nutrient chemistry of the Ob' and Yenisey Rivers, Siberia: results from June 2000 expedition and evaluation of long-term data sets, *Mar. Chem.*, *75*(3), 219–227, doi:10.1016/S0304-4203(01)00038-X.

Holmes, R. M., J. W. McClelland, P. A. Raymond, B. B. Frazer, B. J. Peterson, and M. Stieglitz (2008), Lability of DOC transported by Alaskan rivers to the Arctic Ocean, *Geophys. Res. Lett.*, *35*(3), L03402, doi:10.1029/2007GL032837.

Holmes, R. M. et al. (2012), Seasonal and Annual Fluxes of Nutrients and Organic Matter from Large Rivers to the Arctic Ocean and Surrounding Seas, *Estuaries and Coasts*, *35*(2), 369–382, doi:10.1007/s12237-011-9386-6.

Hurst, J. L., G. J. F. Pugh, and D. W. H. Walton (1985), The effects of freeze-thaw cycles and leaching on the loss of soluble carbohydrates from leaf material of two subantarctic plants, *Polar Biol.*, *4*(1), 27–31, doi:10.1007/BF00286814.

Huryn, A. D., and J. E. Hobbie (2012), *Land of Extremes: A Natural History of the Arctic North Slope of Alaska*, University of Alaska Press.

Huryn, A. D., K. A. Slavik, R. L. Lowe, S. M. Parker, D. S. Anderson, and B. J. Peterson (2005), Landscape heterogeneity and the biodiversity of Arctic stream communities : a habitat template analysis, *Can. J. Fish. Aquat. Sci.*, *62*, 1905–1919, doi:10.1139/F05-100.

IPCC, Trenberth, K.E., P.D. Jones, P. Ambenje, R. Bojariu, D. Easterling, A. Klein Tank, D. Parker, F. Rahimzadeh, J.A. Renwick, M. Rusticucci, B. S. and P. Z. (2007), *Observations: Surface and Atmospheric Climate Change. In: Climate Change 2007: The Physical Science Basis. Contribution of Working Group I to the Fourth Assessment Report of the Intergovernmental Panel on Climate Change*, edited by M. T. and H. L. M. Solomon, S., D. Qin, M. Manning, Z. Chen, M. Marquis, K.B. Averyt, Cambridge University Press, Cambridge, United Kingdom and New York, NY, USA.

Irwin, T., M. Rutherford, K. Banks, K. Gibson, J. Houle, P. Decker, D. Shellenbaum, P. Anderso, J. Meyer, and T. A. Arion (2008), *Regional Geology of the North Slope of Alaska*.

Jaffe, D. A., and M. D. Zukowski (1993), Nitrate deposition to the Alaskan snowpack, *Atmos. Environ. Part A. Gen. Top.*, *27*(17-18), 2935–2941, doi:10.1016/0960-1686(93)90326-T.

Johnson, L. C., G. R. Shaver, A. E. Giblin, K. J. Nadelhoffer, E. R. Rastetter, J. a. Laundre, and G. L. Murray (1996), Effects of drainage and temperature on carbon balance of

tussock tundra microcosms, *Oecologia*, *108*(4), 737–748, doi:10.1007/BF00329050.

Jones, J. B., K. C. Petrone, J. C. Finlay, L. D. Hinzman, and W. R. Bolton (2005), Nitrogen loss from watersheds of interior Alaska underlain with discontinuous permafrost, *Geophys. Res. Lett.*, *32*(2), L02401, doi:10.1029/2004GL021734.

Jones, M. N. (1984), Nitrate reduction by shaking with cadmium; alternate to cadmium columns, *Water Res.*, *18*(5), 643–646.

Jorgenson, M. T., K. Yoshikawa, M. Kanevskiy, Y. Shur, V. E. Romanovsky, S. Marchenko, G. Grosse, J. Brown, and B. Jones (2008), *Permafrost Characteristics of Alaska*.

Judd, K. E., and G. W. Kling (2002), Production and export of dissolved C in arctic tundra mesocosms: The roles of vegetation and water flow, *Biogeochemistry*, *60*(3), 213–234, doi:10.1023/A:1020371412061.

Kane, D. L., L. D. Hinzman, C. S. Benson, and K. R. Everett (1989), Hydrology of Imnavait Creek, an Arctic watershed, *Holarct. Ecol.*, *12*(3), 262–269, doi:10.1111/j.1600-0587.1989.tb00845.x.

Kane, D. L., R. E. Gieck, and L. D. Hinzman (1997), Snowmelt Modeling at Small Alaskan Arctic Watershed, *J. Hydrol. Eng.*, *2*(4), 204–210.

Kane, D. L., J. P. McNamara, D. Yang, P. Q. Olsson, and R. E. Gieck (2003), An Extreme Rainfall / Runoff Event in Arctic Alaska, *J. Hydrometerorology*, *4*, 1220–1228.

Kawahigashi, M., K. Kaiser, A. Rodionov, and G. Guggenberger (2006), Sorption of dissolved organic matter by mineral soils of the Siberian forest tundra, *Glob. Chang. Biol.*, *12*(10), 1868–1877, doi:10.1111/j.1365-2486.2006.01203.x.

Kaye, J. P., and S. C. Hart (1997), Competition for nitrogen between plants and soil microorganisms, *Trends Ecol. Evol.*, *12*(4), 139–143, doi:10.1016/S0169-5347(97)01001-X.

Keller, K., J. D. Blum, and G. W. Kling (2010), Stream geochemistry as an indicator of increasing permafrost thaw depth in an arctic watershed, *Chem. Geol.*, *273*(1-2), 76–81, doi:10.1016/j.chemgeo.2010.02.013.

Kendall, C., S. R. Silva, and V. J. Kelly (2001), Carbon and nitrogen isotopic compositions of particulate organic matter in four large river systems across the United States, *Hydrol. Process.*, *15*(7), 1301–1346, doi:10.1002/hyp.216.

Kling, G. W. et al. (2014), Land-Water Interactions, in *Alaska's Changing Arctic: Ecological Consequences for Tundra, Streams, and Lakes*, edited by J. E. Hobbie and G. W. Kling, pp. 143–172, Oxford University Press, New York.

Koven, C. D., B. Ringeval, P. Friedlingstein, P. Ciais, P. Cadule, D. Khvorostyanov, G. Krinner, and C. Tarnocai (2011), Permafrost carbon-climate feedbacks accelerate

global warming., *Proc. Natl. Acad. Sci. U. S. A.*, *108*(36), 14769–74, doi:10.1073/pnas.1103910108.

Kriet, K., B. J. Peterson, and T. L. Corliss (1992), Water and sediment export of the upper Kuparuk River drainage of the North Slope of Alaska, *Hydrobiologia*, *240*(1-3), 71–81, doi:10.1007/BF00013453.

Levine, M. A., and S. C. Whalen (2001), Nutrient limitation of phytoplankton production in Alaskan Arctic foothill lakes, *Hydrobiologia*, *455*, 189–201, doi:10.1023/A:1011954221491.

MacIntyre, S., J. O. Sickman, S. A. Goldthwait, and G. W. Kling (2006), Physical pathways of nutrient supply in a small, ultraoligotrophic arctic lake during summer stratification, *Limnol. Oceanogr.*, *51*(2), 1107–1124, doi:10.4319/lo.2006.51.2.1107.

Mack, M. C., E. a. G. Schuur, M. S. Bret-Harte, G. R. Shaver, and I. Chapin, F. Stuart (2004), Ecosystem carbon storage in arctic tundra reduced by long-term nutrient fertilization., *Nature*, *431*(7007), 440–3, doi:10.1038/nature02887.

MacLean, R., M. W. Oswood, J. G. Irons, and W. H. Mcdowell (1999), The effect of permafrost on stream biogeochemistry : A case study of two streams in the Alaskan (U. S. A.) taiga, *Biogeochemistry*, *47*(1999), 239–267.

McClelland, J. W., M. Stieglitz, F. Pan, R. M. Holmes, and B. J. Peterson (2007), Recent changes in nitrate and dissolved organic carbon export from the upper Kuparuk River, North Slope, Alaska, *J. Geophys. Res.*, *112*(G4), G04S60, doi:10.1029/2006JG000371.

McClelland, J. W., A. Townsend-Small, R. M. Holmes, F. Pan, M. Stieglitz, M. S. Khosh, and B. J. Peterson (2014), River export of nutrients and organic matter from the North Slope of Alaska to the Beaufort Sea, *Water Resour. Res.*, 1823–1839, doi:10.1002/2013WR014722.Received.

McDowell, W. H., and G. E. Likens (1988), Origin, composition, and flux of dissolved organic carbon in the Hubbard Brook Valley, *Ecol. Monogr.*, *58*(3), 177–195, doi:10.2307/2937024.

McGuire, D. A., L. G. Anderson, T. R. Christensen, S. Dallmore, L. Guo, D. J. Hayes, T. D. Lorenson, R. W. Macdonald, and N. T. Roulet (2009), Sensitivity of the carbon cycle in the Arctic to climate change, *Ecol. Monogr.*, *79*(4), 523–555.

McNamara, J. P., D. L. Kane, L. D. Hinzman, and A. Storm (1997), Hydrograph separations in an Arctic watershed using mixing model and graphical techniques in the Upper Kuparuk, *Water Resour. Res.*, *33*(7), 1707–1719.

McNamara, J. P., D. L. Kane, and L. D. Hinzman (1998), An analysis of streamflow hydrology in the Kuparuk River Basin, Arctic Alaska: a nested watershed approach, *J. Hydrol.*, *206*(1-2), 39–57, doi:10.1016/S0022-1694(98)00083-3.

McNamara, J. P., D. L. Kane, J. E. Hobbie, and G. W. Kling (2008), Hydrologic and biogeochemical controls on the spatial and temporal patterns of nitrogen and phosphorus in the Kuparuk River, arctic Alaska, *Hydrol. Process.*, *22*, 3294–3309, doi:10.1002/hyp.

Melick, D. R., and R. D. Seppelt (1992), Loss of soluble carbohydrates and changes in freezing point of Antarctic bryophytes after leaching and repeated freeze-thaw cycles, *Antarct. Sci.*, *4*(4), 399–404, doi:10.1017/S0954102092000592.

Menard, H. W., and S. M. Smith (1966), Hypsometry of Ocean Basin Provinces, *J. Geophys. Res.*, *71*(18), 4305–4325.

Meyer, J. L., and J. B. Wallace (1998), Leaf Litter as a Source of Dissolved Organic Carbon in Streams, *Ecosystems*, *1*(3), 240–249, doi:10.1007/s100219900019.

Milliman, J. D., and J. P. M. Syvitski (1992), Geomorphic/Tectonic Control of Sediment Discharge to the Ocean: The Importance of Small Mountainous Rivers, *J. Geol.*, *100*(5), 525–544, doi:10.1086/629606.

Mook, W. G., and F. C. Tan (1991), *Biogeochemistry of Major World Rivers, SCOPE Report Volume 42*, edited by E. T. Degens, S. Kempe, and J. E. Richey, Hoboken, N. J.

Nadelhoffer, K. J., A. E. Giblin, G. R. Shaver, and J. A. Laundre (1991), Effects of temperature and substrate quality on element mineralization in six Arctic soils, *Ecology*, *72*(1), 242–253, doi:10.2307/1938918.

Neff, J. C., and G. P. Asner (2001), Dissolved Organic Carbon in Terrestrial Ecosystems: Synthesis and a Model, *Ecosystems*, *4*(1), 29–48, doi:10.1007/s100210000058.

Neff, J. C., and D. U. Hooper (2002), Vegetation and climate controls on potential CO2, DOC and DON production in northern latitude soils, *Glob. Chang. Biol.*, *8*(9), 874–884.

Neff, J. C., J. C. Finlay, S. a. Zimov, S. P. Davydov, J. J. Carrasco, E. a. G. Schuur, and a. I. Davydova (2006), Seasonal changes in the age and structure of dissolved organic carbon in Siberian rivers and streams, *Geophys. Res. Lett.*, *33*(23), L23401, doi:10.1029/2006GL028222.

O'Leary, M. H. (1988), Carbon Isotopes in Photosynthesis Fractionation techniques may reveal new aspects of carbon dynamics in plants, *Bioscience*, *38*(5), 328–336.

Oechel, W. C., S. J. Hastings, G. L. Vourlitis, M. Jenkins, G. Riechers, and N. Grulke (1993), Recent change of Arctic tundra ecosystems from a net carbon dioxide sink to a source, *Nature*, *361*(February), 520–523.

Osterkamp, T. E., and M. W. Payne (1981), Estimates of permafrost thickness from well logs in northern Alaska, *Cold Reg. Sci. Technol.*, *5*(1), 13–27, doi:10.1016/0165-232X(81)90037-9.

Pearson, R. G., S. J. Phillips, M. M. Loranty, P. S. A. Beck, T. Damoulas, S. J. Knight, and S. J. Goetz (2013), Shifts in Arctic vegetation and associated feedbacks under climate change, *Nat. Clim. Chang.*, *3*(7), 673–677, doi:10.1038/nclimate1858.

Peterson, B. J., J. E. Hobbie, T. L. Corliss, and K. Kriet (1983), A continuous-flow periphyton bioassay: Tests of nutrient limitation in a tundra stream, *Limnol. Oceanogr.*, *28*(3), 583–591, doi:10.4319/lo.1983.28.3.0583.

Peterson, B. J., J. E. Hobbie, and T. L. Corliss (1986), Carbon Flow in a Tundra Stream Ecosystem, *Can. J. Fish. Aquat. Sci.*, *43*(1978), 1259–1270.

Peterson, B. J., T. Corliss, K. Kriet, and J. E. Hobbie (1992), Nitrogen and phosphorus concentrations and export for the upper Kuparuk River on the North Slope of Alaska in 1980, *Hydrobiologia*, *240*(1-3), 61–69, doi:10.1007/BF00013452.

Peterson, B. J., M. Bahr, and G. W. Kling (1997), A tracer investigation of nitrogen cycling in a pristine tundra river, *Can. J. Fish. Aquat. Sci.*, *54*(10), 2361–2367, doi:10.1139/cjfas-54-10-2361.

Peterson, B. J., R. M. Holmes, J. W. McClelland, C. J. Vörösmarty, R. B. Lammers, A. I. Shiklomanov, I. Shiklomanov, and S. Rahmstorf (2002), Increasing river discharge to the Arctic Ocean., *Science*, *298*(5601), 2171–2173, doi:10.1126/science.1077445.

Peterson, B. J., J. W. McClelland, R. Curry, R. M. Holmes, J. E. Walsh, and K. Aagaard (2006), Trajectory shifts in the Arctic and subarctic freshwater cycle., *Science*, *313*(5790), 1061–1066, doi:10.1126/science.1122593.

Petrone, K. C., J. B. Jones, L. D. Hinzman, and R. D. Boone (2006), Seasonal export of carbon, nitrogen, and major solutes from Alaskan catchments with discontinuous permafrost, *J. Geophys. Res.*, *111*(G2), G02020, doi:10.1029/2005JG000055.

Peuravuori, J., and K. Pihlaja (1997), Molecular size distribution and spectroscopic properties of aquatic humic substances, *Anal. Chim. Acta*, *337*(2), 133–149, doi:10.1016/S0003-2670(96)00412-6.

Ping, C. L., J. G. Bockheim, J. M. Kimble, G. J. Michaelson, and D. A. Walker (1998), Characteristics of cryogenic soils along a latitudinal transect in Arctic Alaska, *J. Geophys. Res.*, *103*.

Pomeroy, J. W., H. G. Jones, M. Tranter, and G. R. O. Lilbæk (2005), Hydrochemical Processes in Snow-covered Basins, *Encycl. Hydrol. Sci.*, 1–14, doi:10.1002/0470848944.

Rawlins, M. A. et al. (2010), Analysis of the Arctic system for freshwater cycle intensification: Observations and expectations, *J. Clim.*, *23*(21), 5715–5737, doi:10.1175/2010JCLI3421.1.

Raymond, P. A., J. W. McClelland, R. M. Holmes, A. V. Zhulidov, K. Mull, B. J. Peterson, R. G. Striegl, G. R. Aiken, and T. Y. Gurtovaya (2007), Flux and age of dissolved

organic carbon exported to the Arctic Ocean: A carbon isotopic study of the five largest arctic rivers, *Global Biogeochem. Cycles*, *21*(4), n/a–n/a, doi:10.1029/2007GB002934.

Rember, R. D., and J. H. Trefry (2004), Increased concentrations of dissolved trace metals and organic carbon during snowmelt in rivers of the Alaskan Arctic, *Geochim. Cosmochim. Acta*, *68*(3), 477–489, doi:10.1016/S0016-7037(03)00458-7.

Romanovsky, V. E., S. L. Smith, and H. H. Christiansen (2010), Permafrost thermal state in the polar Northern Hemisphere during the international polar year 2007-2009: a synthesis, *Permafr. Periglac. Process.*, *21*(2), 106–116, doi:10.1002/ppp.689.

Schell, D. M. (1983), Carbon-13 and Carbon-14 Abundances in Alaskan Aquatic Organisms : Delayed Production from Peat in Arctic Food Webs, *Science (80-. ).*, *219*(4588), 1068–1071.

Schimel, J. P., C. Bilbrough, and J. M. Welker (2004), Increased snow depth affects microbial activity and nitrogen mineralization in two Arctic tundra communities, *Soil Biol. Biochem.*, *36*(2), 217–227, doi:10.1016/j.soilbio.2003.09.008.

Schuur, E. A. G. et al. (2013), Expert assessment of vulnerability of permafrost carbon to climate change, *Clim. Change*, *119*(2), 359–374, doi:10.1007/s10584-013-0730-7.

Schuur, E. A. G. et al. (2015), Climate change and the permafrost carbon feedback, *Nature*, *520*(October), 171–179, doi:10.1038/nature14338.

Sereda, J., K. Hunter, D. Vandergucht, and J. Hudson (2012), Photochemical mineralization of dissolved organic nitrogen to ammonia in prairie lakes, *Hydrobiologia*, *693*(1), 71–80, doi:10.1007/s10750-012-1087-z.

Shaver, G. R., and I. Chapin, F. Stuart (1986), Effect of Fertilizer on Production and Biomass of Tussock Tundra, Alaska, U.S.A., *Arct. Alp. Res.*, *18*(3), 261–268, doi:10.1657/1938-4246-42.1.45.

Shaver, G. R., W. D. Billings, I. Chapin, F. Stuart, A. E. Giblin, K. Nadelhoffer, W. C. Oechel, and E. B. Rastetter (1992), Global Change and the Carbon Balance of Arctic Ecosystems, *Bioscience*, *42*(6), 433–441.

Shaver, G. R., L. C. Johnson, D. H. Cades, G. Murray, J. A. Laundre, E. B. Rastetter, K. J. Nadelhoffer, and A. E. Giblin (1998), Biomass and CO2 flux in wet sedge tundras: Responses to nutrients, temperature, and light, *Ecol. Monogr.*, *68*(1), 75–97, doi:10.1890/0012-9615(1998)068[0075:BACFIW]2.0.CO;2.

Shaver, G. R. et al. (2014), Terrestrial Ecosystems at Toolik Lake, Alaska, in *Alaska's Changing Arctic: Ecological Consequences for Tundra, Streams, and Lakes*, edited by J. E. Hobbie and G. W. Kling, pp. 90–142, Oxford University Press, New York.

Spencer, R. G. M., G. R. Aiken, K. P. Wickland, R. G. Striegl, and P. J. Hernes (2008), Seasonal and spatial variability in dissolved organic matter quantity and

composition from the Yukon River basin, Alaska, *Global Biogeochem. Cycles*, *22*(4), n/a–n/a, doi:10.1029/2008GB003231.

Steiglitz, M., J. Hobbie, A. Giblin, and G. Kling (2000), Effects of climate change and climate variability on carbon dynamics in Arctic tundra., *Global Biogeochem. Cycles*, *14*(4), 1123–1136.

Strahler, A. N. (1957), Quantitative analysis of watershed geomorphology, *Trans. Am. Geophys. Union*, *38*(6), 913–920, doi:10.1130/0016-7606.

Striegl, R. G., G. R. Aiken, M. M. Dornblaser, P. A. Raymond, and K. P. Wickland (2005), A decrease in discharge-normalized DOC export by the Yukon River during summer through autumn, *Geophys. Res. Lett.*, *32*(21), L21413, doi:10.1029/2005GL024413.

Suberkropp, K., G. Godshalk, and M. Klug (1976), Changes in the chemical composition of leaves during processing in a woodland stream, *Ecology*, *57*(4), 720–727, doi:10.2307/1936185.

Tank, S. E., M. Manizza, R. M. Holmes, J. W. McClelland, and B. J. Peterson (2012), The Processing and Impact of Dissolved Riverine Nitrogen in the Arctic Ocean, *Estuaries and Coasts*, *35*(2), 401–415, doi:10.1007/s12237-011-9417-3.

Tarnocai, C., J. G. Canadell, E. A. G. Schuur, P. Kuhry, G. Mazhitova, and S. A. Zimov (2009), Soil organic carbon pools in the northern circumpolar permafrost region, *Global Biogeochem. Cycles*, *23*, doi:10.1029/2008GB003327.

Townsend-Small, A., J. W. McClelland, R. Max Holmes, and B. J. Peterson (2011), Seasonal and hydrologic drivers of dissolved organic matter and nutrients in the upper Kuparuk River, Alaskan Arctic, *Biogeochemistry*, *103*(1-3), 109–124, doi:10.1007/s10533-010-9451-4.

Tukey, H. B. (1970), The Leaching of Substances from Plants, *Annu. Rev. Plant Physiol.*, *21*(1), 305–324, doi:10.1146/annurev.pp.21.060170.001513.

Ueyama, M., H. Iwata, Y. Harazono, E. S. Euskirchen, W. C. Oechel, and D. Zona (2013), Growing season and spatial variations of carbon fluxes of Arctic and boreal ecosystems in Alaska (USA), *Ecol. Appl.*, *23*(8), 1798–1816, doi:10.1890/11-0875.1.

Verardo, D. J., P. N. Froelich, and A. McIntyre (1990), Determination of organic carbon and nitrogen in marine sediments using the Carlo Erba NA-1500 analyzer, *Deep Sea Res. Part A. Oceanogr. Res. Pap.*, *37*(1), 157–165, doi:10.1016/0198-0149(90)90034-S.

Walker, D. A., and K. R. Everett (1987), Road Dust and Its Environmental Impact on Alaskan Taiga and Tundra, *Arct. Alp. Res.*, *19*(4), 479–489, doi:10.1657/1523-0430(07-021).

Walker, D. A., E. Binnian, B. M. Evans, N. D. Lederer, E. Nordstrand, and P. J. Webber (1989), Terrain, vegetation and landscape evolution of the R4D research site, Brooks Range Foothills, Alaska, *Holarct. Ecol.*, *12*(3), 238–261.

Walther, G.-R., E. Post, P. Convey, A. Menzel, C. Parmesan, T. J. C. Beebee, J.-M. Fromentin, O. Hoegh-Guldberg, and F. Bairlein (2002), Ecological responses to recent climate change., *Nature*, *416*(6879), 389–395, doi:10.1038/416389a.

Walvoord, M. A., and R. G. Striegl (2007), Increased groundwater to stream discharge from permafrost thawing in the Yukon River basin: Potential impacts on lateral export of carbon and nitrogen, *Geophys. Res. Lett.*, *34*(12), doi:10.1029/2007GL030216.

Wein, R. W., and L. C. Bliss (1973), Changes in arctic Eriophorum tussock communities following fire, *Ecology*, *54*(4), 845–852.

Wein, R. W., and L. C. Bliss (1974), Primary Production in Arctic Cottongrass Tussock Tundra Communities, *Arct. Alp. Res.*, *6*(3), 261–274, doi:10.1657/1938-4246-42.1.45.

Weishaar, J., and G. Aiken (2001), Evaluation of specific ultra-violet absorbance as an indicator of the chemical content of dissolved organic carbon, *Environ. Chem.*, *41*(2), 843–845.

White, D. et al. (2007), The arctic freshwater system: Changes and impacts, *J. Geophys. Res.*, *112*(G4), G04S54, doi:10.1029/2006JG000353.

Wickland, K. P., J. C. Neff, and G. R. Aiken (2007), Dissolved Organic Carbon in Alaskan Boreal Forest: Sources, Chemical Characteristics, and Biodegradability, *Ecosystems*, *10*(8), 1323–1340, doi:10.1007/s10021-007-9101-4.

Wollheim, W. M., B. J. Peterson, L. A. Deegan, J. E. Hobbie, B. Hooker, W. B. Bowden, K. J. Edwardson, D. B. Arscott, A. E. Hershey, and J. C. Finlay (2001), Influence of stream size on ammonium and suspended particulate nitrogen processing, *Limn*, *46*(1), 1–13.

Woo, M. (1986), Permafrost hydrology in North America, *Atmosphere-Ocean*, *24*(3), 201–234, doi:10.1080/07055900.1986.9649248.

Yano, Y., G. R. Shaver, A. E. Giblin, E. B. Rastetter, and K. J. Nadelhoffer (2010), Nitrogen dynamics in a small arctic watershed: Retention and downhill movement of15N, *Ecol. Monogr.*, *80*(2), 331–351, doi:10.1890/08-0773.1.

Yavitt, J. B., and T. J. Fahey (1986), Litter decay and leaching from the forest floor in Pinus contorta (lodgepole pine) ecosystems, *J. Ecol.*, *74*(2), 525–545, doi:10.2307/2260272.

Yoneyama, T. (1996), *Mass Spectrometry of Soils*, edited by T. W. Boutton and S. Yamasaki, Marcel Dekker, Inc.

Zhang, T., T. E. Osterkamp, and K. Stamnes (1996), Some Characteristics of the Climate in Northern Alaska, USA, *Arct. Alp. Res.*, *28*(4), 509–518.

Zsolnay, A., and H. Steindl (1991), Geovariability and biodegradability of the Water-Extractable Organic Material in an agricultural soil, *Soil Biol. Biochem.*, *23*(11), 1077–1082, doi:10.1016/0038-0717(91)90047-N.